RAPID MONITORING OF BRAIN AUDITORY EVOKED POTENTIALS FOR ASSESSING CEREBRAL HYPOXIA

by

DMITRY KHAVULYA

A thesis submitted to the

Graduate School-New Brunswick

Rutgers, The State University of New Jersey

And The Graduate School of Biomedical Sciences

University of Medicine and Dentistry of New Jersey

In partial fulfillment of the requirements

For the degree of

Master of Science

Graduate Program in Biomedical Engineering

Written under the direction of

Dr. John K-J. Li, Ph.D

And approved by

_____

_____

_____

New Brunswick, New Jersey

May 2012

ABSTRACT OF THE THESIS

RAPID MONITORING OF BRAIN AUDITORY EVOKED POTENTIALS FOR ASSESSING CEREBRAL HYPOXIA

By DMITRY KHAVULYA

Thesis Director:

Dr. John K-J. Li, Ph.D

The brain is critically dependent on blood flow and oxygen supply for its normal function. Few existing methods allow rapid noninvasive assessment during critical hypoxic events. A novel technique for recording and analyzing brain auditory evoked potential (BAEP) under hypoxic conditions was developed. Experiments were performed on a healthy subject during hyperventilation (HV) and episodes of periodic breath-holding. Surface electrodes were used to measure EEG (electro-encephalogram) and also BAEP in A2-Cz configuration. Auditory stimuli were applied in the form of 0.1 seconds stream of clicks. An analog circuit and data acquisition system was developed for amplifying, filtering and recording the EEG from Cz-A2 position. Data were digitized online. Signal processing techniques were performed to extract and analyze BAEP using

Latency Correction (LC), Ensemble Averaging, Continuous Wavelet Transform (CWT), and Principal Component Analysis (PCA). Results showed that the hypoxic conditions caused depolarization and hyperpolarization, producing aggregate potentials or field potentials. BAEPs can be extracted and analyzed under hypoxic conditions with minimum averaging (400 realizations) allowing real time evaluation of the auditory pathway. Increased activity in the auditory pathway directly following depletion of oxygen to the brain was observed. The hypoxic condition was confirmed when BAEP was used in combination with a near-infrared spectroscopic device for quantifying oxygenation. Thus, the BAEP system designed here can be used for non-invasive, real-time assessment of the auditory pathway, in identifying abnormal breathing and hypoxic events, and in the evaluation of patients suffering from cerebrospinal injury when used in conjunction with near-infrared oxygenation monitoring system.

Acknowledgements

I would first and foremost like to thank my thesis advisor Dr. John K-J. Li for his encouragement and support, both financial and intellectual, during my thesis work. Through Dr. Li I have gained extensive knowledge in the field of neuro-engineering and cardiovascular engineering. Dr. Li is a leading expert in the field of cardiovascular engineering, and I feel privileged to have had the chance to work with him on my project.

I would also like to thank my committee members Dr. Gary M. Drzewiecki and Dr. George K. Shoane for taking the time to participate in my thesis defense. Their questions and comments have significantly contributed to the organization and completion of my thesis.

I would like to give a special thanks to my wife Saroja and my daughter Savithri. Their presence in my life has contributed to my healthy state of mind, which made it possible for me to complete my master's studies. I would like to thank my wife for the countless hours she spent pretending to listen to the most mundane details of my research.

I would like to thank my very good friends Monica M. Rodas and Michael Grabchak for all their great advise and encouragement. They have greatly contributed to the rich experience I had during my time at Rutgers.

Finally, I would like to thank Dr. Evangelia Micheli-Tzanakou for introducing me to wavelets and principal component analysis, and providing me with insight into neural processes.

Table of Contents

Lists of tables

List of illustrations

Chapter 1. INTRODUCTION

1.1 The Electroencephalogram (EEG): Background

Electroencephalography is the measurement of aggregate electrical activity generated in the brain [14]. This activity comes about due to the passive in and out movement of ions through the neural cell membrane. Several ions are transported across the membrane, however the voltage gradient is mostly governed by the flow of Na^+, K^+, and Cl^- ions. At rest the permeability to K^+ is greater than other ions so K^+ diffuses out of the neuron creating a net negative voltage inside the cell. This voltage has been measured to be approximately -70 mv [8]. When a neuron receives input from its surrounding neurons the cell membrane depolarizes, due to the influx of Na^+ ions and the efflux of C^-, bringing the membrane potential closer to 0 [10]. A neuron takes multiple inputs from multiple neural sources through synapses or the axon dendrite connections. Action potentials occur if the inputs to a postsynaptic neuron cause its membrane potential to reach a voltage at which Na^+ K^+ ion channels are activated. These channels pump the ions against their electrochemical gradient by active transport, causing the membrane potential to become positive [10]. Action potentials propagate along the axon and to the postsynaptic neurons that will also generate action potentials if the threshold voltage, which activates ion channels, is reached [8]. For neurons to generate action potentials sufficient oxygen supply is required. Oxygen, together with glucose, convert adenosine diphosphate (ADP) and inorganic phosphate (Pi) to adenosine triphosphate (ATP). ATP is then utilized in driving active transport, which pumps Na^+ and K^+ ions [21]. It has been shown that non-oxidative glycolysis yields 15 times less ATP molecules

than oxidative phosphorylation [21]. Thus, since the brain is highly energetic, it cannot function if the oxygen supply is inadequate. In acute hypoxia where oxygen concentration suddenly decreases the brain will try to rapidly adapt to this sudden change in order to maintain normal neurological processes [17].

1.2 EEG Recording and Analysis

The EEG is typically recorded using surface electrodes positioned on the scalp. A common position pattern is illustrated in figure 1. The names of electrode positions correspond to regions of the cerebral cortex. The electrode names and the corresponding cortex regions are shown in table 1.

EEG Analysis

Spectral characteristics have been widely used to analyze EEG signals [14]. The energy changes of EEG rhythms have been associated with different physiological states [14]. The EEG is commonly broken down in to five frequency bands alpha, beta, theta, delta, and gamma [14]. These bands and the associated frequency ranges are summarized in table 2. Different physiological states can be correlated to energy increases and decreases in the EEG bands. For example low frequency rhythms such as delta and theta have been shown to increase in sleep and sedation [14]. Studies also show that under hypobaric hypoxia conditions alpha rhythms decrease and delta rhythms increase [18]. It has been a standard practice to decompose the EEG into individual frequency bands and monitor the energy in these bands. A Fourier Transform (FT) is commonly implemented for frequency analyses by transforming the EEG signal from the time domain to the frequency domain. This provides a quantitative representation of energy for each frequency band. FT is effective because the constant oscillation of the membrane

potential, do to passive ion movements across the cell membrane, allows the EEG to be represented as a summation of sinusoids that differ in frequency and phase characteristics [19].

The EEG has also been used to evaluate sensory pathways. Auditory and visual evoked potentials have been regularly recorded for assessment of the auditory and visual pathways [14]. An evoked potential (EP) is the brain's electrical response to a stimulus. EPs are recorded by applying a stimulus to a sensory system at a desired frequency while recording the EEG. The response to the stimulus is then extracted from the EEG by averaging over several stimulations.

Table 1: Electrode names and placement

Electrode	Cortex Region
F	Frontal
C	Central
P	Parietal
T	Temporal
O	Occipital
A	Auricular
Fp	Frontopolar

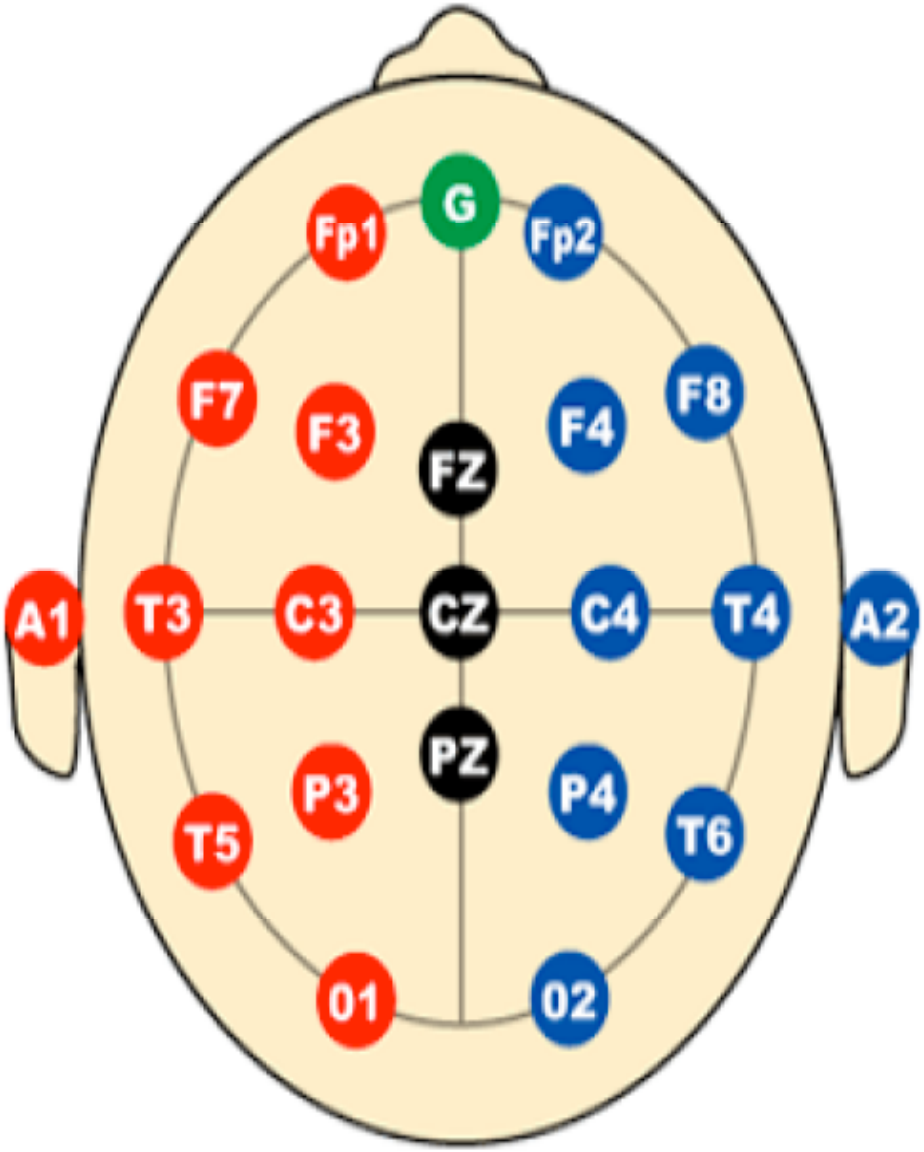

Fig. 1. EEG electrode placement.

Shows the international 10-20 system of electrode placement for EEG recordings.

Image from: **http://www.immrama.org/eeg/electrode.html**

Table 2: EEG frequency bands

Frequency band	Bandwidth
Delta	<4 Hz
Theta	4-7 Hz
Alpha	8-13 Hz
Beta	13-30 Hz
Gamma	>30 Hz

1.3 BAEP Background

The BAEP is the brain's electrical response to an auditory stimulus [2]. First, the ear captures the sound. The main function of the ear in humans illustrated figure 2 is to collect, amplify, and transform mechanical energy. Collection and amplification of this energy is performed mostly by the outer ear, which in turn activates the middle ear for facilitating the transfer of energy from air to fluid in the inner ear or the cochlea. The fluid motion causes the hairs inside the cochlea to move and generate electrical impulses. These impulses stimulate the auditory nerve and initiate an auditory response [20]. This response is characterized by a series of waveforms, which originate in the brainstem and propagate to the auditory cortex. The response is illustrated in figure 3 [2]. BAEP can be separated into two components, the brainstem response (ABR) and the auditory cortex response or Midlatency Auditory Response (MLR). The ABR response is characterized by 5 waveforms that correspond to the 5 sections of the auditory brainstem. Figure 3 shows the auditory pathway. Wave I is produced from the auditory nerve, Wave II from the cochlear nuclei, Wave III from superior olive, Wave IV from lateral lemniscus, and Wave V from inferior colliculus [6]. The brainstem response is typically seen 2 ms after the stimulus application, and lasts approximately 10 ms. The MLR is generated in the auditory cortex and is usually seen between 10 and 60 ms after the stimulus [16].

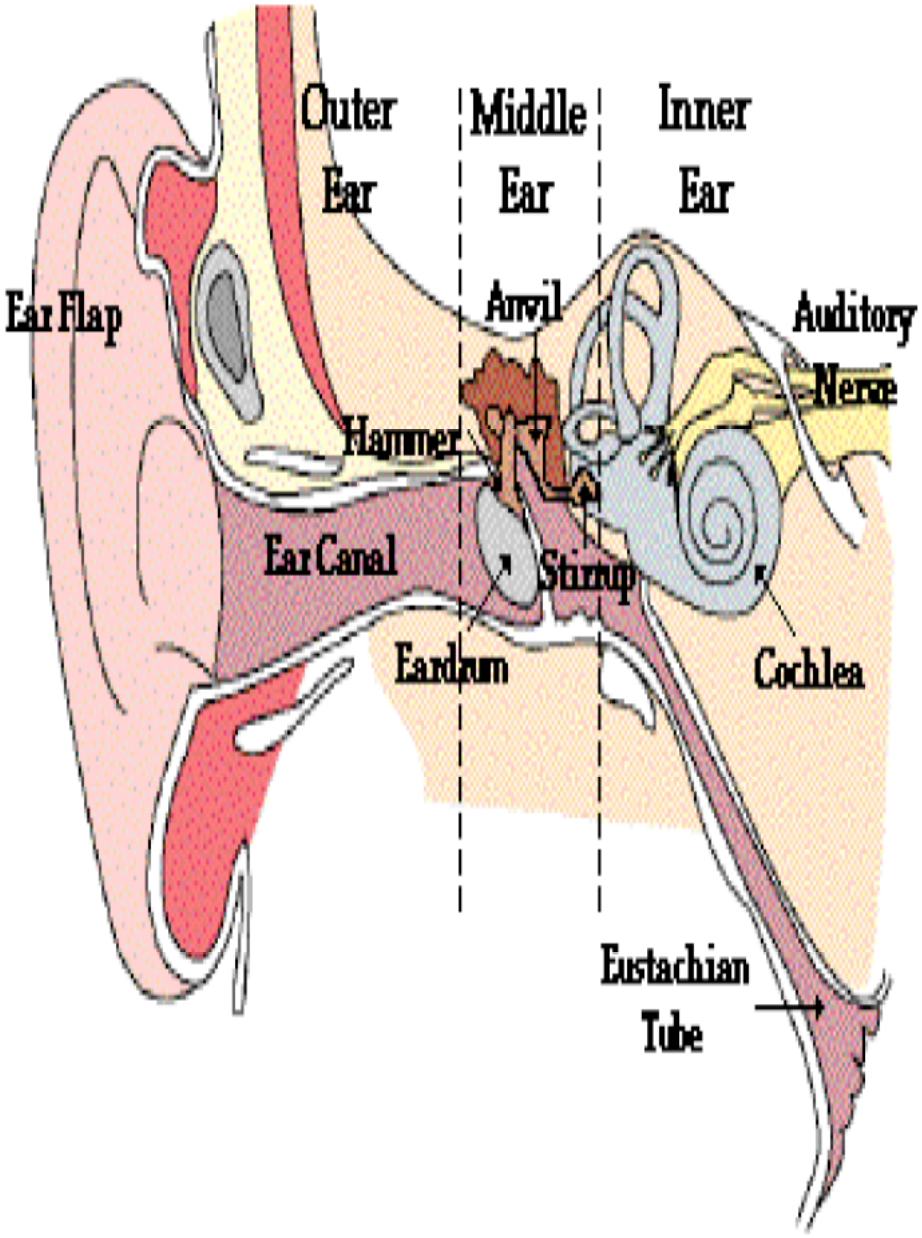

Fig. 2. Diagram of the human ear

Image taken from:

http://www.ndted.org/EducationResources/HighSchool/Sound/humanear.htm

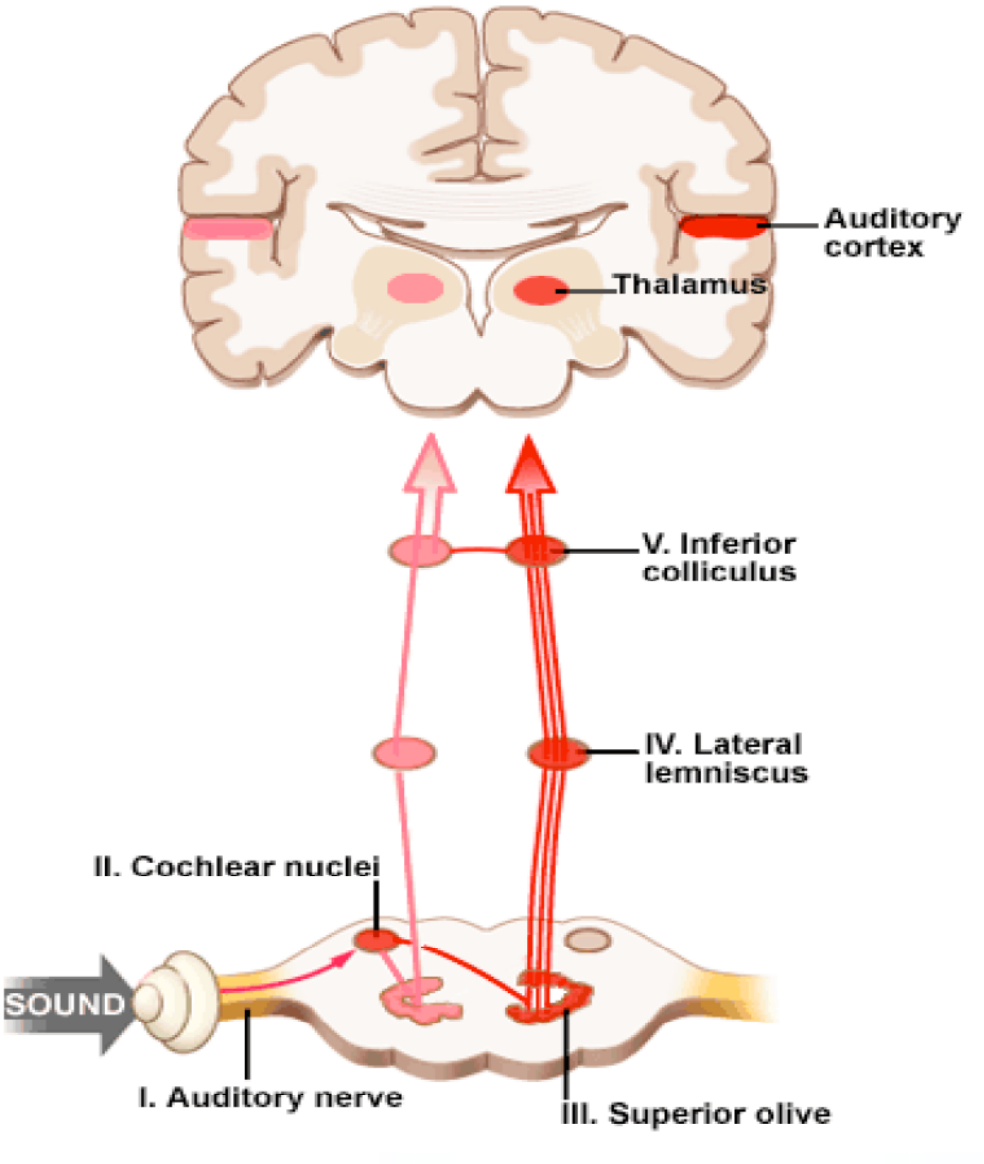

Fig. 3. The auditory pathway

Figure 3 shows the auditory pathway along with a sequence of depolarizations, which produces the BAEP.

Image is taken from: http://www.cochlea.org/en/spe/auditory-pathways-2.html

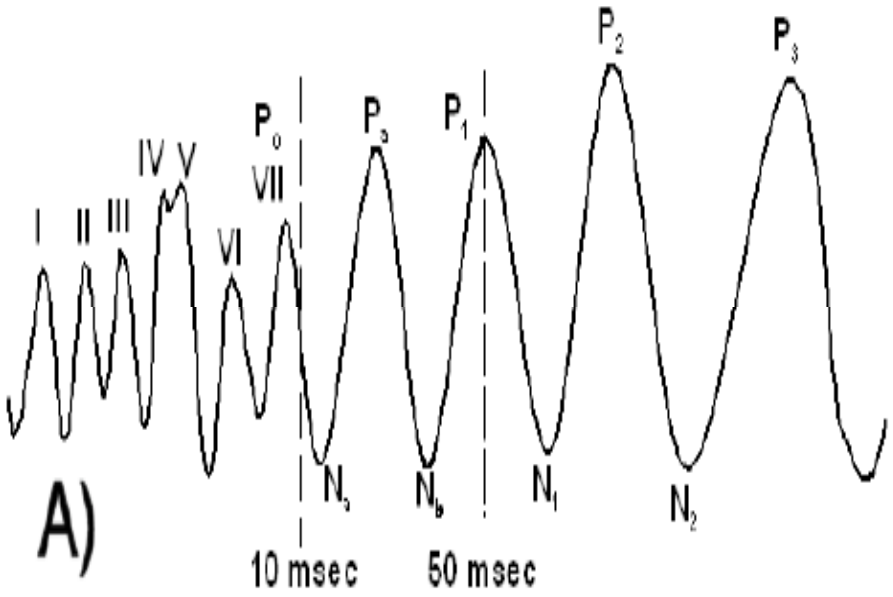

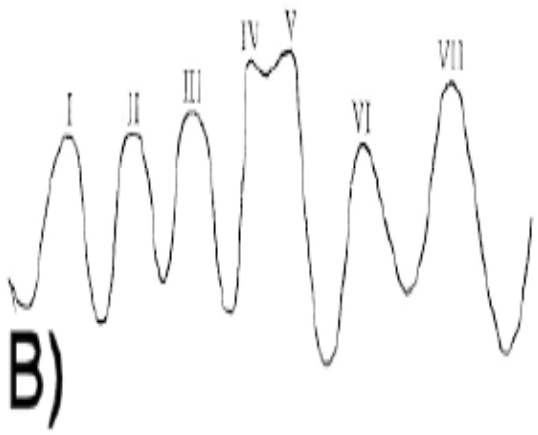

Wave	Ref. Values (ms)	
I	1.35	1.95
II	2.54	3.14
III	3.58	4.18
IV	5.00	5.60
V	5.32	6.12
VI	7.05	7.65
VII	8.70	9.40

Fig. 4. Illustration of the BAEP

Waves I-V are generated in the brainstem. Subsequent waves are generated in the auditory cortex. Image from [2]

1.4 BAEP Recording

The BAEP can be measured non-invasively with the use of surface electrodes placed on top the head. Bipolar recordings are typically used to record the signal. The most common placement of the electrodes is + on top of the head, - behind the ear, and ground on the forehead [5]. The positive and negative leads are inputs to a differential amplifier so that the inputs are subtracted in order to cancel redundant EEG activity. However, regardless of electrode placement, the signal to noise ratio (SNR) is low, which is a key challenge to differentiating the BAEP from the surrounding EEG. The BAEP is significantly smaller in amplitude then the EEG, which is generally in the mV range, while BAEP is in the nV-μV Range [14].

Several statistical techniques have been used to extract the BAEP from the EEG. The most common technique is the ensemble average. A brain signal can be represented by equation 1

$$S_i = d + n_i \tag{1}$$

Where signal S_i is a combination of desired signal d plus noise n_i. In this study d represents the BAEP and n represents the surrounding EEG. The EEG is centered by subtraction of the mean, which insures that the EEG is a 0 mean signal. Under these conditions a mean of S is computed over N samples of the BAEP as shown in equation 2.

$$Y_N = \frac{1}{N}\sum_{i=1}^{N} S_i = d + \frac{1}{N}\sum_{i=1}^{N} n_i \tag{2}$$

Since the EEG is a 0 mean signal $\frac{1}{N}\sum_{i=1}^{N} n_i \Rightarrow 0$. However the EEG is significantly greater in amplitude then the BAEP, and *N* must be very large. Between 1000-4000 stimulus applications is usually needed to reduce the EEG significantly enough for the BAEP to become apparent [3 6]. Depending on the stimulus rate, which is usually between 5-10 times per second, acquiring this many data sets makes real time monitoring of the BAEP impractical.

Chapter 2. AIMS AND SIGNIFICANCE OF THE THESIS

2.1 BAEP Significance

The auditory pathway's electrical response to an auditory stimulus can be used as a diagnostic tool. The most common use of auditory evoked potential is for hearing assessment. However, BAEP recordings have been used in many other clinical applications. Studies have shown that the ABR can be used to detect brain abnormalities in premature infants as well as assess brain function in children with down syndrome [14]. BAEP's have also been used for detection of brain tumors, stroke, multiple sclerosis, coma, and brain death [14]. Spinal cord injury can potentially affect the response due to the brain spinal cord relationship. BAEP's have also been recorded to assess psychological states such as, stress, fear, emotional distress, anxiety, and excitement, and physiological states such as sleep [3].

2.2 Aims Objectives

The focus of this study is to assess how the auditory response is affected by a sudden onset of hypoxia. As stated earlier the brain relies heavily on adequate oxygen supply, therefore we expect to see changes in the auditory response shortly after hypoxia is induced. Monitoring these changes can help in noninvasive assessment of brain functions during surgery, and to develop an early warning system for detecting cerebral hypoxia.

2.3 Specific Aims

A single channel BAEP recorder with a digital signal-processing module is developed in this study. First, software was written for data acquisition in LABVIEW. This software is coupled with an algorithm for extraction of the BAEP from the EEG

using several parameters obtained from the EEG. Parameters that are considered are time, frequency, and phase characteristics of the signal. We show that the BAEP under acute hypoxic conditions can be recorded noninvasively. Further, it can be extracted and analyzed using a minimal amount of averaging, within a reasonable time, and with a single EEG channel. In this study the majority of BAEP extraction and identification is done through digital signal processing allowing the device to be built with minimum amount of electronic components. Thus the device can be easily made and inexpensively produced. Device portability is enhanced by the size reduction due to the lessening of the required hardware components.

Chapter 3. DESIGN METHODS AND EXPERIMENTAL PROTOCOLS

3.1 Circuit Design

BIOPAC EL500 series disposable Ag-ACl electrodes, and 40EL leads were used for all recordings. The placement of electrodes are summarized in table 5. The circuit built for EEG amplification and filtering is shown in figure 5. A1 corresponds to 524 AD precision instrumentation amplifier and A2 corresponds to LM324 operational amplifier. Both amplifiers were powered with +-8V DC. The gain in A1 and A2 is set to 100 with a total gain of 10000. Resistor and capacitor values for the amplification module are summarized in table 3. A highpass filter between A1 and A2 has a cutoff frequency of 0.48 Hz. Addition of this filter removes the DC component and prevents signal saturation caused by DC interference [4]. A2 is set up as an amplifier and an active lowpass filter with a cutoff frequency of 1000 Hz. An additional lowpass passive filter with a cutoff frequency of 530 Hz is added to eliminate high energy electromagnetic noise. Output from the amplifier is the input to the MCC USB-1408 Fs analog to digital converter (DAQ). The timer circuit for click generation is shown in figure 6 and is described further in the experimental set up section. A separate power supply, supplying +7V DC, is used to power the 555 timer chip. This is done to electrically separate the timer circuit from the amplifier circuit. Clicks were generated using a square wave. Potentiometers P1 and P2 were adjusted to achieve a 100 ms duration between clicks. A diode D1 was added in parallel with P2 to achieve a 50% duty cycle.

3.2 Data Acquisition with LabVIEW:

Communication between MCC DAQ and LabVIEW was established using the universal libraries .vi functions developed for DAQ control. The front and the back

panels are shown in figure 6 and figure 7. The front panel, or the graphical user interface, allows the user to specify several parameters such as board number, low channel, high channel, recording time in seconds, and sampling rate. The EEG display shows the recorded EEG. The click display shows the square wave used to drive the speaker in click generation. The power spectrum display shows the power spectrum of the recorded EEG. The data from the EEG and square wave are saved to a text file and stored on the hard drive.

3.3 Protocol for Recordings:

Subject was a young healthy male. Surface electrodes were places at positions shown in table 5. The stimulus was a click generated at 100 ms intervals. The click was applied to the left ear, via headphones, and the positive electrode was at A2 (behind the right ear) in order to record from the contralateral side. The negative electrode was placed at position Cz on top of the head, and ground was placed on the neck below the right ear.

EEGs were recorded for 40 seconds at a sampling rate of 10 kHz. The conditions for all recordings are summarized in table 6. An intervention in this study was 10 seconds of hyperventilation followed by 40 seconds of breath holding. The EEG recording was started immediately after HV. 2 recording sessions were performed during a two-day period. Additional recording sessions were performed at a later time. Each recording session consisted of 3 sets of 4 trials shown in table 6. The subject was allowed to rest for approximately 10 minutes between trials or more if requested. Constraining the subject's field of vision to a homogenous white surface reduced visual evoked potentials.

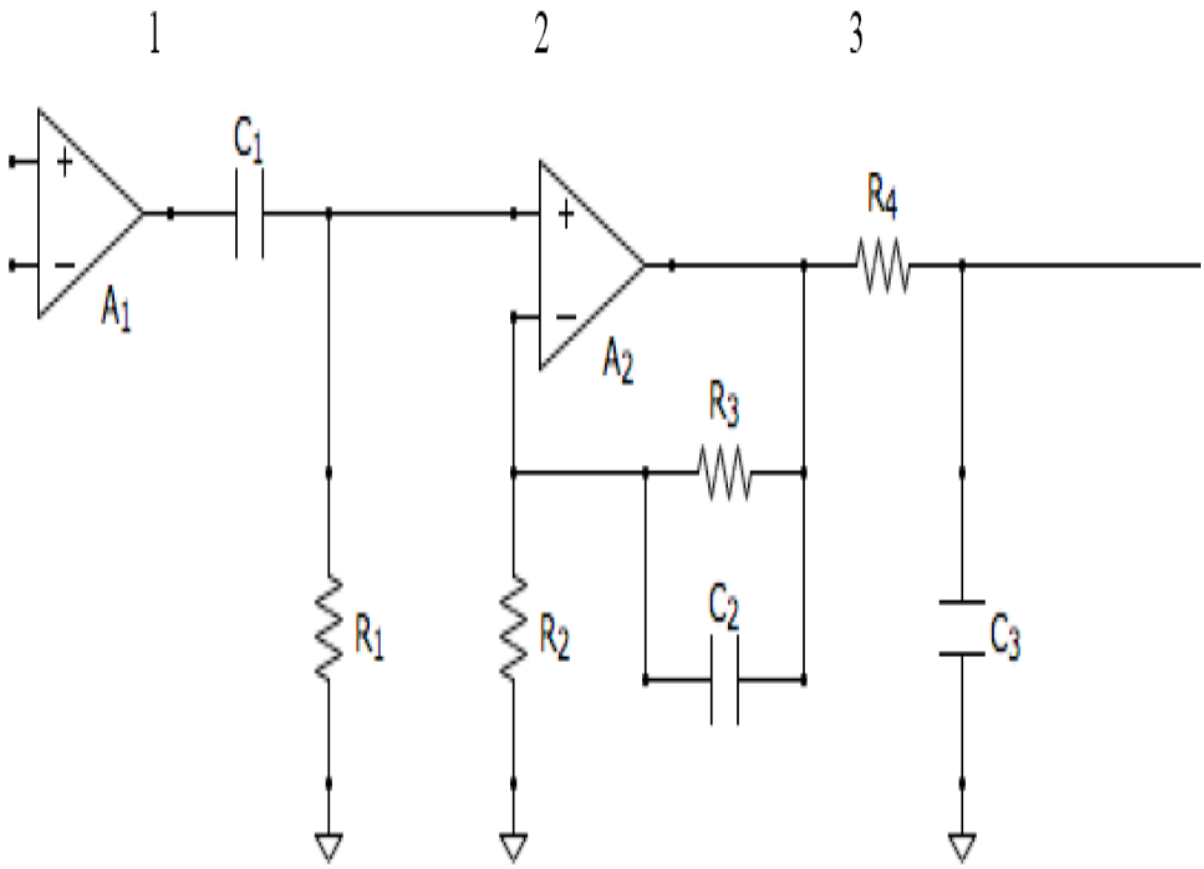

Fig. 5. EEG analog amplifier and filter

Shows the circuit used for bipolar recordings in this study. Electrode at A2 position is the positive input to A1 (524 AD precision instrumentation with gain=100) and Cz is the negative input. C1 and R1 make up the high pass filter with a cutoff frequency of 0.48 Hz. The output from 1 is sent to an operational amplifier A2 (LM324). A2 acts as an amplifier and an active lowpass filter with a cutoff frequency of 1000 Hz. Stage 3 is a low pass passive filter with cutoff frequency of 530 Hz.

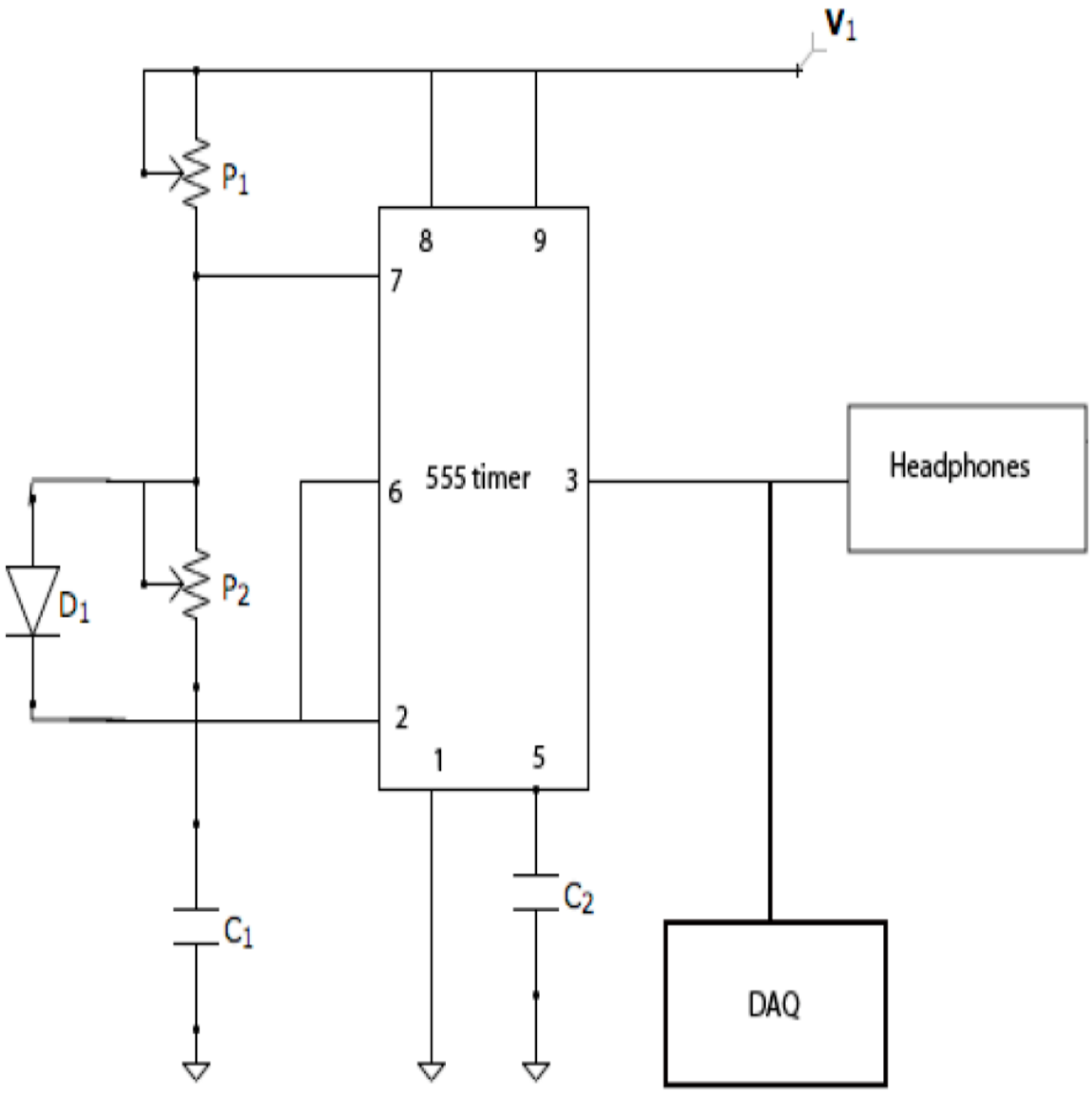

Fig. 6. Stimulus generator

Shows an astable multivibrator circuit used for click generation. P1 and P2 are used as variable resistors to allow adjustable click rates. Diode D1 is placed in parallel with P2 to achieve 50 % duty cycle. Output is recorded and used to partition the EEG into a series of responses.

Table 3: EEG amplifier component descriptions

Component	Value
R1	330 kΩ
R2	1kΩ
R3	100kΩ
R4	10kΩ
C1	1μF
C2	4.72 nF
C3	30 nF

Table 4: Stimulus generator component descriptions

Component	Value
P1	0-10kΩ
P2	0-10kΩ
C1	4.7 μF
C2	10 nF

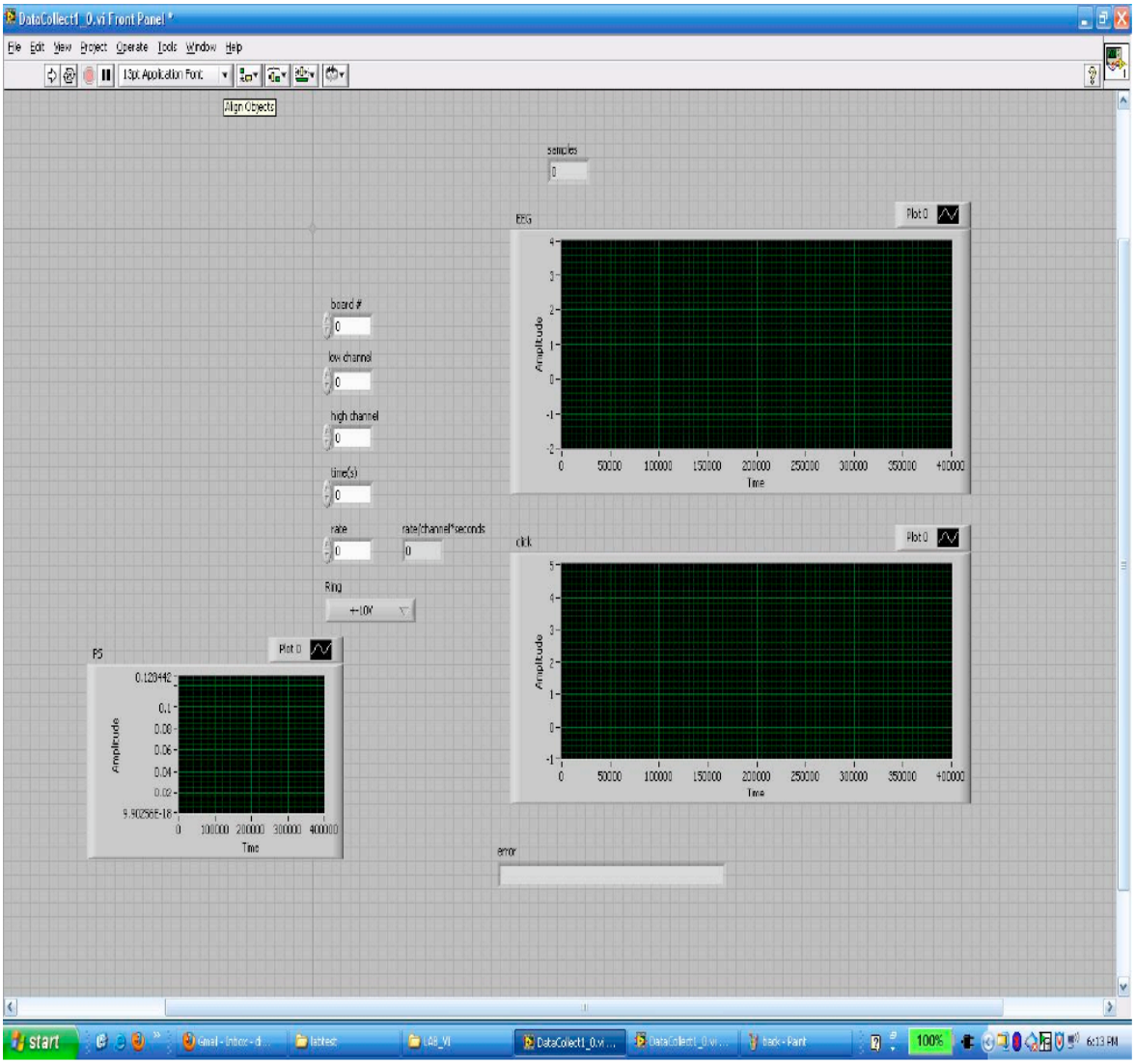

Fig. 7. Data acquisition program front panel

Shows the front panel of the graphical user interface developed in LabView. The interface allows for control of recording time and sampling rate. The three displays show the recorded EEG, recorded click, and the power spectrum of the EEG.

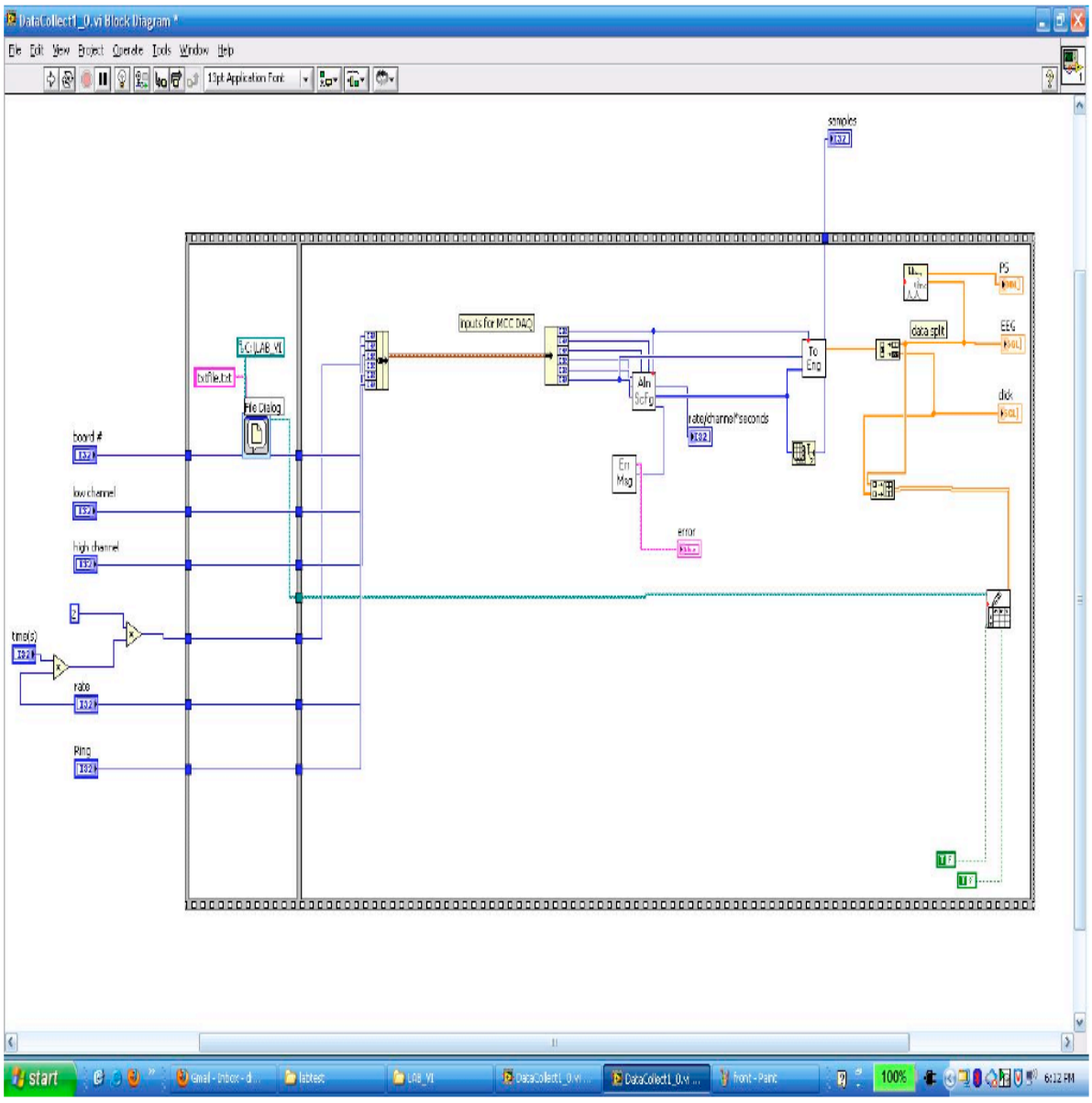

Fig. 8. Data acquisition program back panel

Shows the back panel of the graphical user interface. A sequence structure is used to first open a file and record two data channels, one corresponding to the EEG, and other to the square wave. The output is written to a text file.

Table 5: Electrode placement summary

Leads	Position
Positive	A2
Negative	Cz
Ground	Neck

Table 6: Summary of experimental trials under intervention and regular breathing, in the presence and absence of stimuli

trial #	stimulus	HV hold breath
1	yes	No
2	no	No
3	yes	Yes
4	no	Yes

3.4 Stimulus Generation and Data Recording

Audible clicks were generated using a 555 timer astable multivibrator circuit shown in figure 6, and the electrical component values for the timer circuit are listed in table 4. A 50% duty cycle square wave was used to drive the headphone speaker. $t_1 = t_2$ = click interval =100 ms. Thus, the click rate was (1/0.1s) = 10 Hz. The click and EEG data are recorder simultaneously via a custom LabVIEW program written for data acquisition shown in figures 7 and 8. Two streams of data, EEG and click generating square wave, were sampled by the MCC USB-1406FS DAQ at a rate of 10 kHz per channel.

Figure 9 shows the click and its magnitude spectra. MATLAB function sound() was used to play the square wave through MacBook pro speakers. An open source wave editor app was used to record the output. The duration of the click is approximately 0.18 ms with the prominent click frequencies located between 100 and 1000 Hz. Figure 10 shows the frequency and phase response of an FIR bandpass filter used in this study. The frequencies in the pass band correspond to frequencies of the click with the greatest magnitude.

3.5 Signal Processing and Data Analysis with MATLAB

Preprocessed data and results:

A MATLAB Fast Fourier Transform (FFT) algorithm was applied on the stimulus to identify the relevant frequency band. Data is filtered based on frequencies characteristics of the stimulus shown in figure 8.

1.) Band pass filter with l=100 Hz h=1000 Hz was used to filter the EEG.

2.) IIR comb filter was applied which had a notch at 60 Hz and all subsequent harmonics

FFT was applied on filtered data and spectral characteristics evaluated. Figures 12 a and 12 b show progression of the filtering process.

Table 7: Data acquisition set up

Channel number	2
Sampling frequency	10 kHz
Total recording time	40 s
Click rate	10 Hz

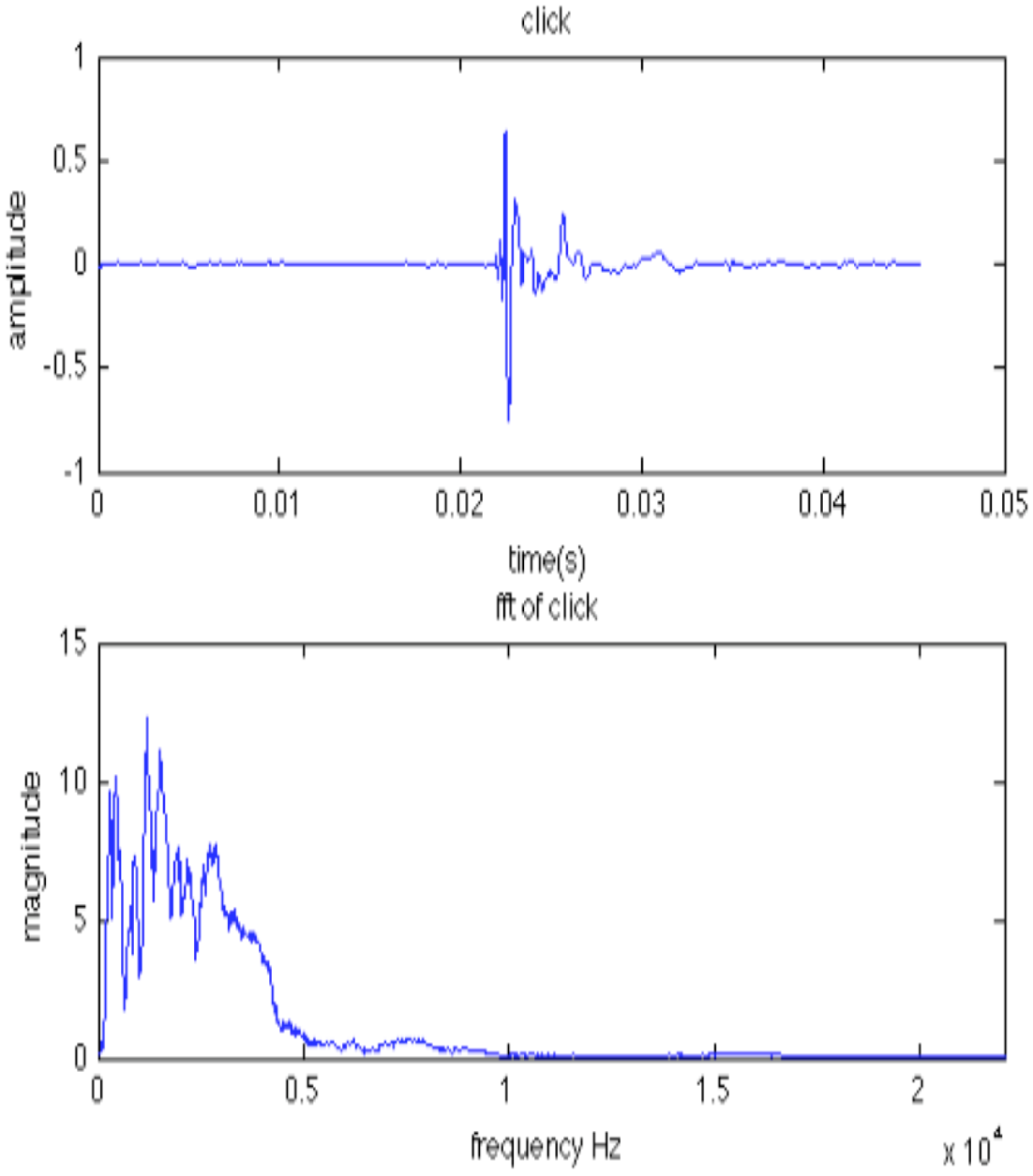

Fig. 9. Stimulus time and frequency domain plots

Shows the click and its magnitude spectra. Frequencies of interest are between 200 and 1000 Hz.

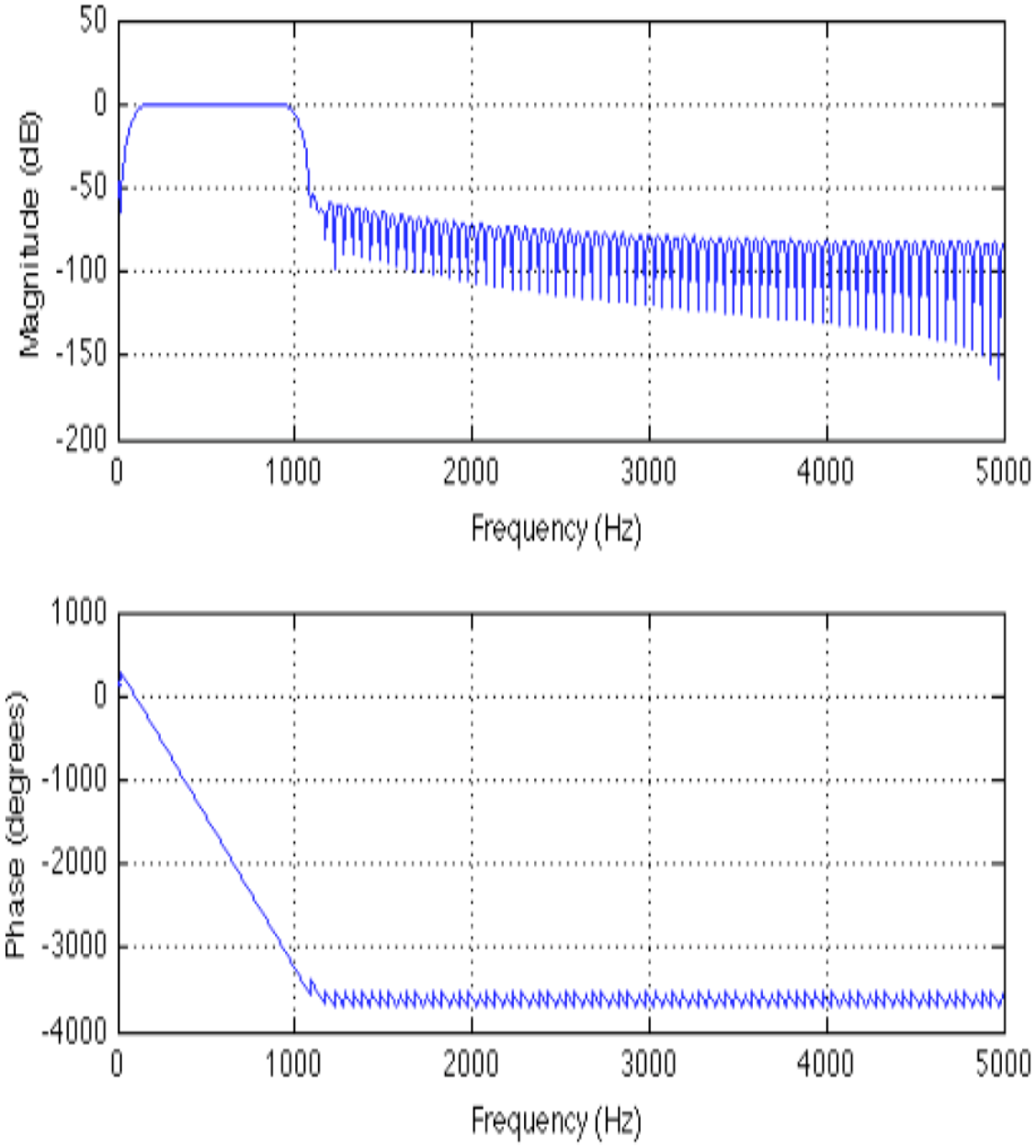

Fig. 10. Bandpass filter response

Shows the frequency and phase response of an FIR filter used in this study.

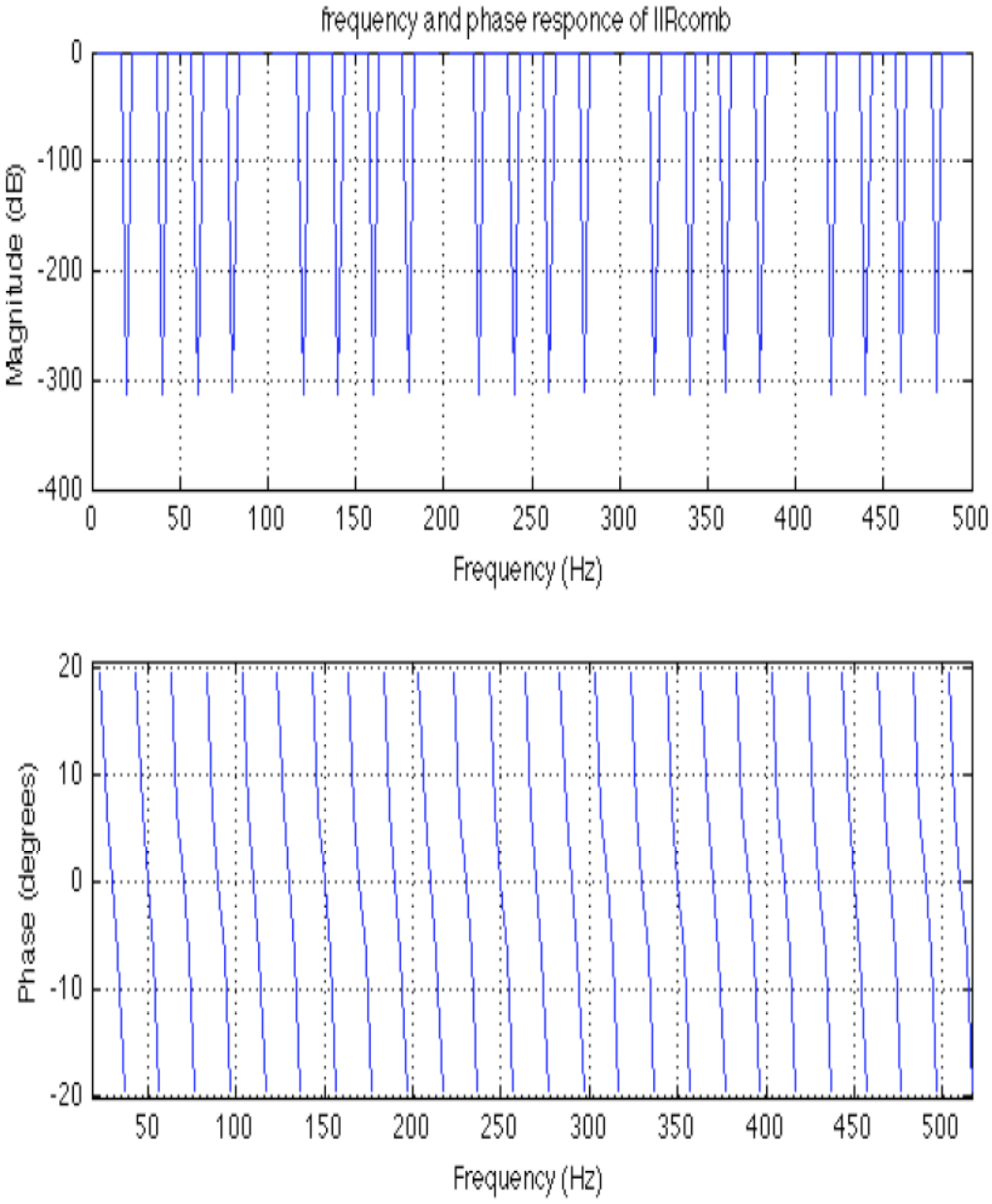

Fig. 11. IIR filter response

Shows the frequency and phase response of an IIR filter used in this study.

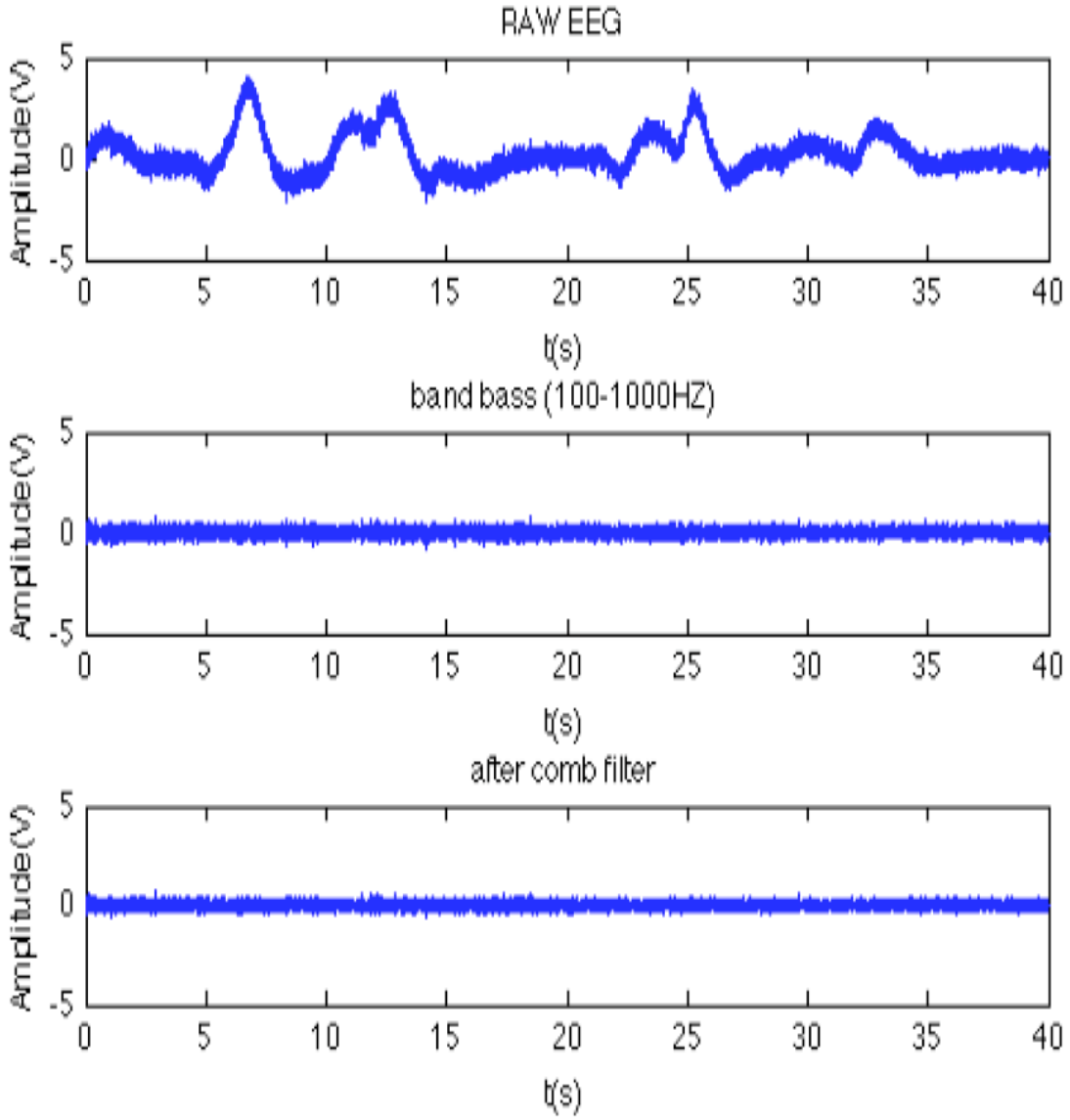

Fig. 12 a. Digital filters on EEG

Shows the two stages of digital filtering. First a bandpass filter (100-1000Hz) is applied to filter out the EEG frequency bands delta through beta. Second a comb filter is used to filter the 60 Hz noise and all harmonics.

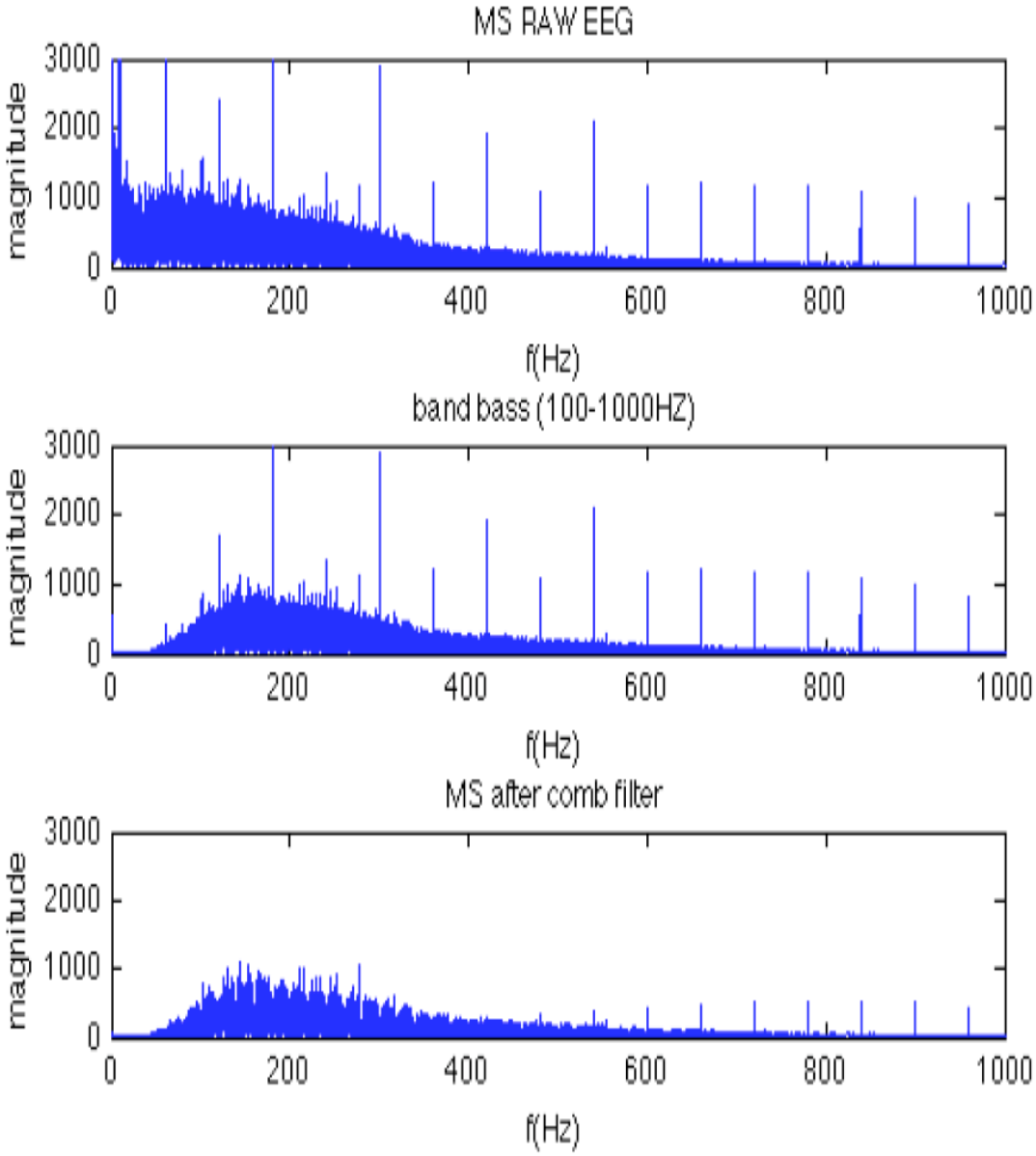

Fig. 12 b. Magnitude spectra of EEG before and after filter application

Shows the magnitude spectra of the EEG prefiltering, after 100-1000Hz bandpass filter and after comb filter.

BAEP extraction:

The auditory evoked potential is stimulated ones every 100 ms. Let *N* represent the total number of realizations per one recording. A realization is an auditory response buried in the EEG.

$$N = \frac{T_{rec}}{click\ interval} \tag{3}$$

We acquired 40s/0.1s = 400 realizations. A MATLAB function was written to partition the data into individual realizations.

Data Partitioning:

Let $x(t_{rec})$ represent the EEG data and $c(t_{rec})$ represent the square wave used in click generation. A new function $del(t_{rec})$, given in equation (4), is obtained from the absolute value of the derivative of $c(t)$ and enables representation of the clicks as a spike series with 100*ms* between spikes.

$$del(t_{rec}) = \left| \frac{d}{dt} c(t_{rec}) \right| \tag{4}$$

Let $x_n(t_{resp})$, represent the portion of the EEG signal $x(t_{rec})$ between each spike, where $n=1...N$. Each interval contains one realization. A matrix *M* is built where the rows are 100 ms portions of the signal and the columns are voltage values over time.

Latency correction (LC):

Since BAEP is highly non-stationary we do not expect that each response will appear at the same delay time after the stimulus is applied [1]. Averaging without consideration of this delay difference will cause distortions in the averaged response [15]. Latency correction is preformed by convolving each realization with the first realization, and is defined in equation 5.

$$C_n(\tau) = \sum_{n=1}^{N} x_1(t)x_n(t+\tau) \tag{5}$$

$C(\tau)$ is the correlation vector at each phase shift τ, and t is the time of the realization. The delay between the stimulus and response is reported to be approximately 2 ms, therefore τ is varied between -2 2 ms. Each realization is shifted to where the correlation is greatest. The phase shift at which the correlation is the maximum is obtained using equation 6.

$$C_{\max}(\tau_{\max}) = \max(C(\tau)) \tag{6}$$

Where τ_{max} is the phase shift, which results in the greatest correlation. If τ_{max} is positive then x_n is padded with 0's. If τ_{max} is negative then the first $|\ \tau_{max}\ |$ values are removed from x_n. The first 50 ms of x_n are considered for averaging. Vector X of latencies corrected responses is defined in Equation 7.

$$X = [x_1 x_2 x_3 \ldots x_N]^{\mathrm{T}} \tag{7}$$

Finely, the auditory response can be obtained by ensemble averaging of all realizations shown in equation 8.

$$BAEP = \frac{1}{N}\sum_{n=1}^{N} x_n^{(i)}(t_{resp}) \quad i = 1 \ldots t_{resp} \times fs \tag{8}$$

The magnitude spectra is obtained by applying the MATLAB Fast Fourier Transform (FFT) algorithm and the frequency characteristics are evaluated by taking the mean of the magnitude spectra as shown in equation 9. Mag_{ave} is the average power W is the length of signal in the frequency domain. This shows the average magnitude of the signal. The results are shown in table 3

$$Mag_{ave} = \frac{1}{W}\sum_{n=1}^{W} \left| FFT(BAEP(n)) \right| \tag{9}$$

Continuous wavelet transform (CWT):

As stated earlier the BAEP is highly non-stationary, meaning the frequency characteristics change with time. Therefore the time-frequency characteristics can be useful features for BAEP evaluation. The CWT has been readily applied to EEG signals [9]. The concept of the CWT is to use a probing function with know frequency characteristics to probe a time series function *x(t)*. The probing function (wavelet) is a symmetric damp oscillation such that the function starts at 0, reaches a peak value, then reduces back to 0 [7]. Wavelet is then translated across *x(t)* at different scales (stretched along the time axis) and correlated with *x(t)*. CWT is defined in equation 10.

$$X_{\omega}(a,b) = \frac{1}{\sqrt{a}} \int_{-\infty}^{\infty} x(t)\psi * \left(\frac{t-b}{a} \right) dt \tag{10}$$

Where a is the scale b is a translation and ψ is the wavelet. $X_{\omega}(a,b)$ is a matrix of correlation coefficients as a function of scale and translation [19]. Wavelet analysis was performed using MATLAB 2007 wavelet toolbox. Daubechies 6 (db6) wavelet was chosen due to its resolution at frequencies between 100-1000 Hz.

Principal Component Analysis (PCA)

Although the BAEP varies between each stimulus application it is still induced at a fix rate. For this reason there is a stationary aspect introduced into the EEG. This aspect can be retrieved using PCA by transforming the data into mutually orthogonal components. Because the correlation between the EEG and the stationary aspect is small we expect that some components will represent the BAEP and others will represent the EEG. We also expect that the BAEP, because of the stationary aspect, will have the greatest variance from the EEG, assuming machine noise is extracted from the signal. In this study PCA is computed using the method described in [19]. Singular Value Decomposition (SVD) is performed on latency corrected M, the matrix of responses. SVD is show in equation 11.

$$M = USV^{\mathrm{T}} \tag{11}$$

M is decomposed into left singular vector U, a singular matrix of eigenvalues S, and right singular vector V. V represents the principal components and the eigenvalues in S

represent the variances in each component [19]. The eigenvalues are arranged from greatest to smallest and are on the diagonal of S such that $S_{11} > S_{22} > S_{33} > \ldots S_{nn}$. Each column of V is then scaled by its corresponding eigenvalue. Since the BAEP should have the highest variance with the EEG it can be represented by the first principal component.

Chapter 4. RESULTS

4.1 Raw EEG Data

The preprocessed EEGs and the magnitude spectrum are shown in figures 13-18a. Two features can be observed from looking at the raw EEG. First, the EEG trials corresponding to HV and oxygen reduction show more fluctuation than the ones where the oxygen supply is undisturbed. This is also apparent in the magnitude spectra shown in figures 13-18b. Second, the magnitude spectra for trials 3 and 4 show a magnitude increase between 300 and 1000 Hz. The EEG signal is broadband with frequencies between 0 and 1000 Hz, which is expected since the active filter in the circuit illustrated in figure 4 had a lowpass cutoff frequency at 1000 Hz. 60 Hz power supply noise and the reproduction at every harmonic can be identified in the spectra. The EEG signal in trial 3 from data set 4 (figure 18a) saturated at 5 seconds after HV. The DAQ used for analog to digital conversion is limited to voltage inputs between -10 and 10 Volts and was not able to capture the high amplitude depolarization.

4.2 Raw Data and Signal Enhancement

The BAEP were initially extracted with out the use of digital filters and using only ensemble average shown in equations 1 and 2. This analysis was performed to see if any BAEP features can be determined directly from the raw average of responses.

The raw average data show increase in activity trial 3, however it is difficult to analyze the response due the distortions caused by the ensemble average. To enhance BAEP features, LC defined in equations 5 and 6 is applied. Figure 20 shows BAEPs extracted using ensemble average after the application of LC.

After an application of LC shown in figures 20 and 21 the detail of the BAEP start to become more apparent in trials 3. However in the remaining trials a narrow-band signal around 200 Hz is observed in the magnitude spectra. The periodicity in these signals leads to the assumption that it is an artifact of the latency correction process and can be considered as noise. To further examine this signal a CWT is performed in order to assess its stationarity.

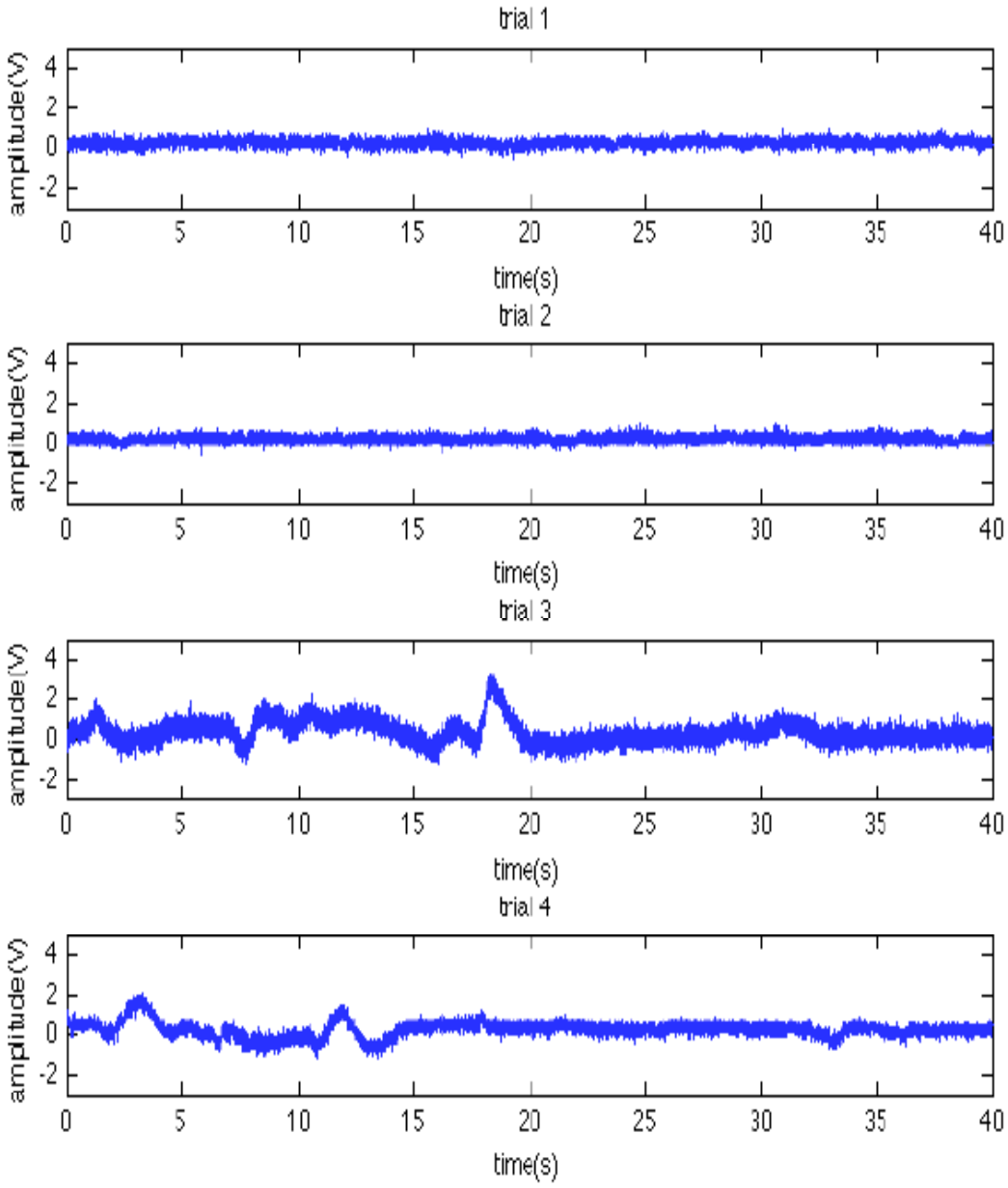

Fig. 13 a. EEG amplitude vs time plots for data set 1

Shows the four trials of EEG data set 1 from first recording session

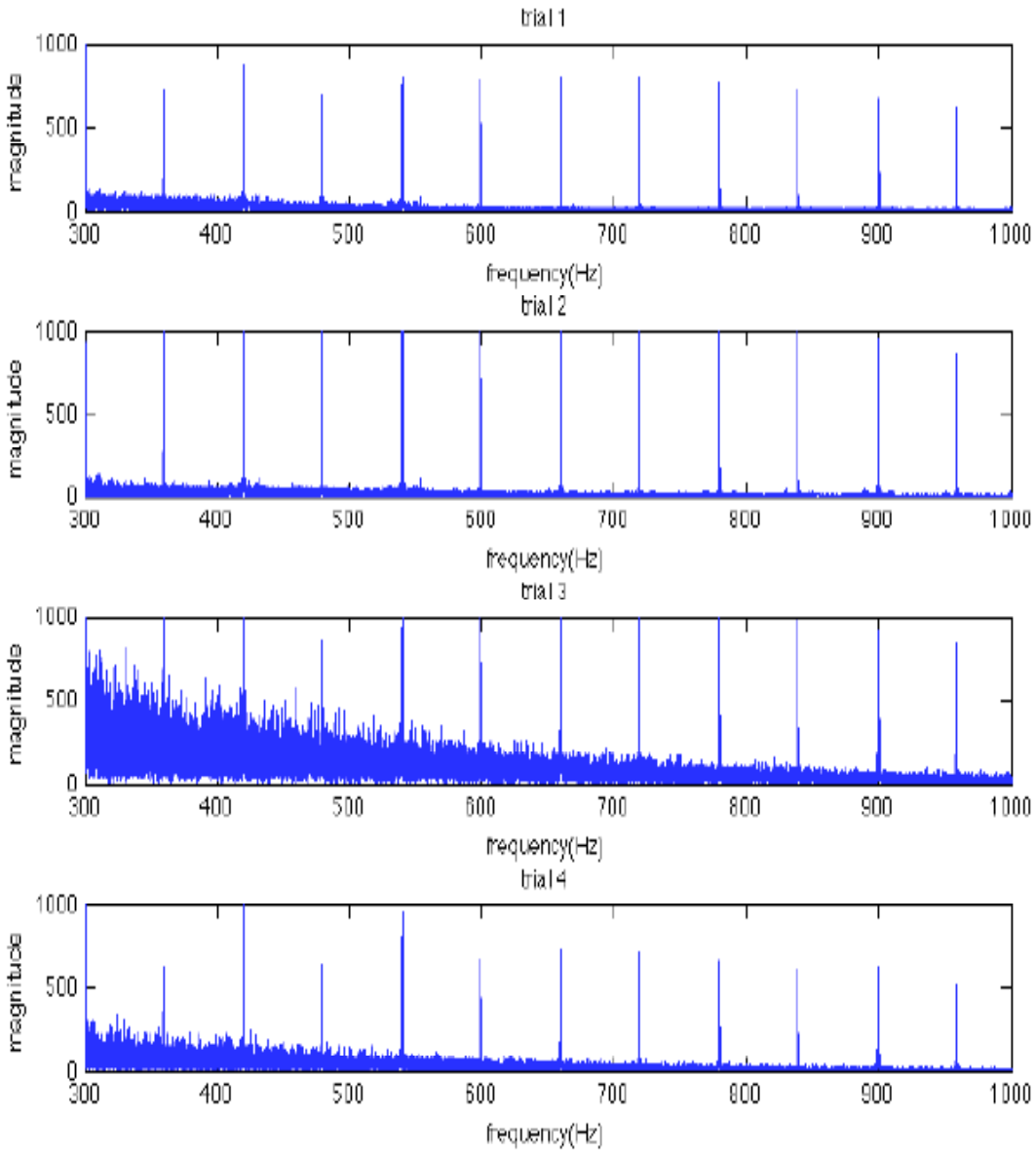

Fig. 13 b. EEG magnitude vs frequency plots for data set 1

Shows the magnitude spectral of the four trials from data set 1 from the first recording session

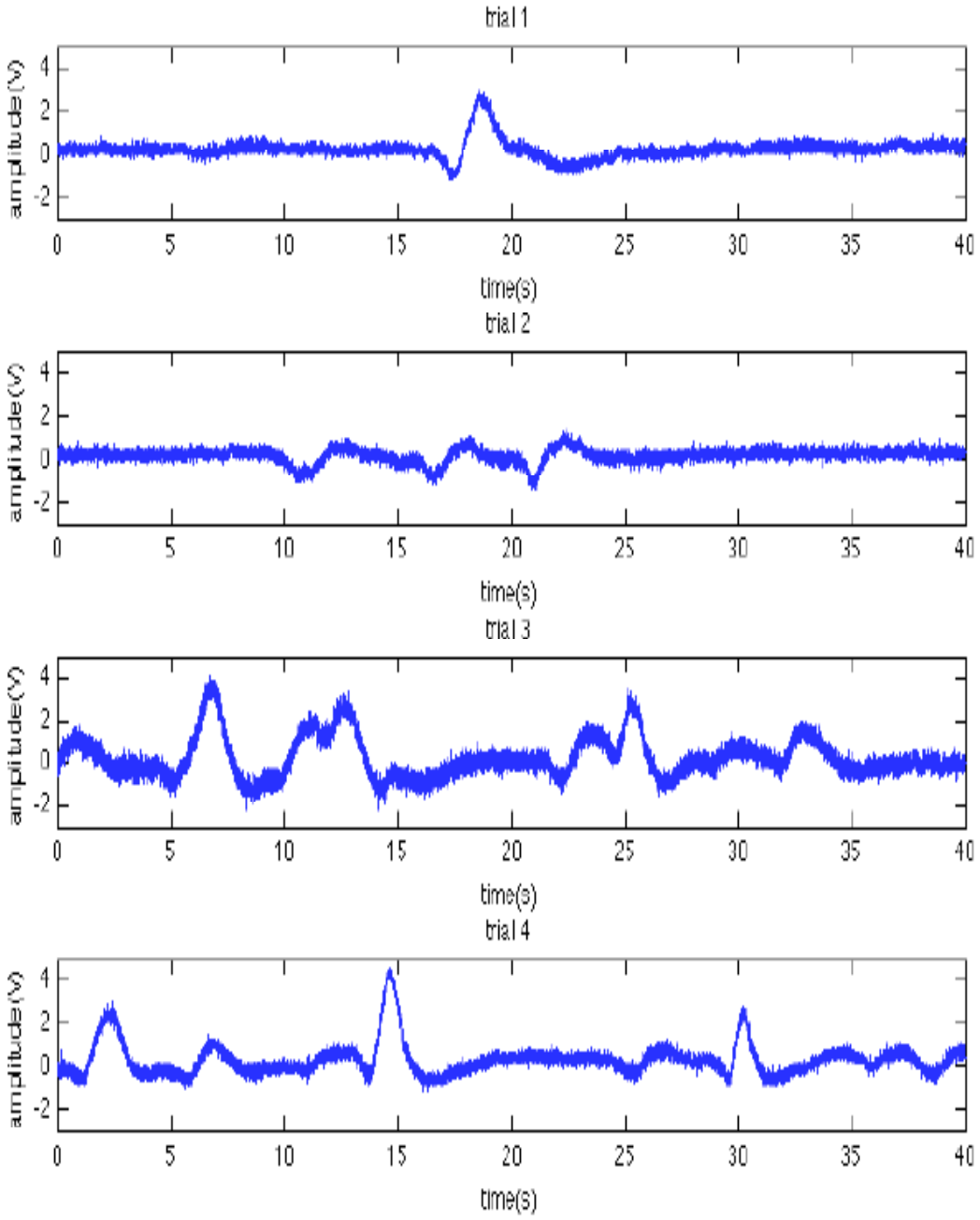

Fig. 14 a. EEG amplitude vs time plots for data set 2

Shows the four trials of EEG data set 2 from first recording session

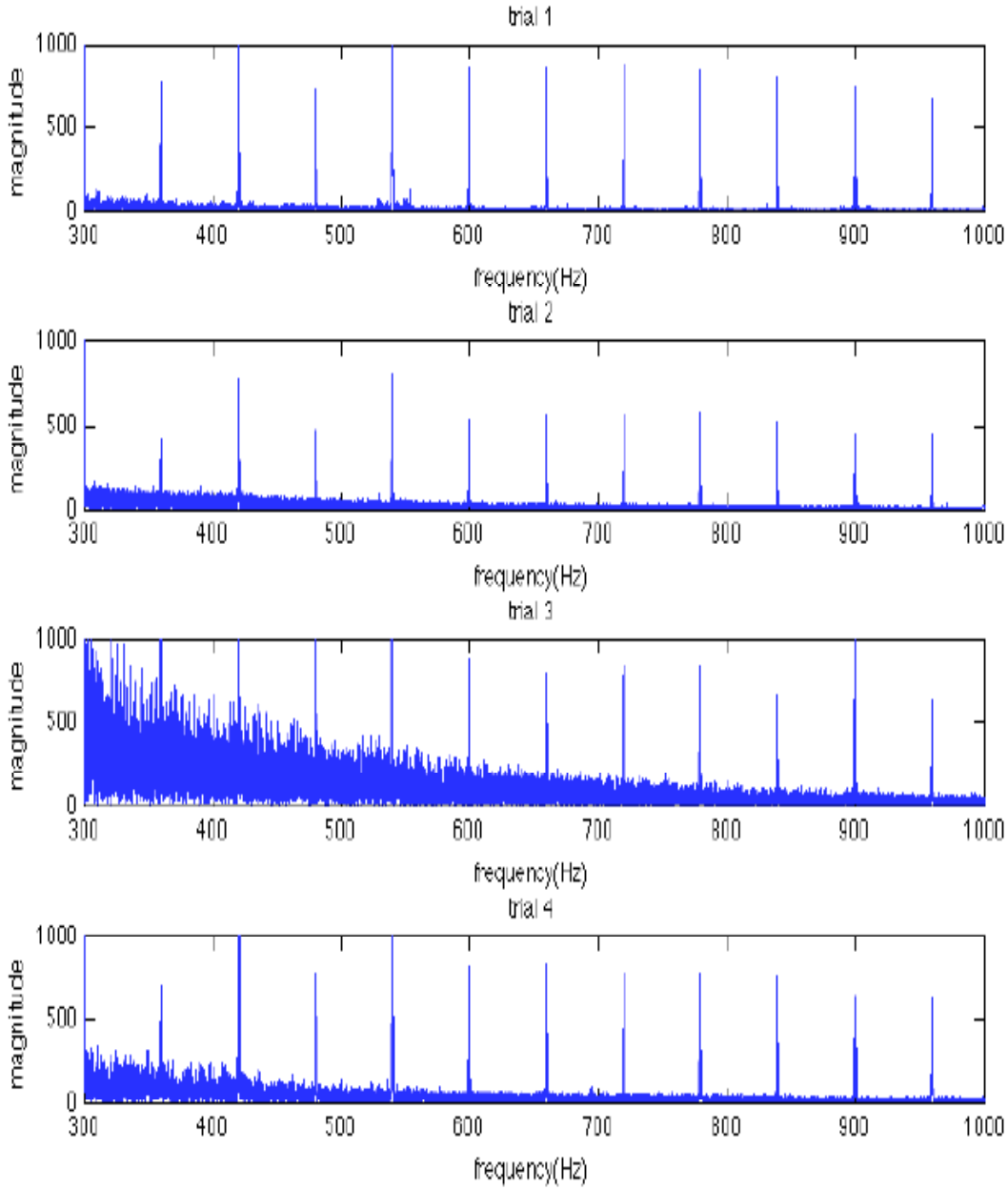

Fig. 14 b. EEG magnitude vs frequency plots for data set 2

Shows the magnitude spectral of the four trials from data set 2 from the first recording session.

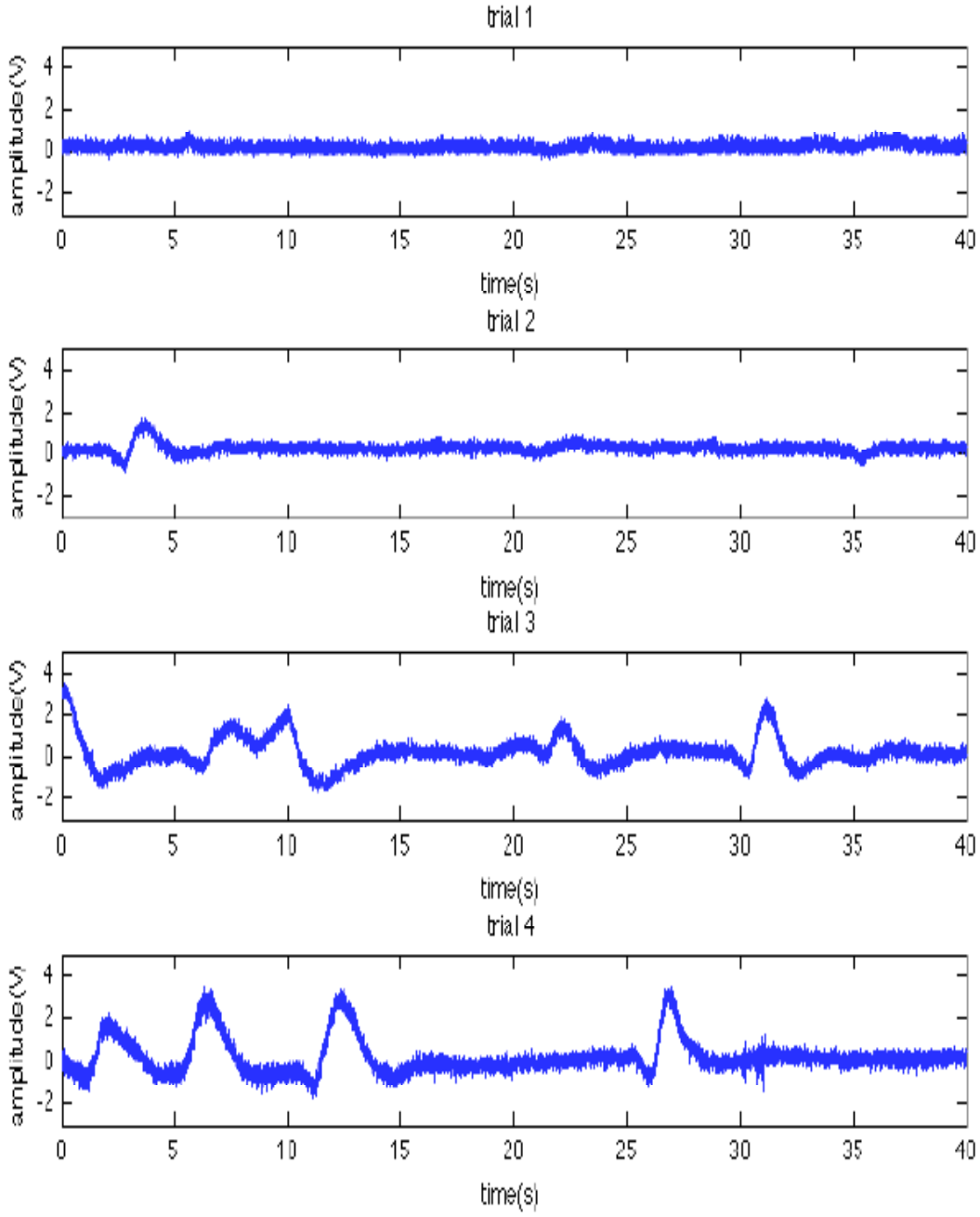

Fig. 15 a. EEG amplitude vs time plots of data set 3

Shows the four trials of EEG data set 3 from first recording session

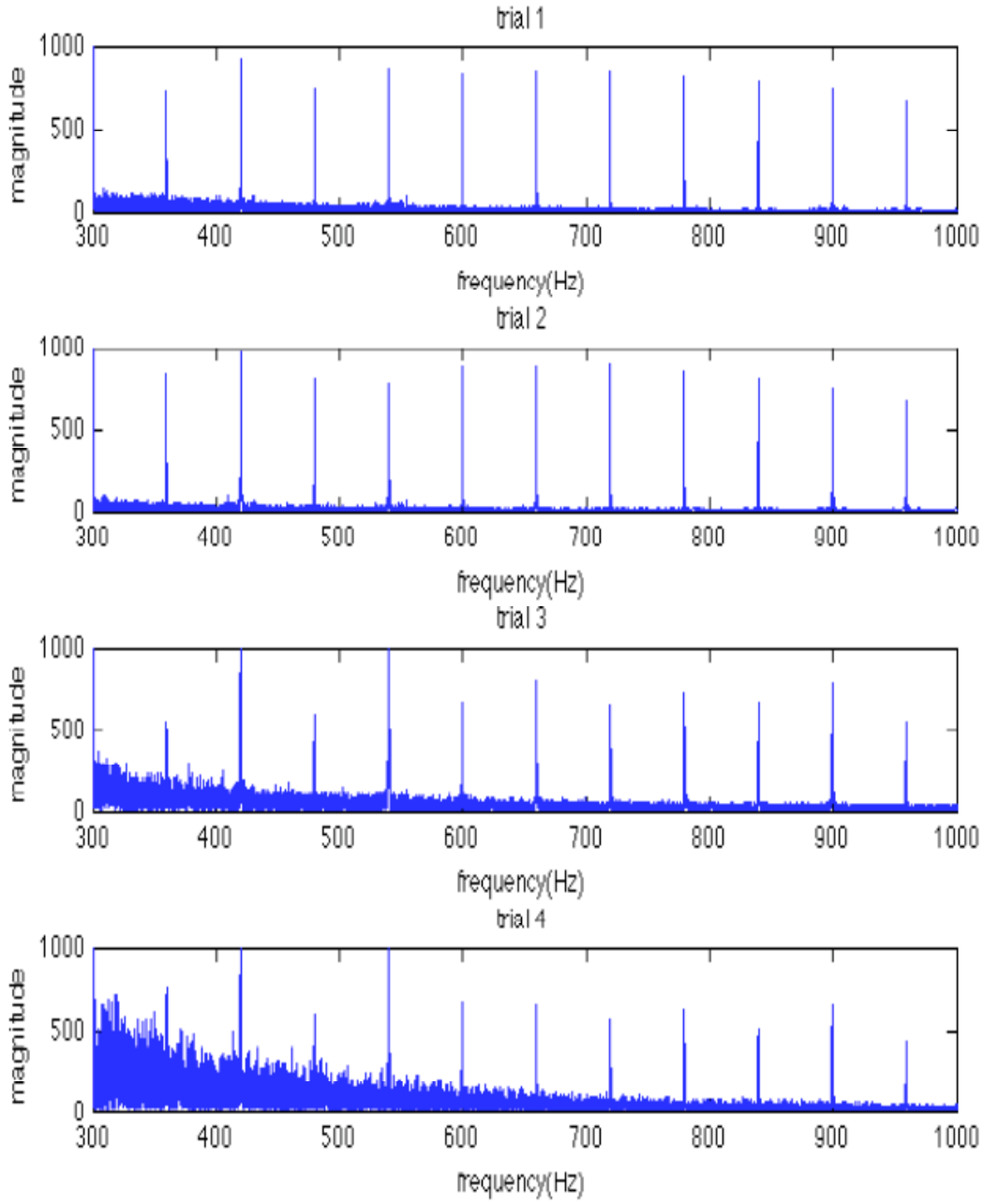

Fig. 15 b. EEG magnitude vs frequency plots of data set 3

Shows the magnitude spectral of the four trials from data set 3 from the first recording session

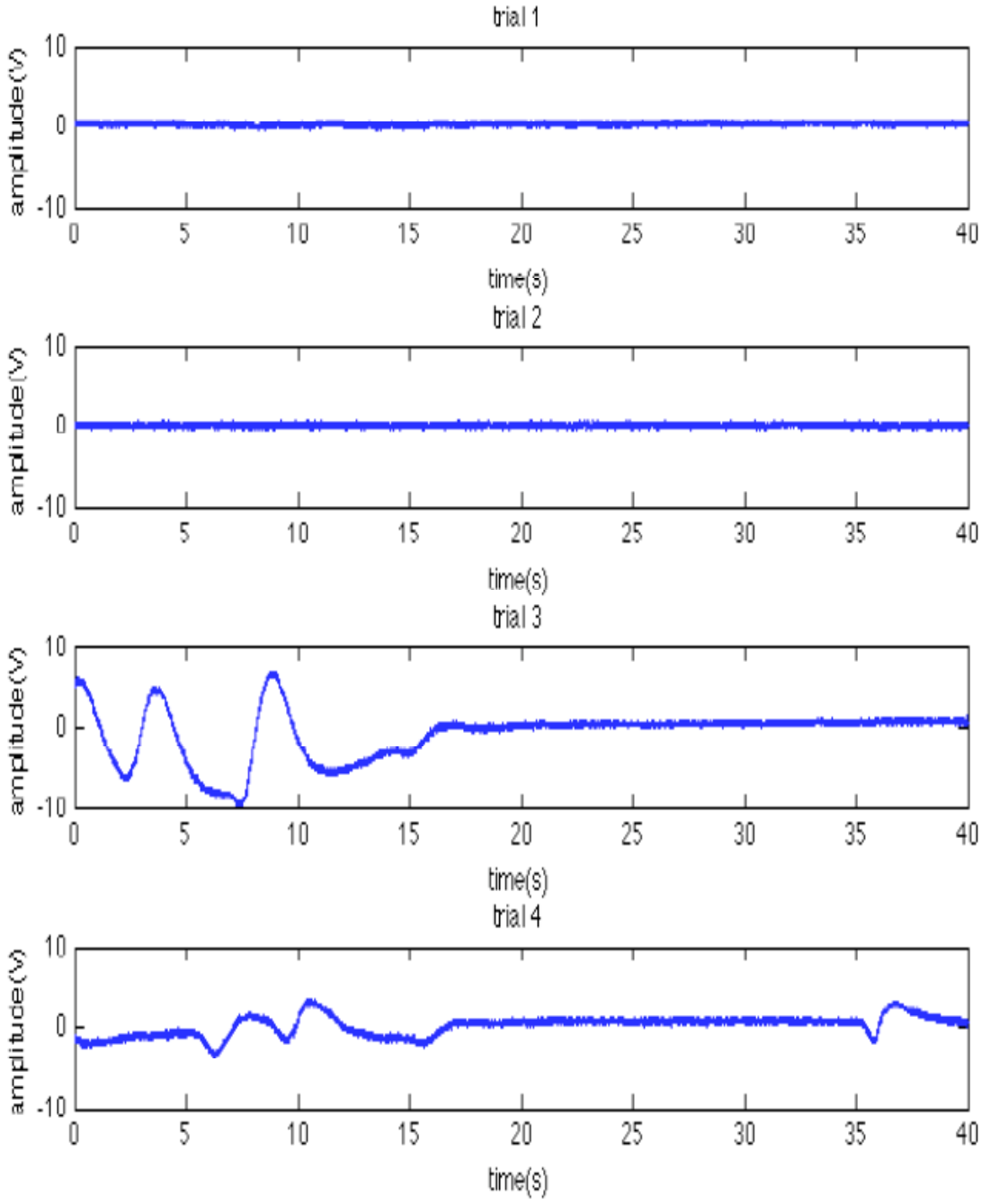

Fig. 16 a. EEG amplitude vs time plots for data set 4

Shows the four trials of EEG data set 4 from second recording session

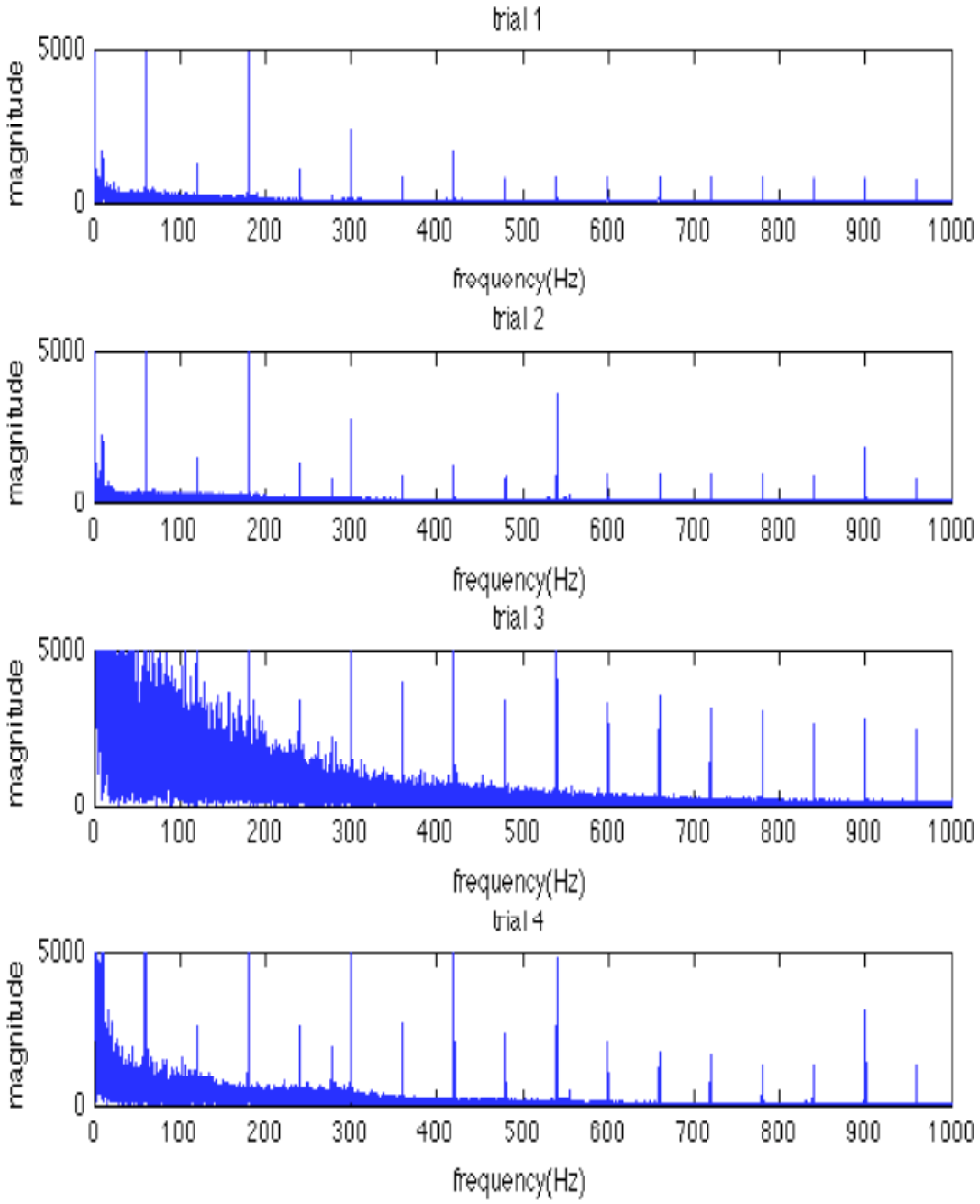

Fig. 16 b. EEG magnitude vs frequency plots for data set 4

Shows the magnitude spectral of the four trials from data set 4 from the second recording session.

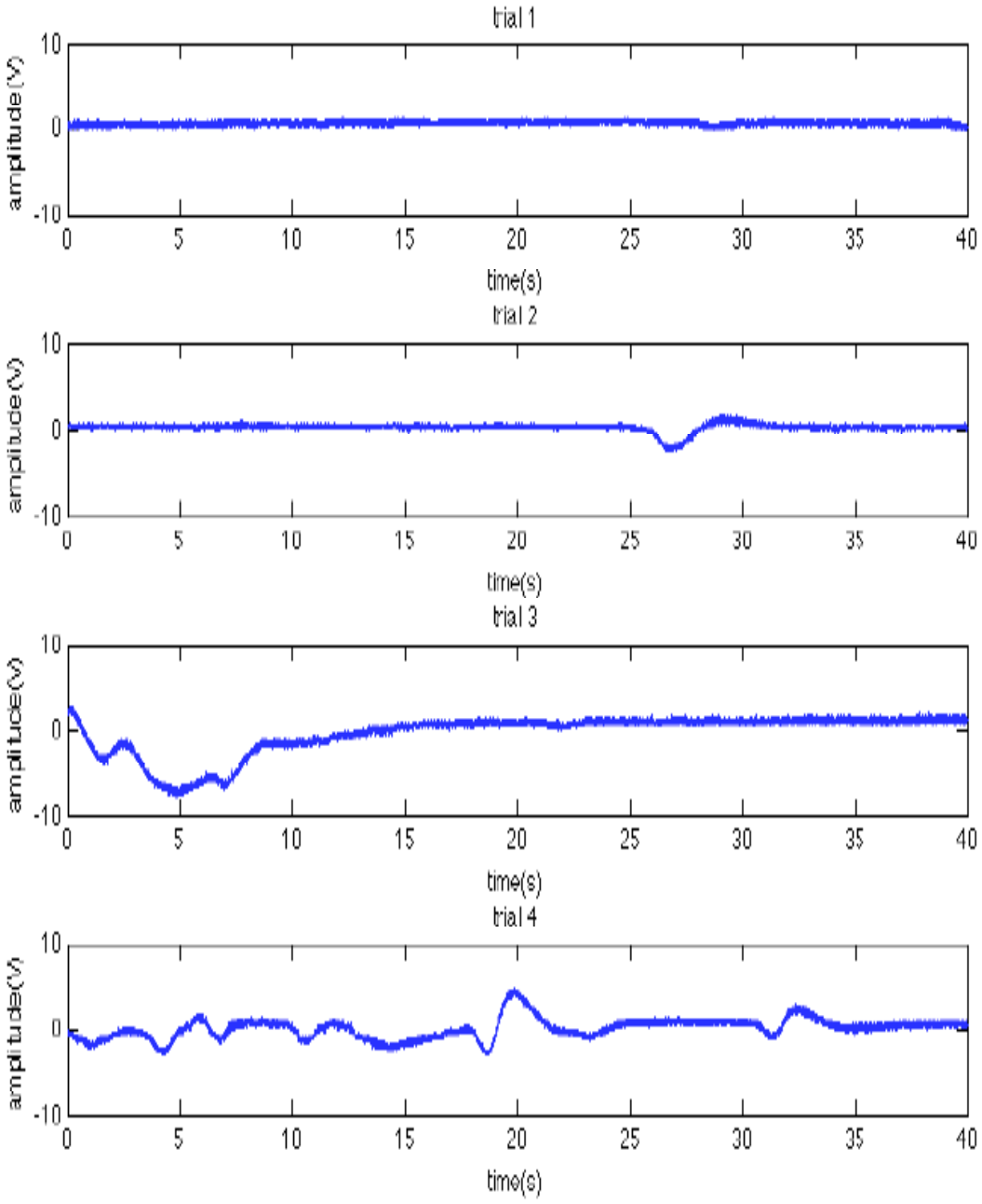

Fig. 17 a. EEG amplitude vs time plots for data set 5

Shows the four trials of EEG data set 5 from second recording session

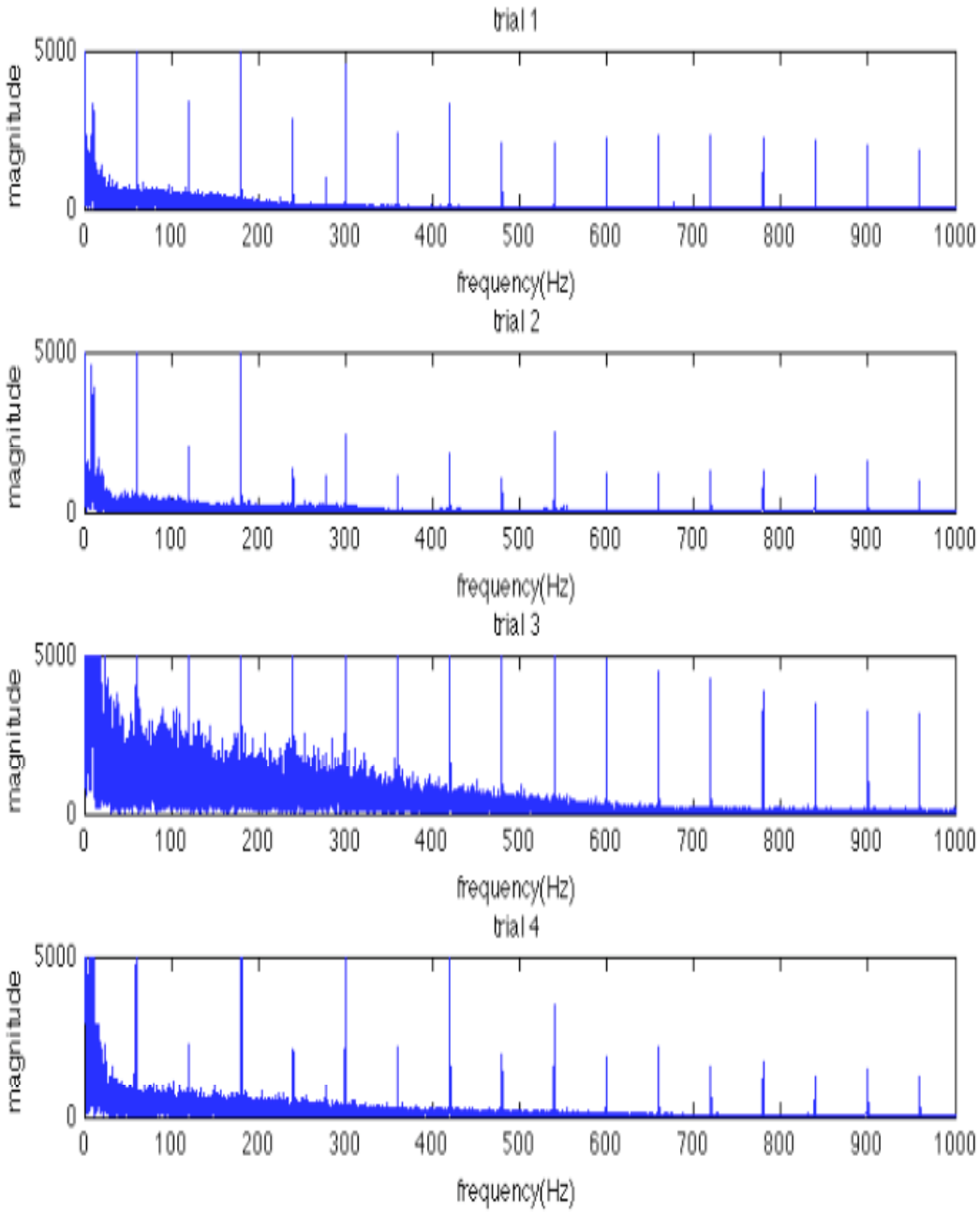

Fig. 17 b. EEG magnitude vs frequency plots for data set 5

Shows the magnitude spectral of the four trials from data set 5 from the second recording session.

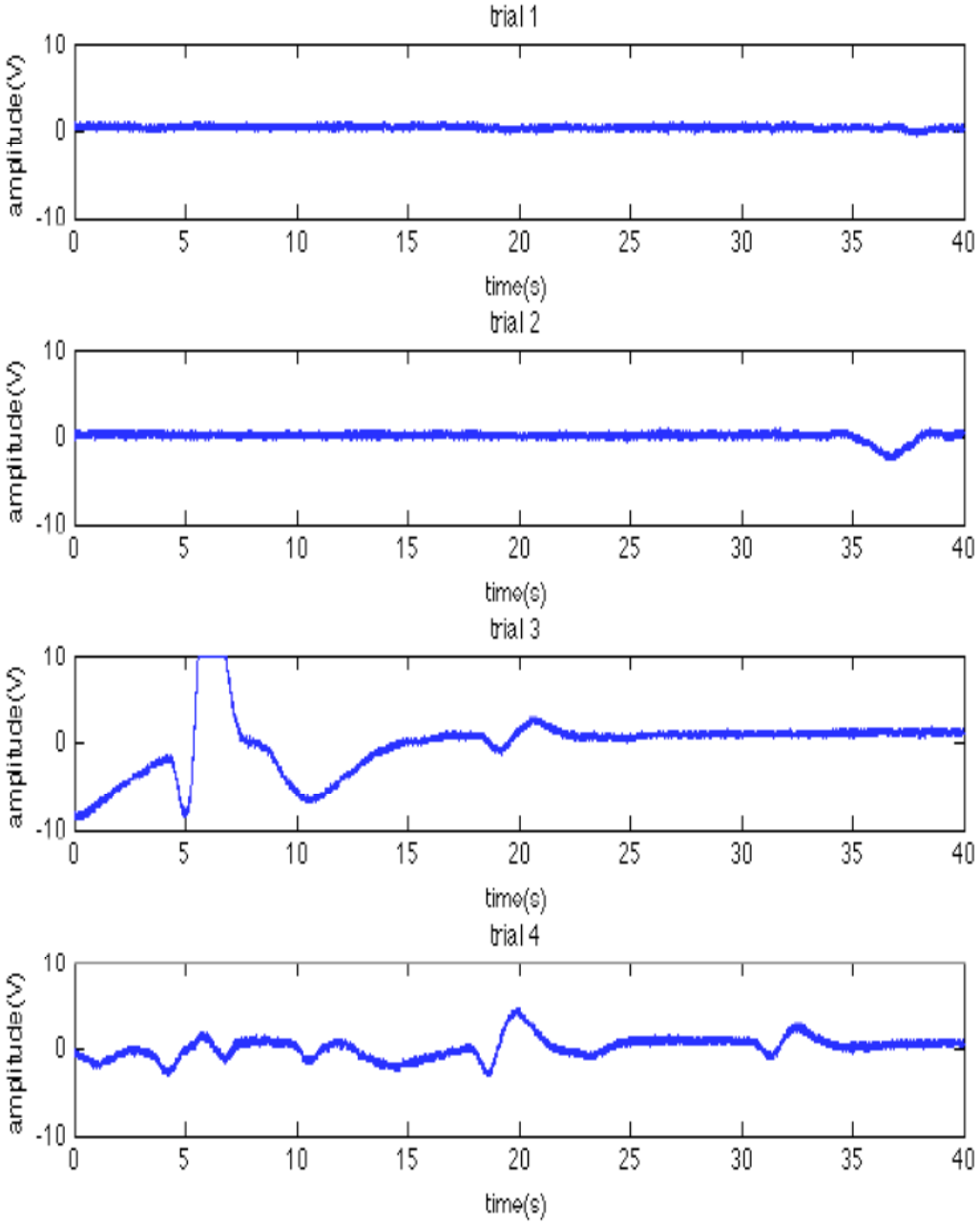

Fig. 18 a. EEG amplitude vs time plots for data set 6

Shows the four trials of EEG data set 6 from second recording session.

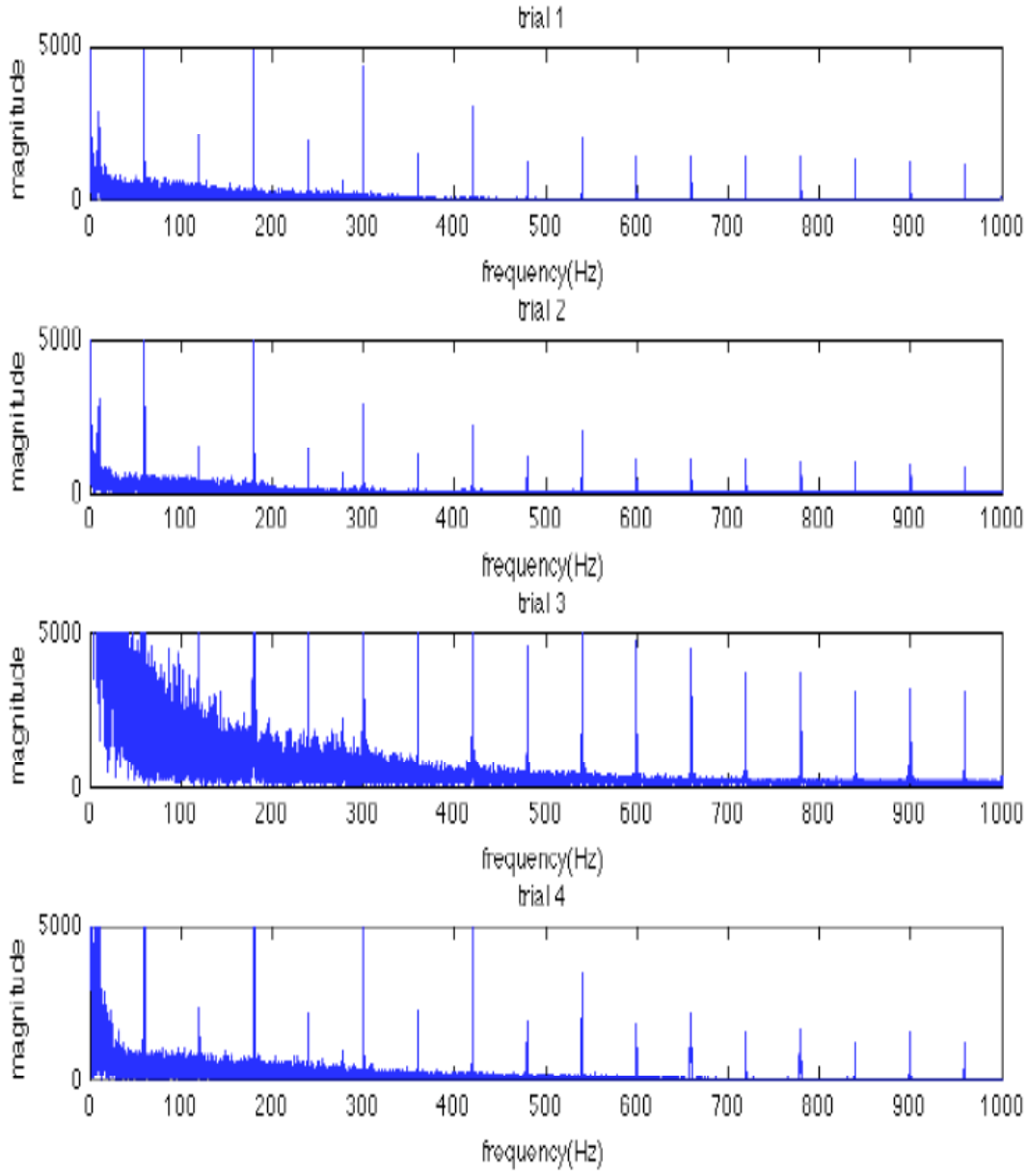

Fig. 18 b. EEG magnitude vs frequency plots for data set 6

Shows the magnitude spectral of the four trials from data set 6 from the second recording session

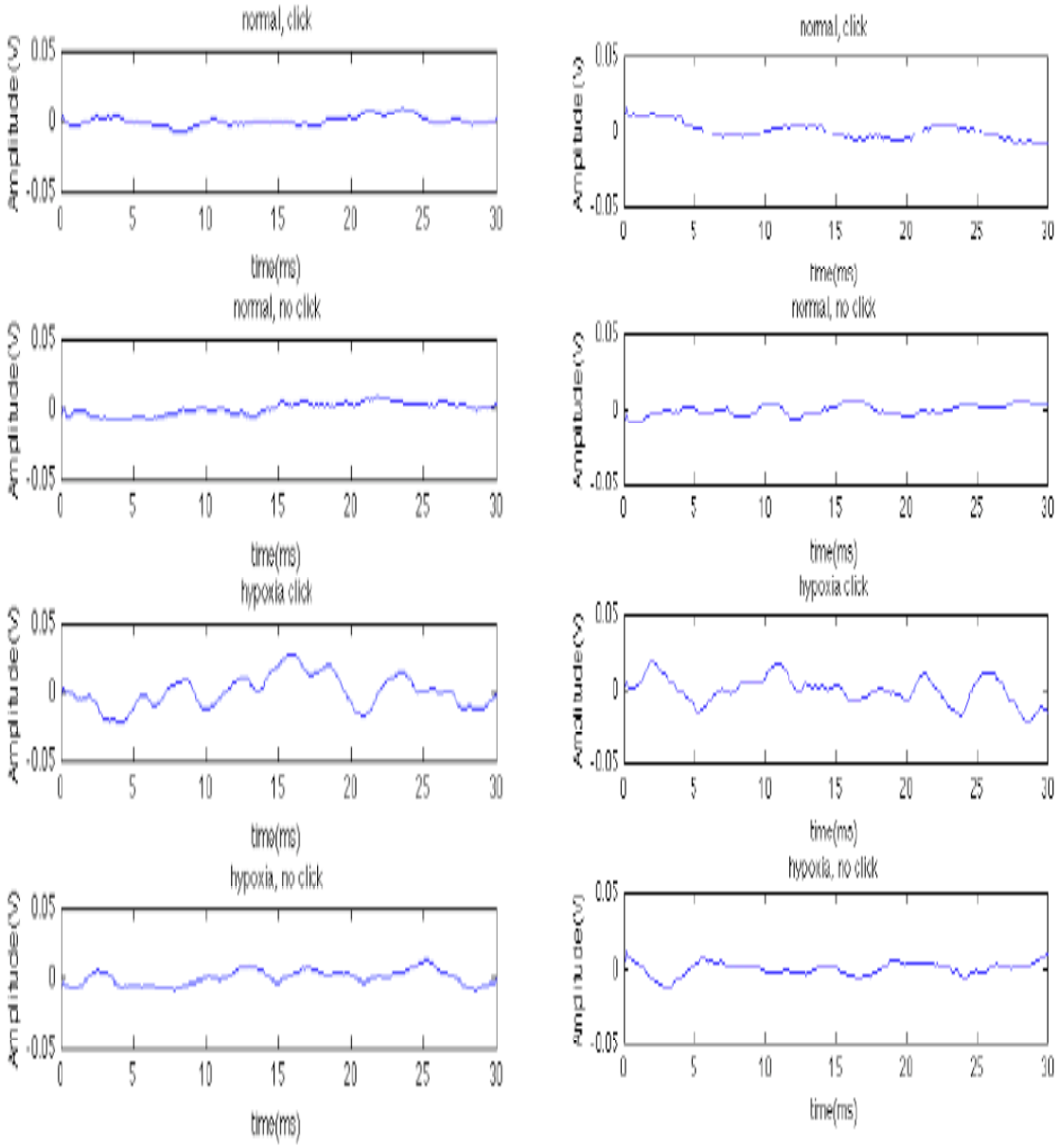

Fig. 19. Raw average for data set 1 and 2

Shows ensemble average of raw data. BAEP features are observed mostly in the trial where the stimulus is applied and hypoxia is induced.

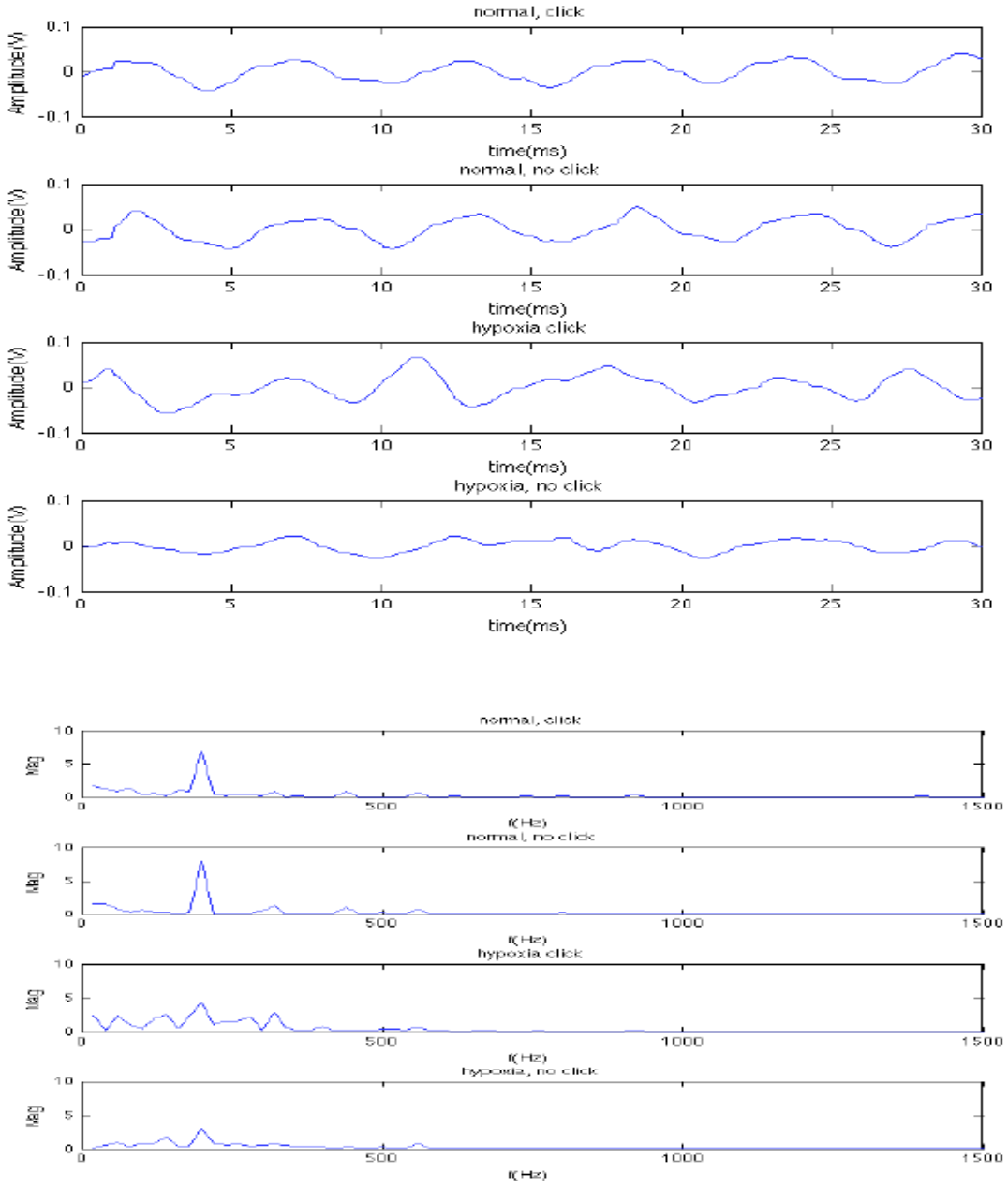

Fig. 20. BAEP time and frequency domain plots after LC application for data set 1

Top plots show BAEP extracted using LC, the bottom plots show the magnitude spectra of the BAEP.

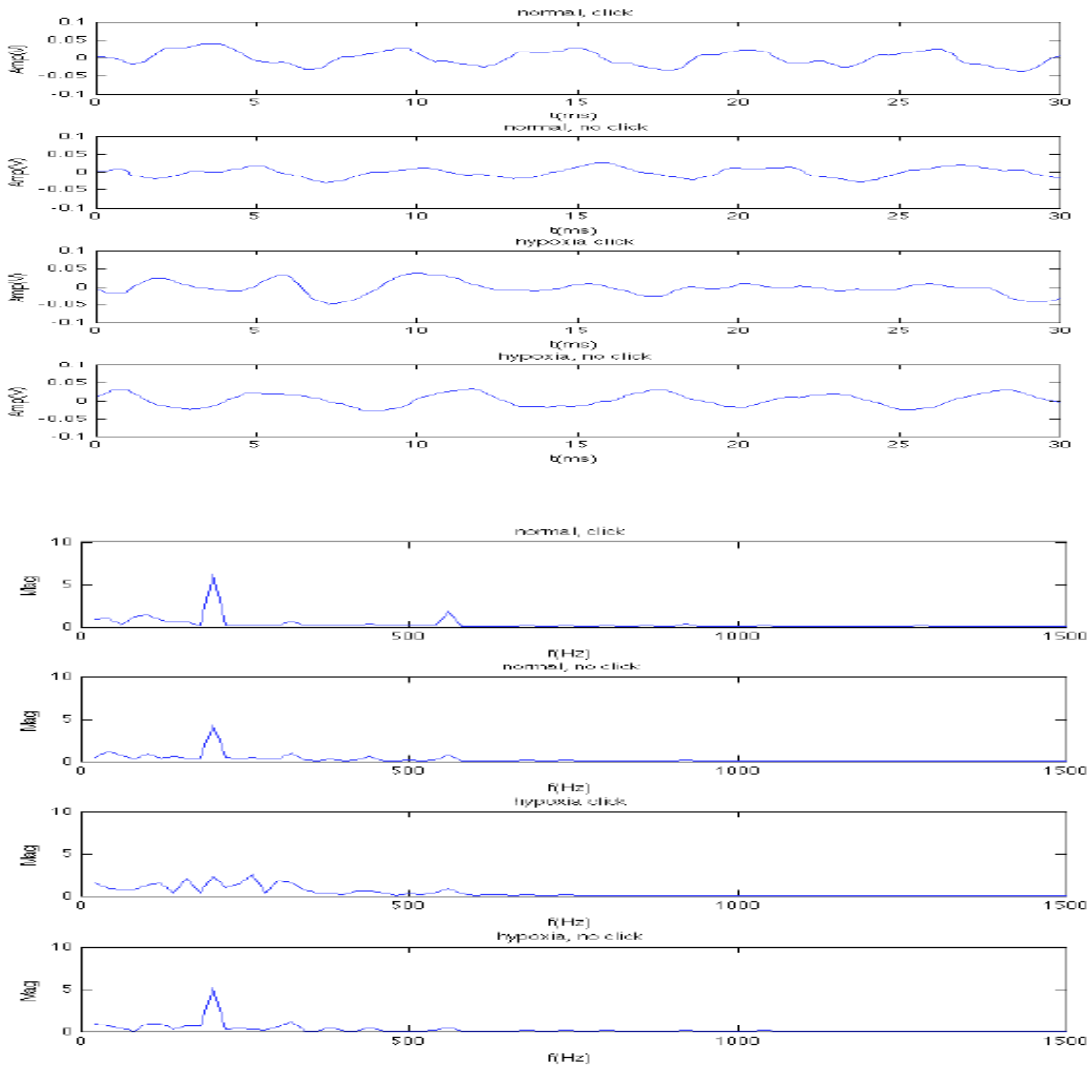

Fig. 21. BAEP time and frequency domain plots after LC application for data set 2

Top plots show BAEPs after LC, and the bottom plots show the magnitude spectra for data set 2.

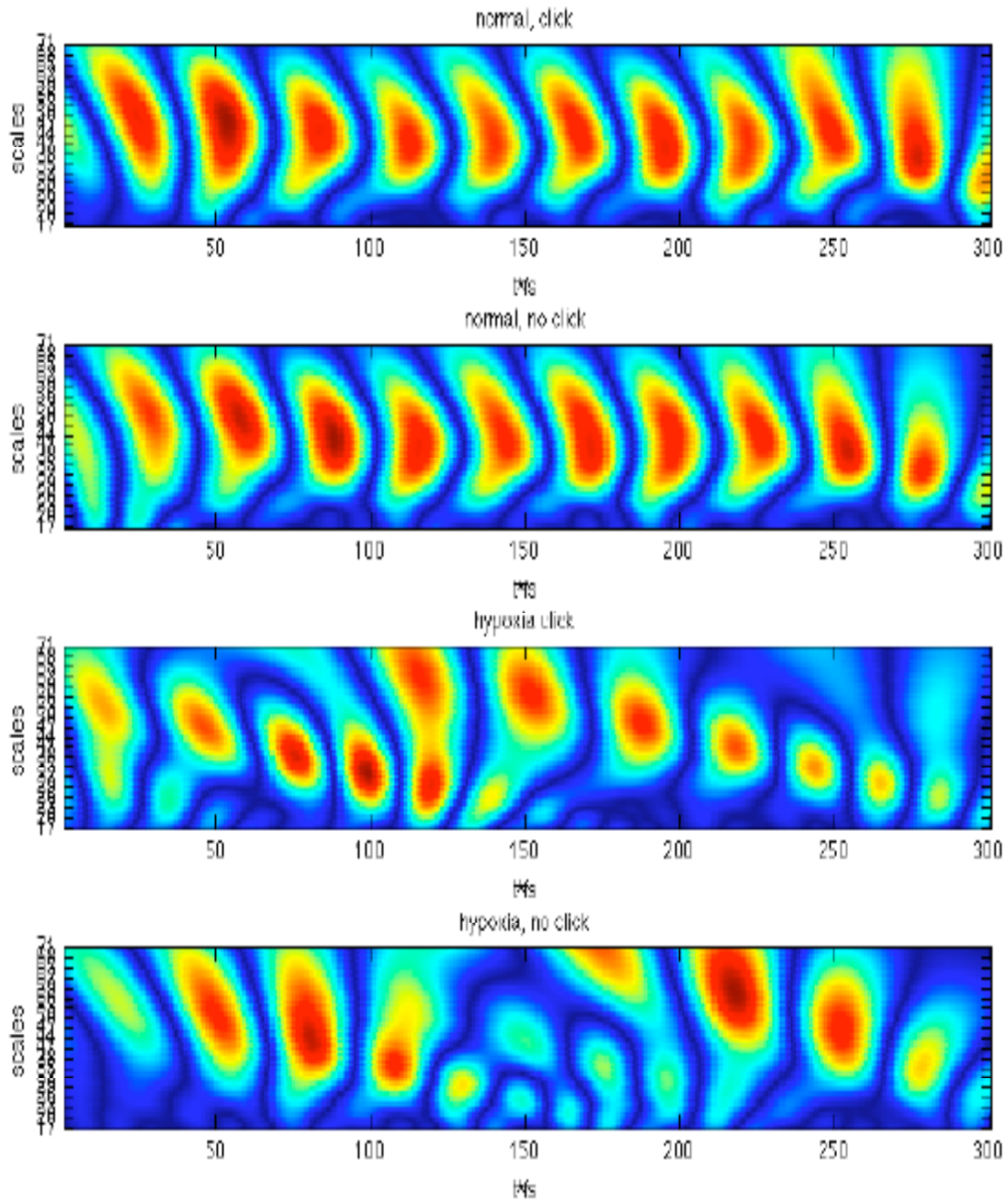

Fig. 22. CWT plots of BAEP after application of LC for data set 1

Shows CWT plots for data set 1. Scales correspond to frequencies between 100 and 1000 Hz

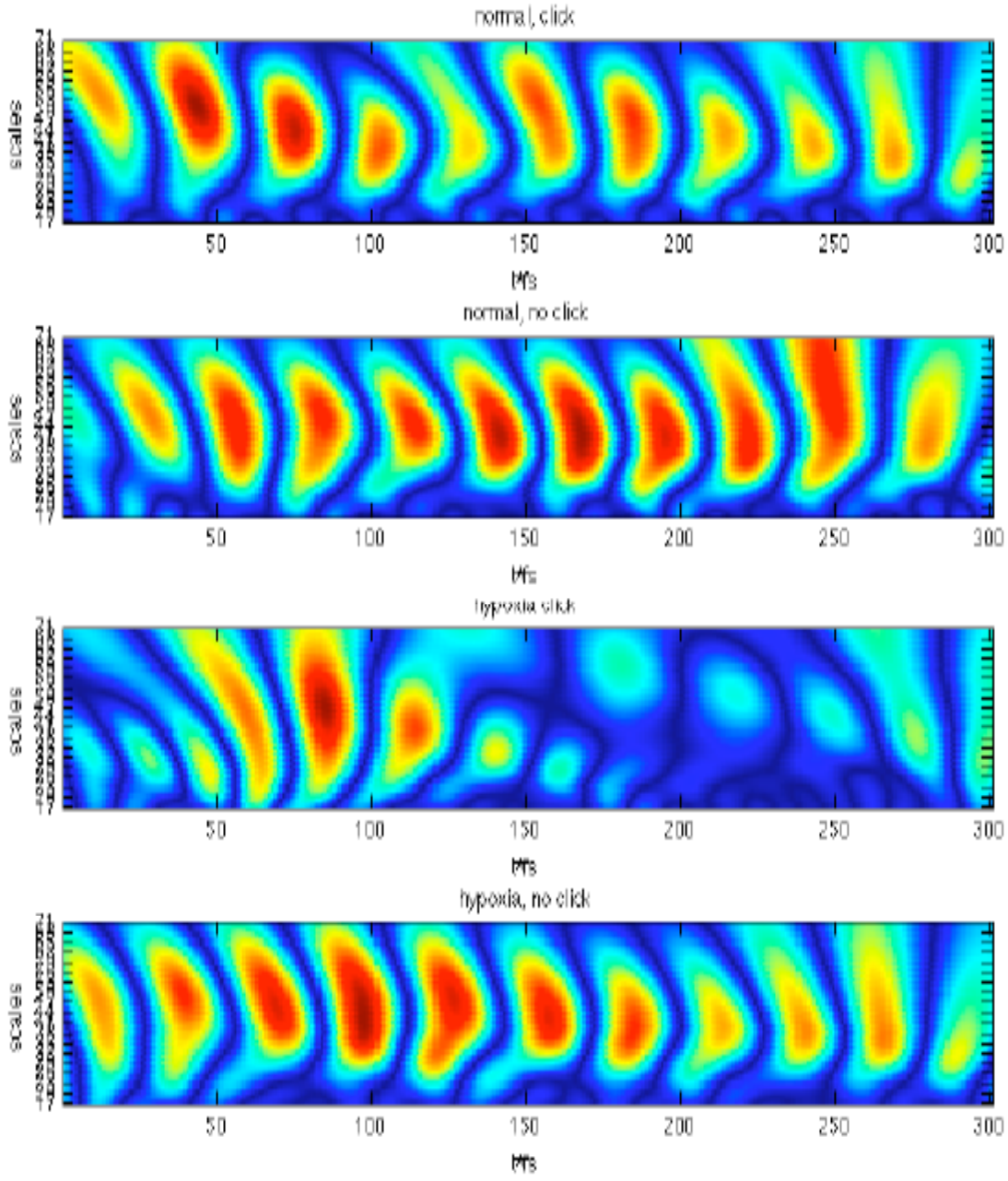

Fig. 23. CWT plots of BAEP after application of LC for data set 2

Shows CWT plots for data set 2. Scales correspond to frequencies between 100 and 1000 Hz

4.3 Processed Data

From figures 22 and 23 time frequency characteristics of the BAEP can be examined. The trials where hypoxia is not induced show a constant energy between 100-1000 Hz over the duration of the response, confirming that the waveform is an artifact of the LC. In the hypoxia trials the CWT plots show change in energy over time, which is characteristic of the dynamic activity of the brain. Two remove the stationarity from all signals a comb filter shown in figure 11. Finally, the band pass filter in figure 10 is applied in order to analyze the response in the frequency range of the BAEP and the stimulus.

Figures 24-29 a show the processed averaged signals. The magnitude spectra of the averaged response is shown in figures 24-29 b. Data in table 8 shows that the average magnitude obtained using equation 9. Average power was greater in the trials where the subject hyperventilated and held his breath then in trials where the subject was breathing normally. The average power for trial 3 for both sessions is greater then all other trials except in session 1 in data set 3. The results from the CWT plots show the majority of activity in the third trial for the majority of data sets occur 15 ms after the response. This activity falls within the time frame of MLR as shown in figure 4. From figure 27 it can be seen that the responses generated with PCA are strongly correlated with their averaged counterparts. Figure 27a shows trial 3 responses from data sets 1-3 and Figure 27b shows trial 3 responses from data sets 4-6. Data sets 5 and 6 show an anti-correlation between the averaged response and the PCA response. Trial 3 from the third and sixth data set varies from the trial 3 in the other data sets as shown in table 8. CWT shows that in these two trials the energy is greater in the first 10 ms of the response.

4.6 Oxygen Monitoring

To insure that hypoxia was induced a custom infrared spectroscopy device (NIR), in conjunction with the BAEP monitor, was used to simultaneously monitor the EEG and brain oxygen concentration. The device detects absorption of near infrared light in the 780 and 870 nm range [12]. Oxygen bound hemoglobin absorbs light at the lower end of NIR range (approximately 700nm), while free hemoglobin absorbs light at around 800 nm [13]. The NIR probe was places on the left side of the forehead with electrodes positions as described in table 5. MCC USB-1608FS DAQ was used of analog to digital conversion. LABVIEW was used to record the data. The onset of hypoxia can be seen in trials 3 and 4 from the NIR data. The corresponding BAEP can be seen in figure 38.

Table 8 BAEP average magnitude

a.)

2/18/11	data set 1	data set 2	Data set 3
Trial 1	0.0665	0.0418	0.0535
Trial 2	0.0578	0.0723	0.0453
Trial 3	0.2086	0.1771	0.0739
Trial 4	0.1063	0.0813	0.1339

b.)

2/25/11	data set 1	data set 2	Data set 2
Trial 1	0.062	0.0431	0.0698
Trial 2	0.066	0.0457	0.0673
Trial 3	0.0929	0.0853	0.133
Trial 4	0.0672	0.0737	0.0786

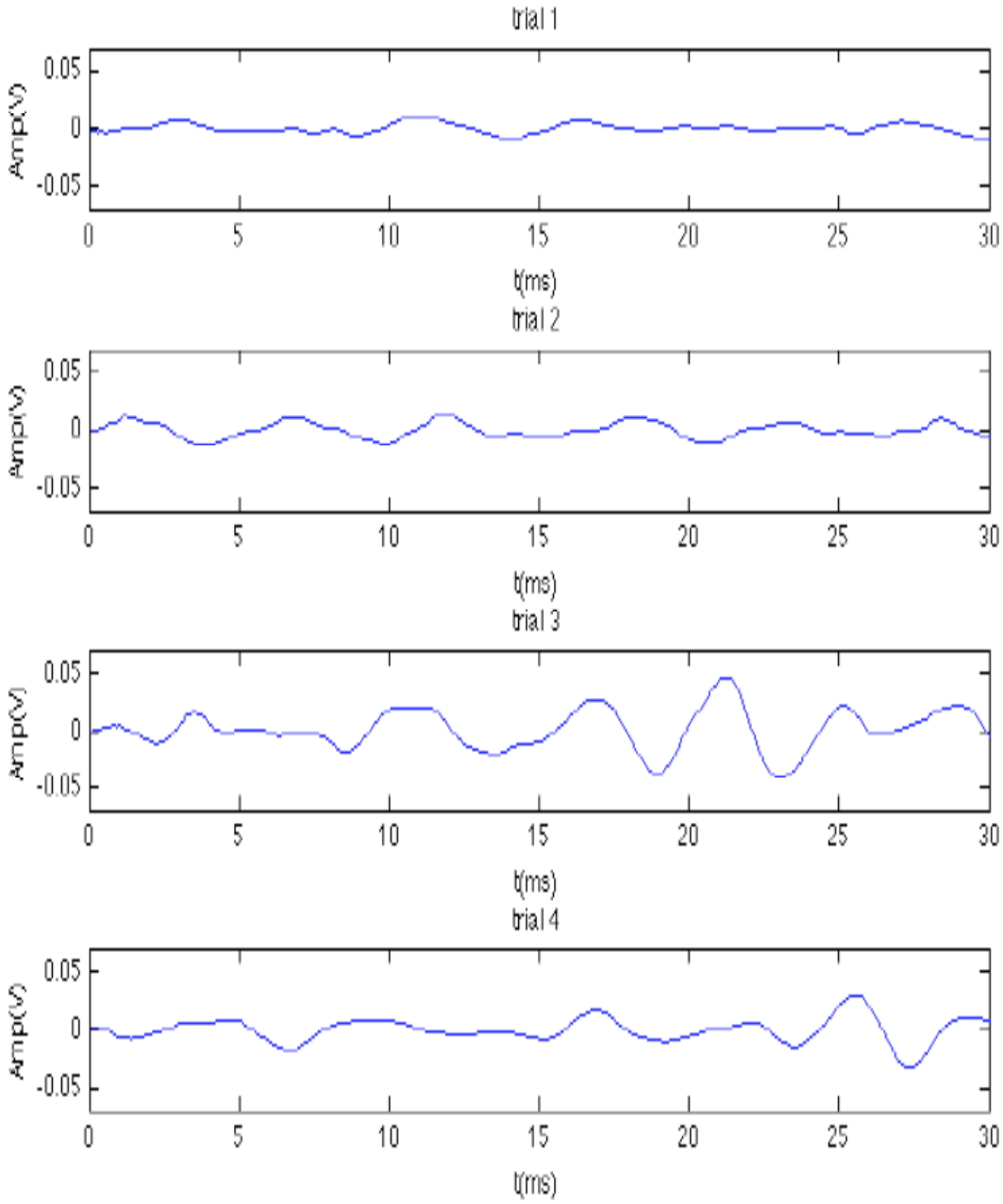

Fig. 24 a. BAEP amplitude vs time plots for data set 1

Shows the auditory response for each trial in data set 1.

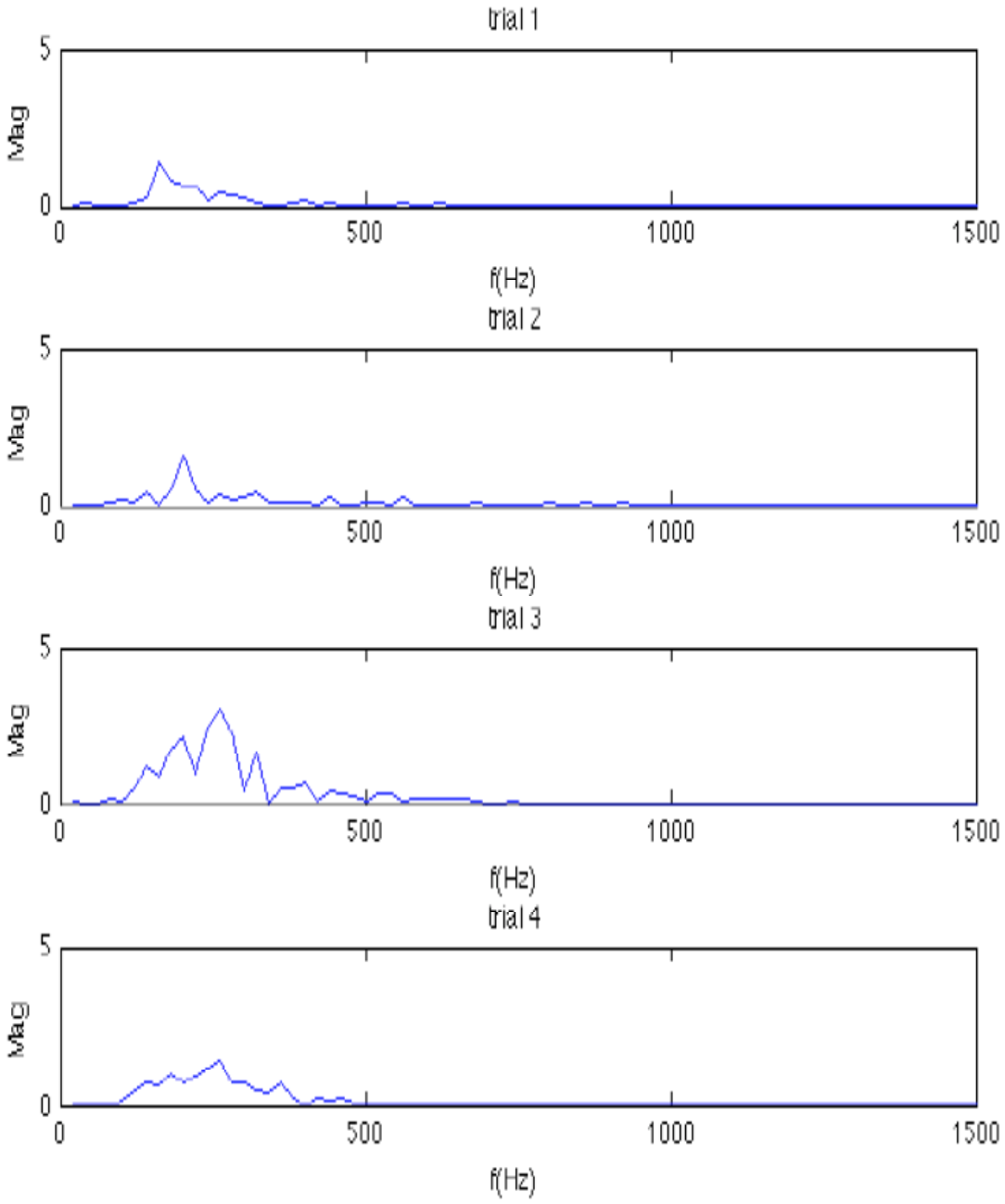

Fig. 24 b. BAEP magnitude vs frequency plots for data set 1

Shows the magnitude spectra for each auditory response in data set 1.

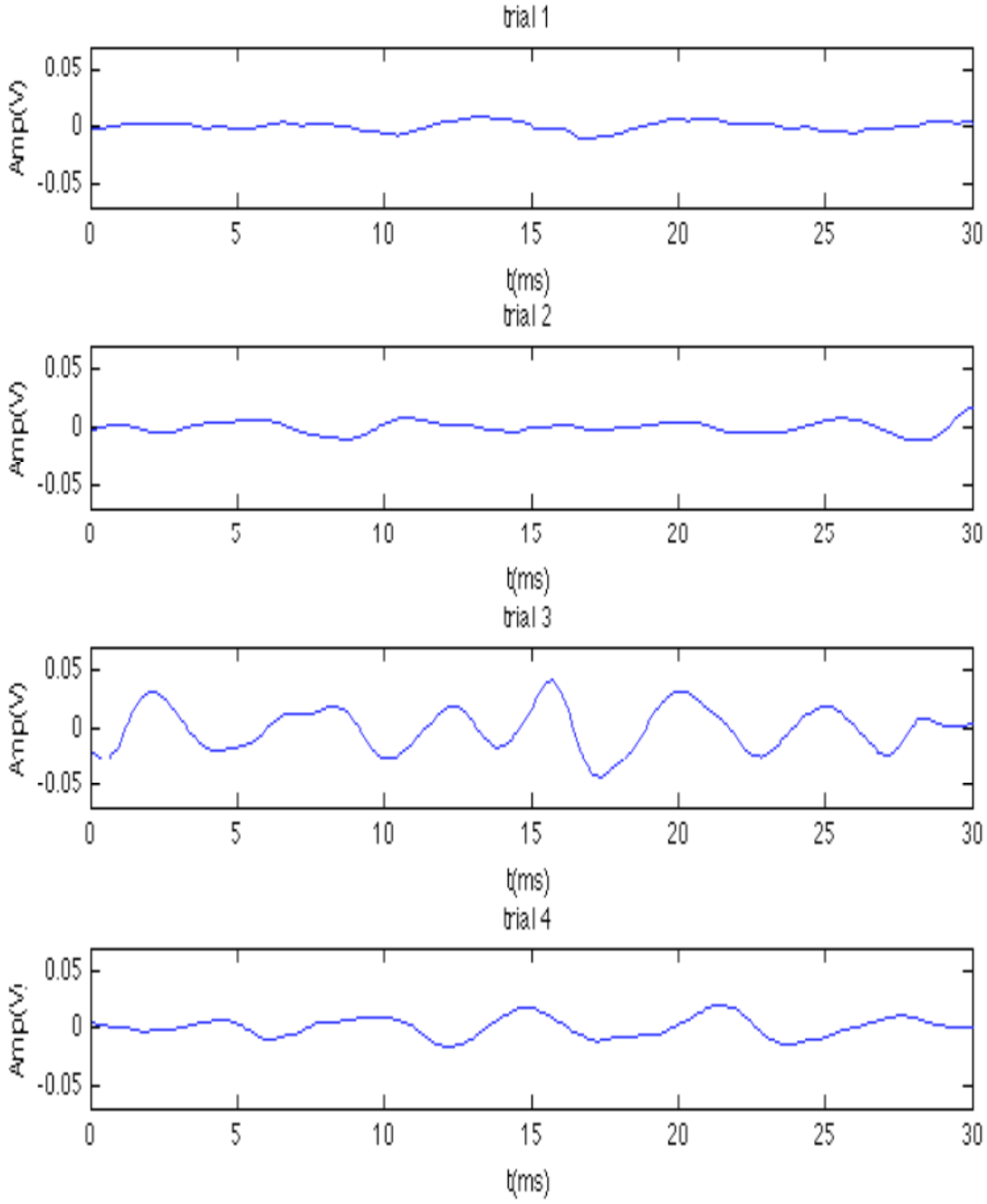

Fig. 25 a. BAEP amplitude vs time plots for data set 2

Figure 25 a shows the auditory response for each trial in data set 2.

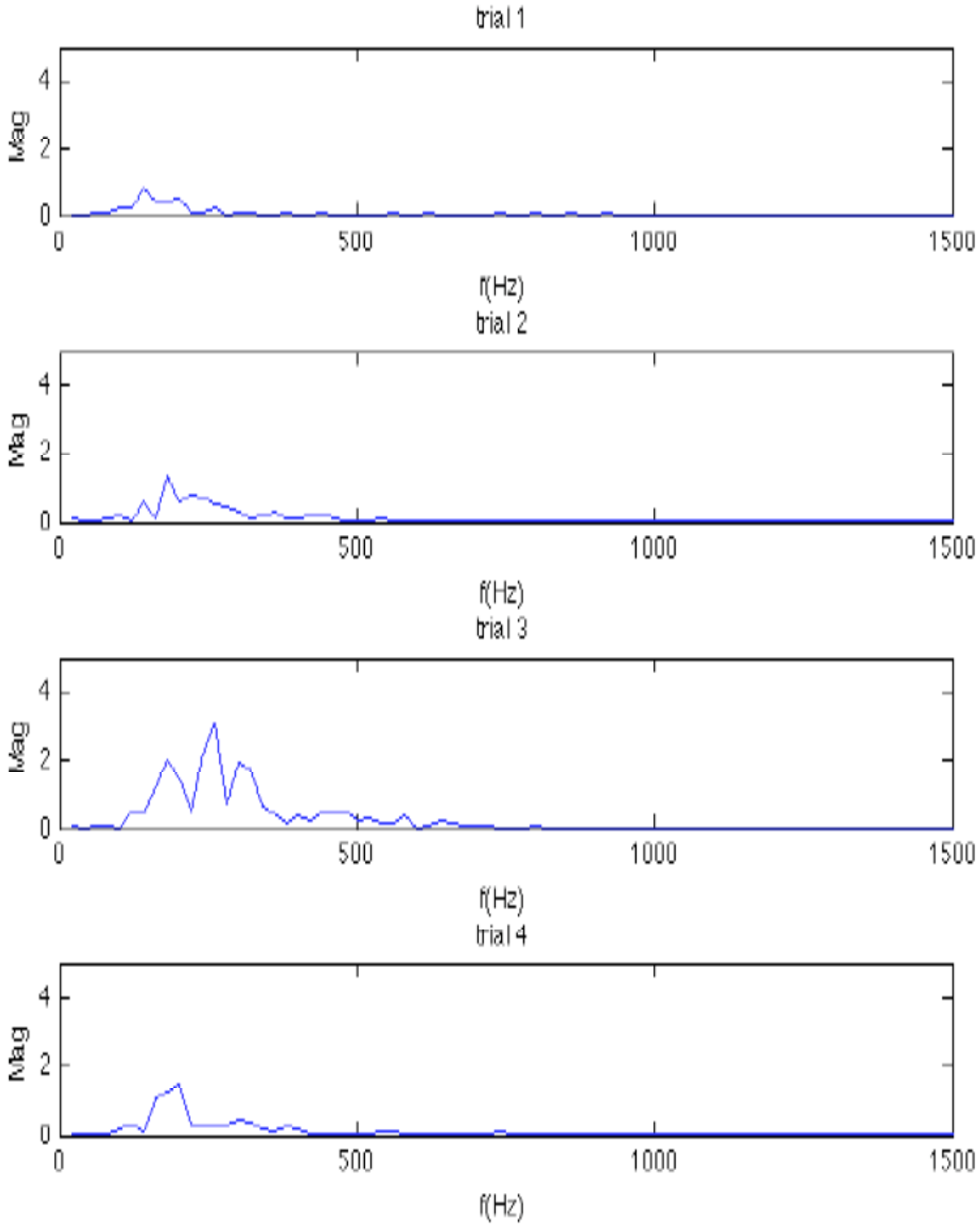

Fig. 25 b. BAEP magnitude vs frequency plots for data set 2

Figure 25 b shows the magnitude spectra for each auditory response in data set 2.

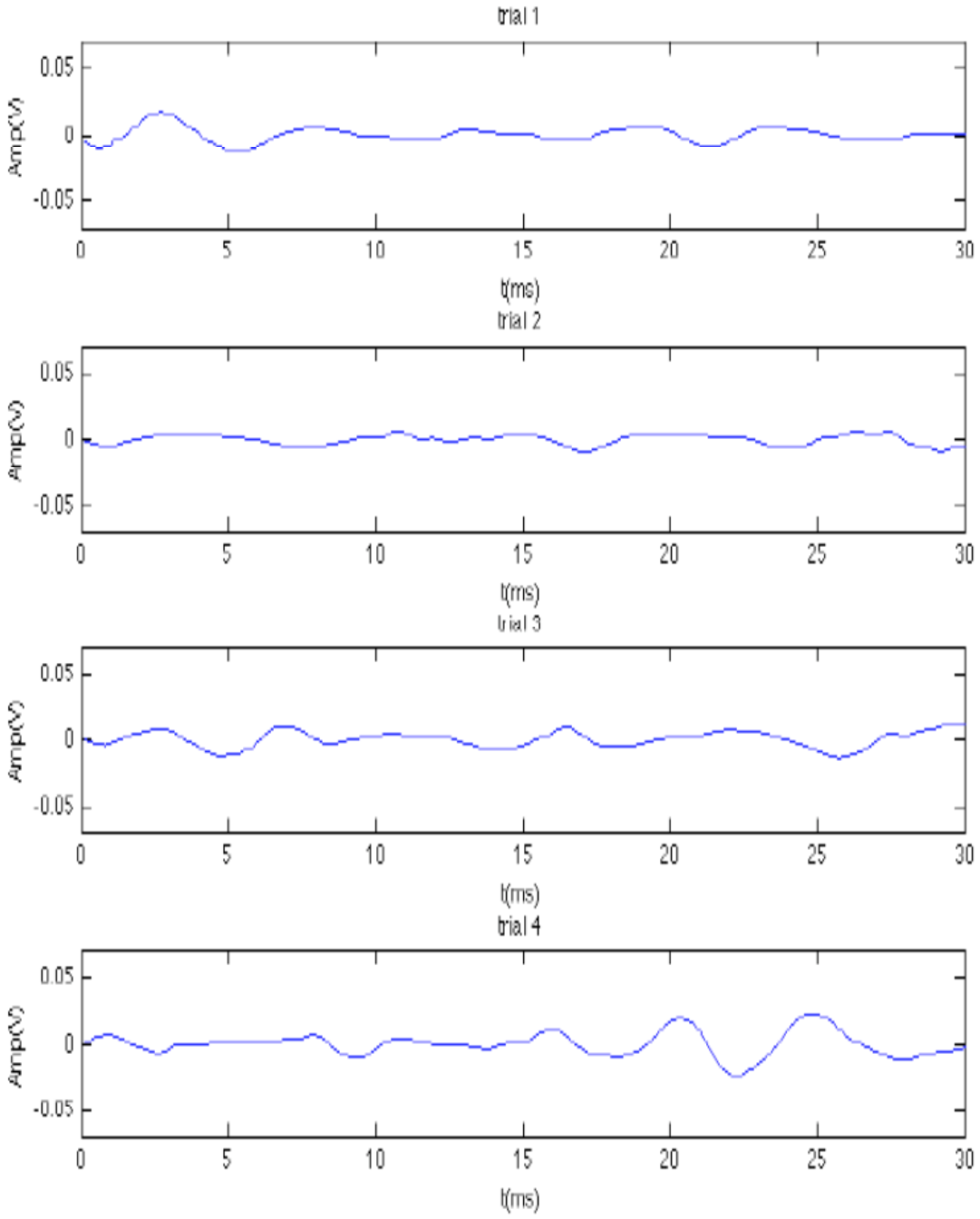

Fig. 26 a. BAEP amplitude vs time plots for data set 3

Figure 26 a shows the auditory response for each trial in data set 3.

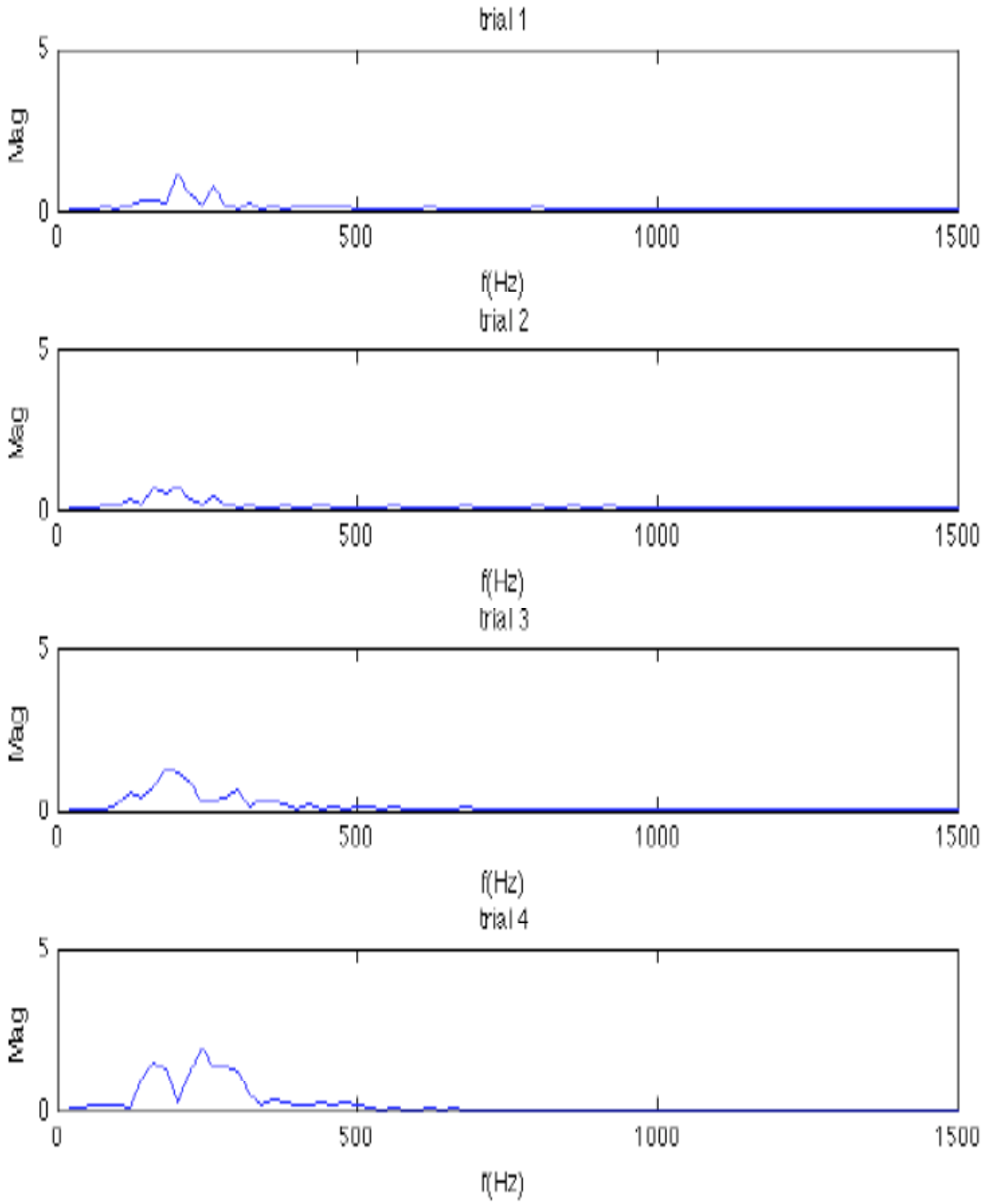

Fig. 26 b. BAEP magnitude vs frequency plots for data set 3

Figure 26 b shows the magnitude spectra for each auditory response in data set 3.

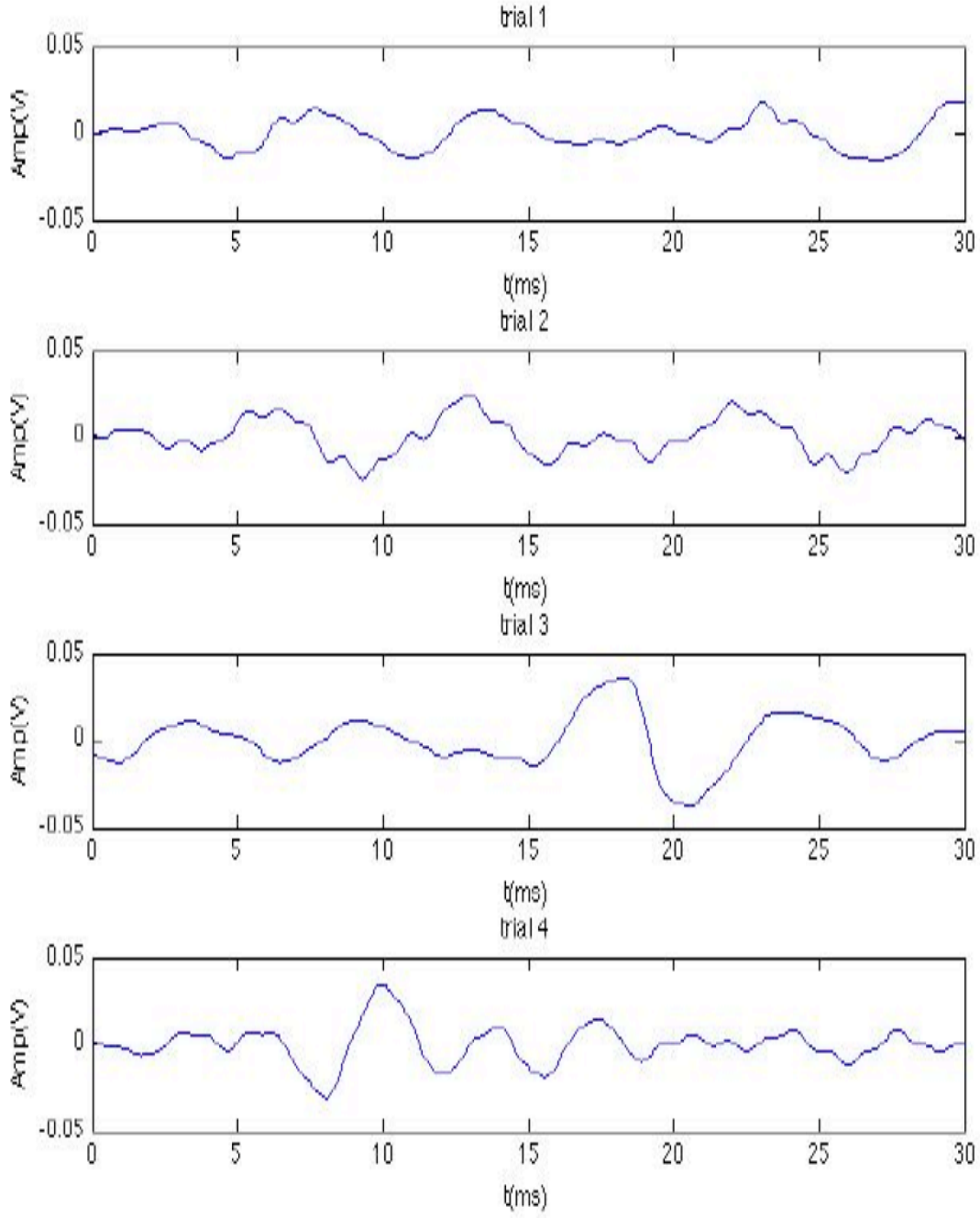

Fig. 27 a. BAEP amplitude vs time plots for data set 4

Figure 27 a shows the auditory response for each trial in data set 4.

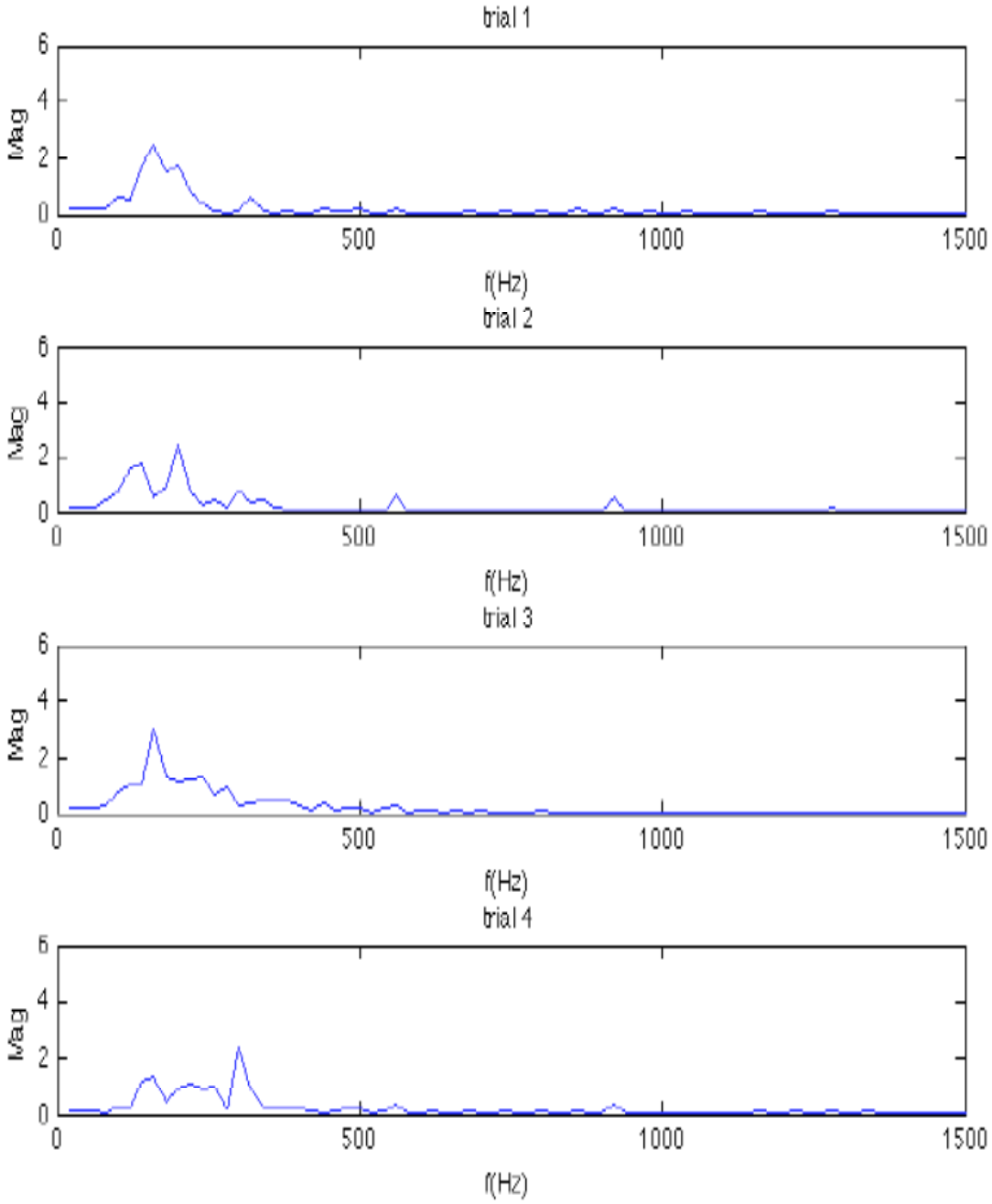

Fig. 27 b. BAEP magnitude vs frequency plots for data set 4

Figure 27 b shows the magnitude spectra for each auditory response in data set 4.

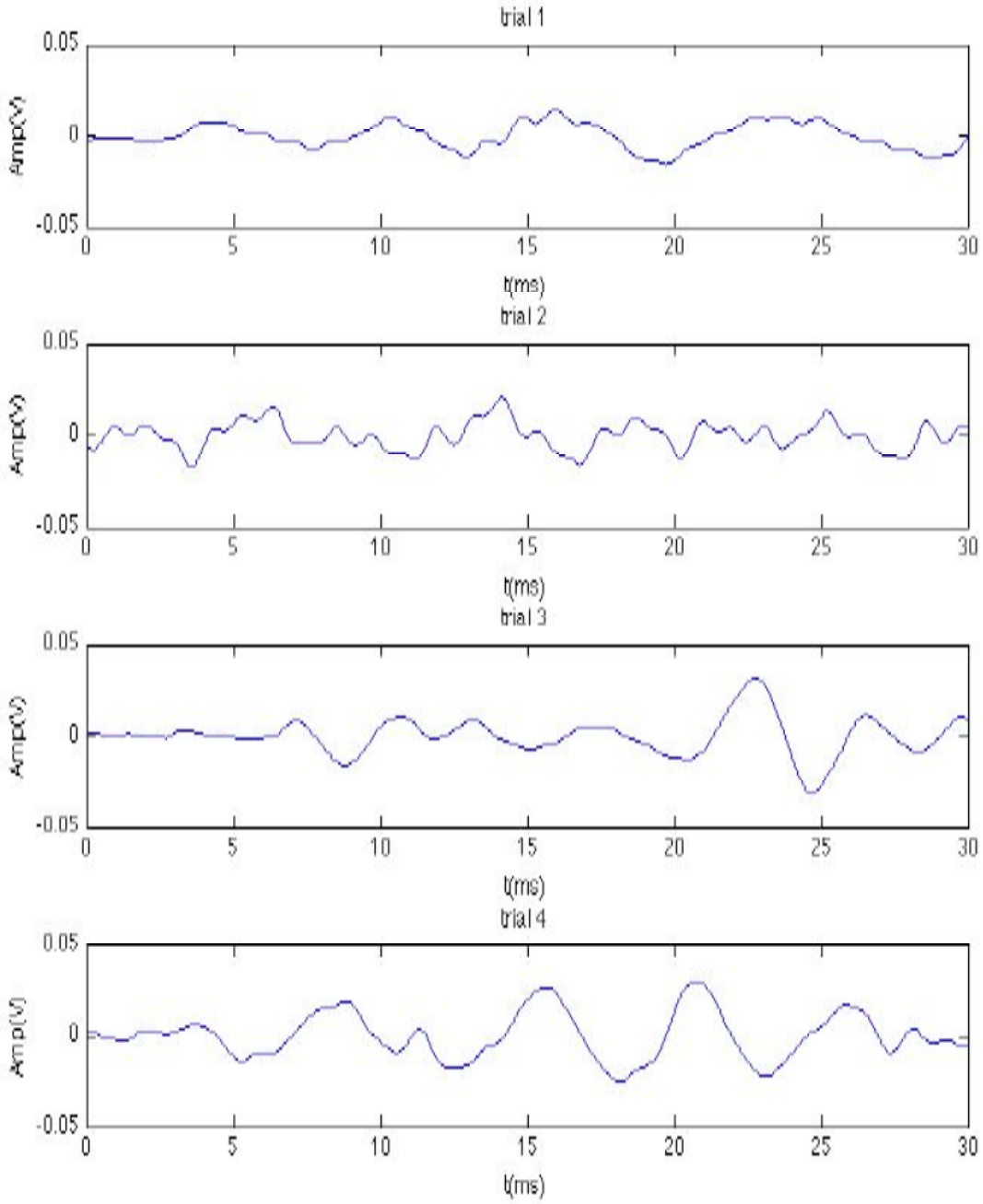

Fig. 28 a. BAEP amplitude vs time plots for data set 5

Figure 28 a shows the auditory response for each trial in data set 5.

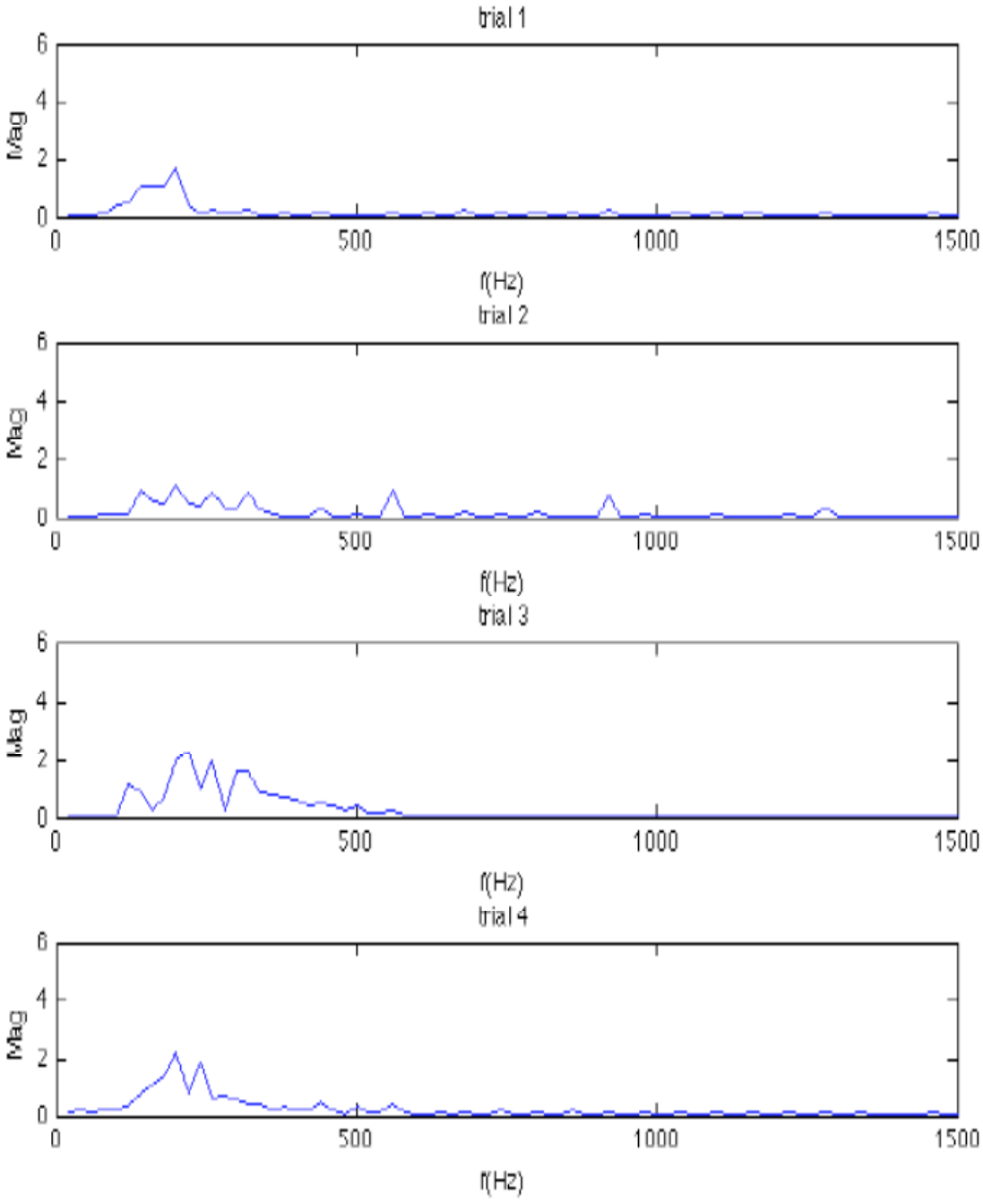

Fig. 28 b. BAEP magnitude vs frequency plots for data set 5

Shows the magnitude spectra for each auditory response in data set 5

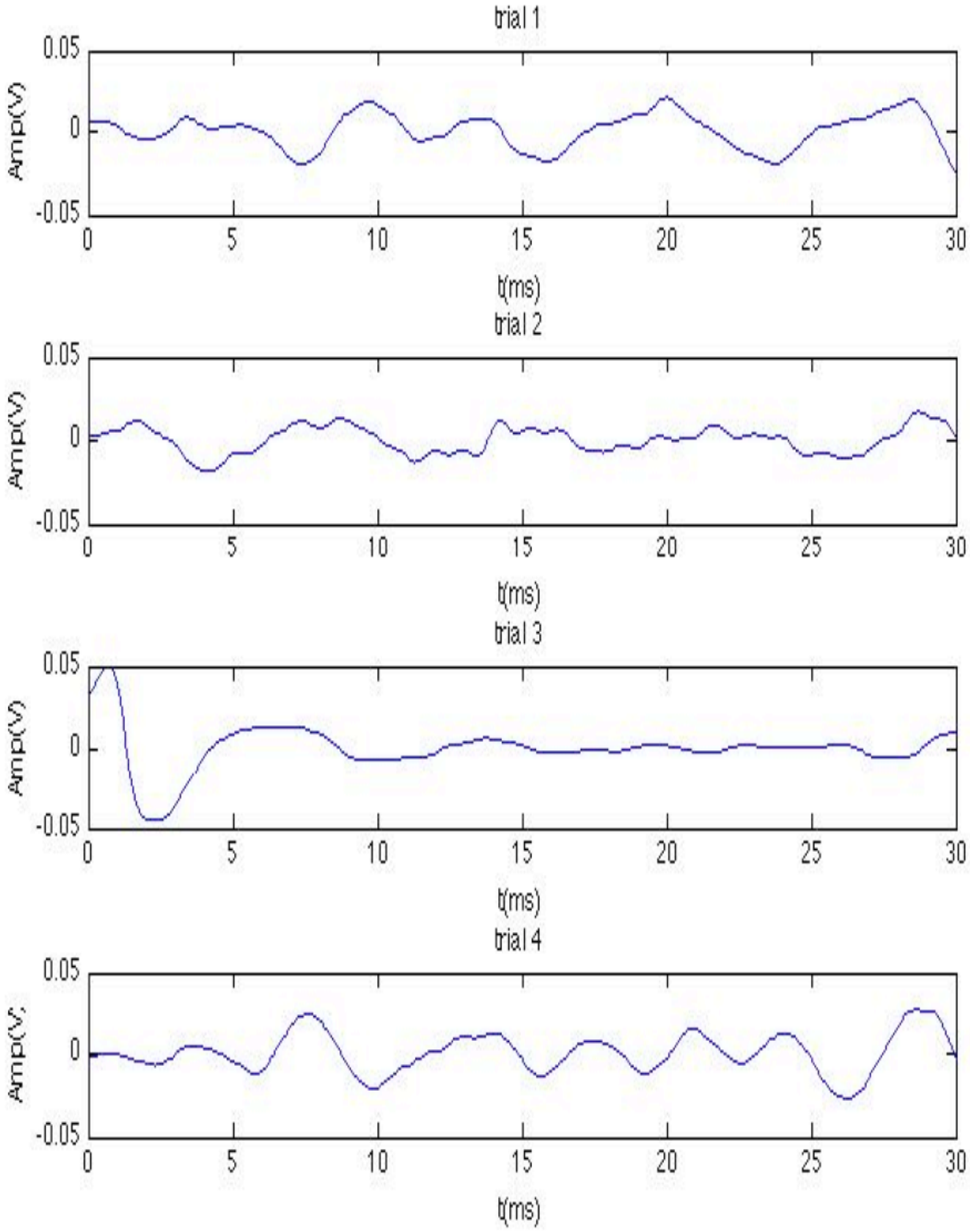

Fig. 29 a. BAEP amplitude vs time plots for data set 6

Shows the auditory response for each trial in data set 6

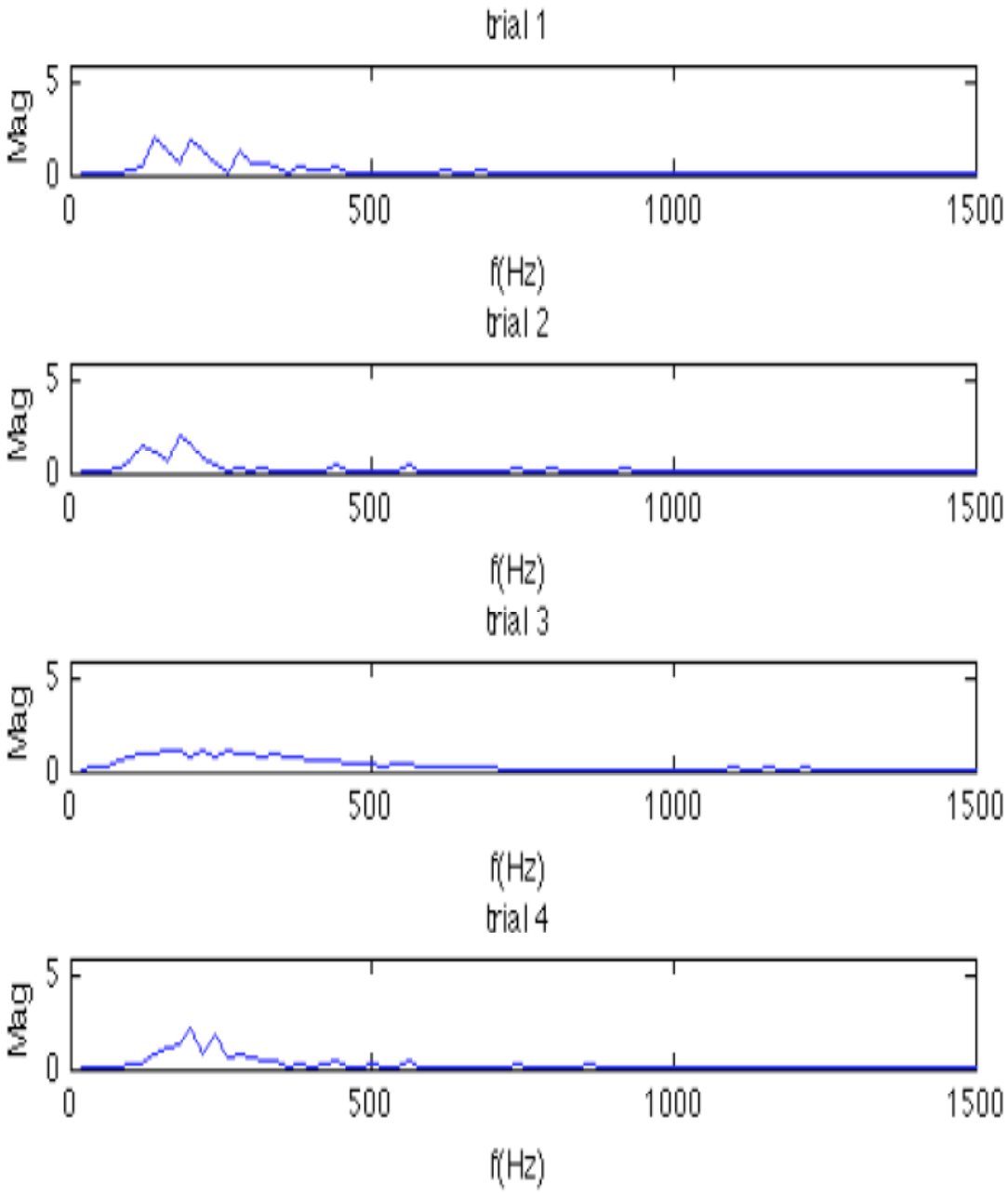

Fig. 29 b. BAEP magnitude vs frequency plots for data set 6

Shows the magnitude spectra for each auditory response in data set 6

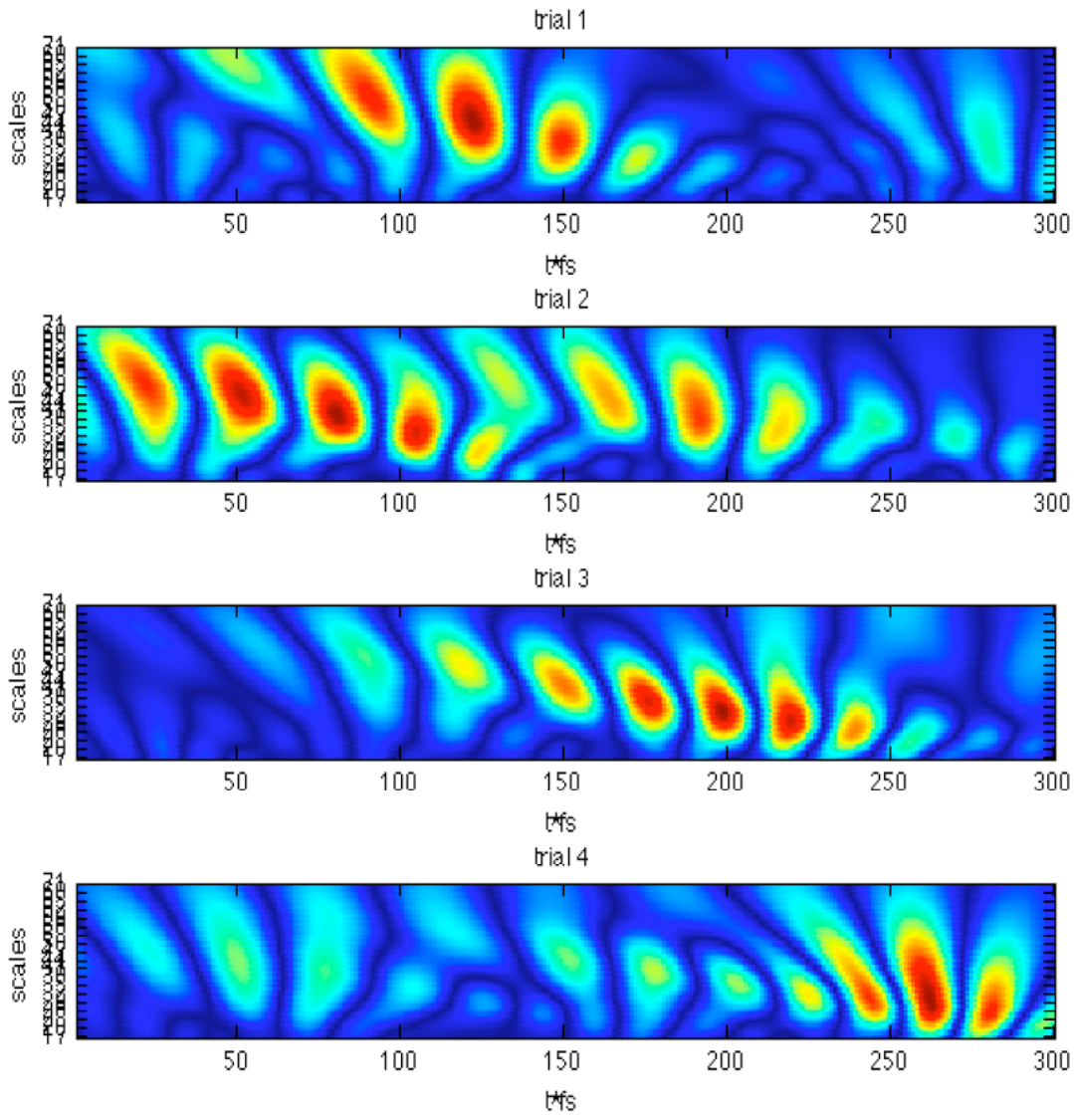

Fig. 30. BAEP CWT plots for data set 1.

Shows the CWT applied on averaged responses for data set 1. The graph shows time frequency representation. The X axis is time*sampling rate and Y axis shows scales 17-71 corresponding to frequencies 100-1000 Hz. The red regions represent high power in the frequency band while the blue regions show low power.

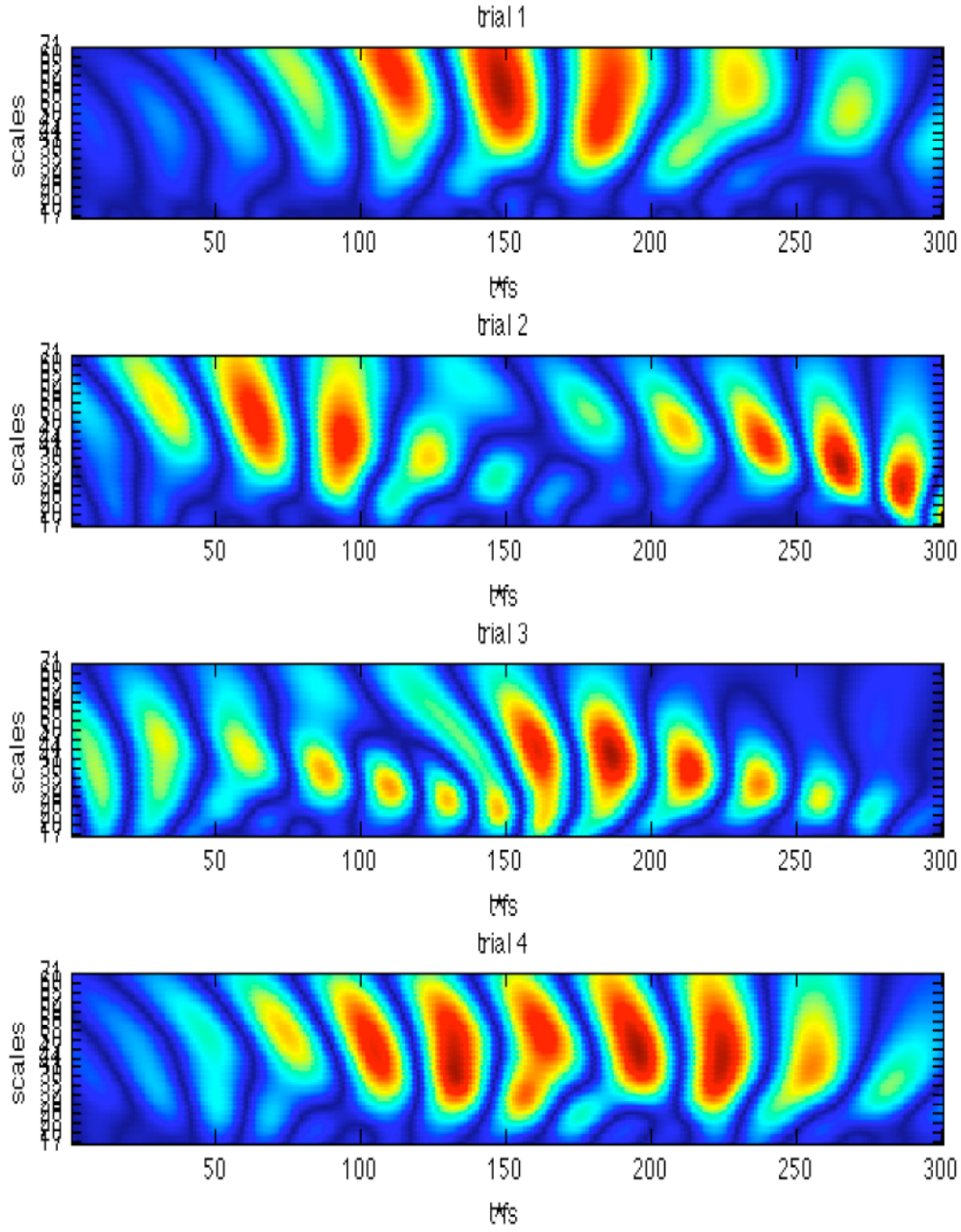

Fig. 31. BAEP CWT plots for data set 2

Shows the CWT applied on averaged responses for data set 2

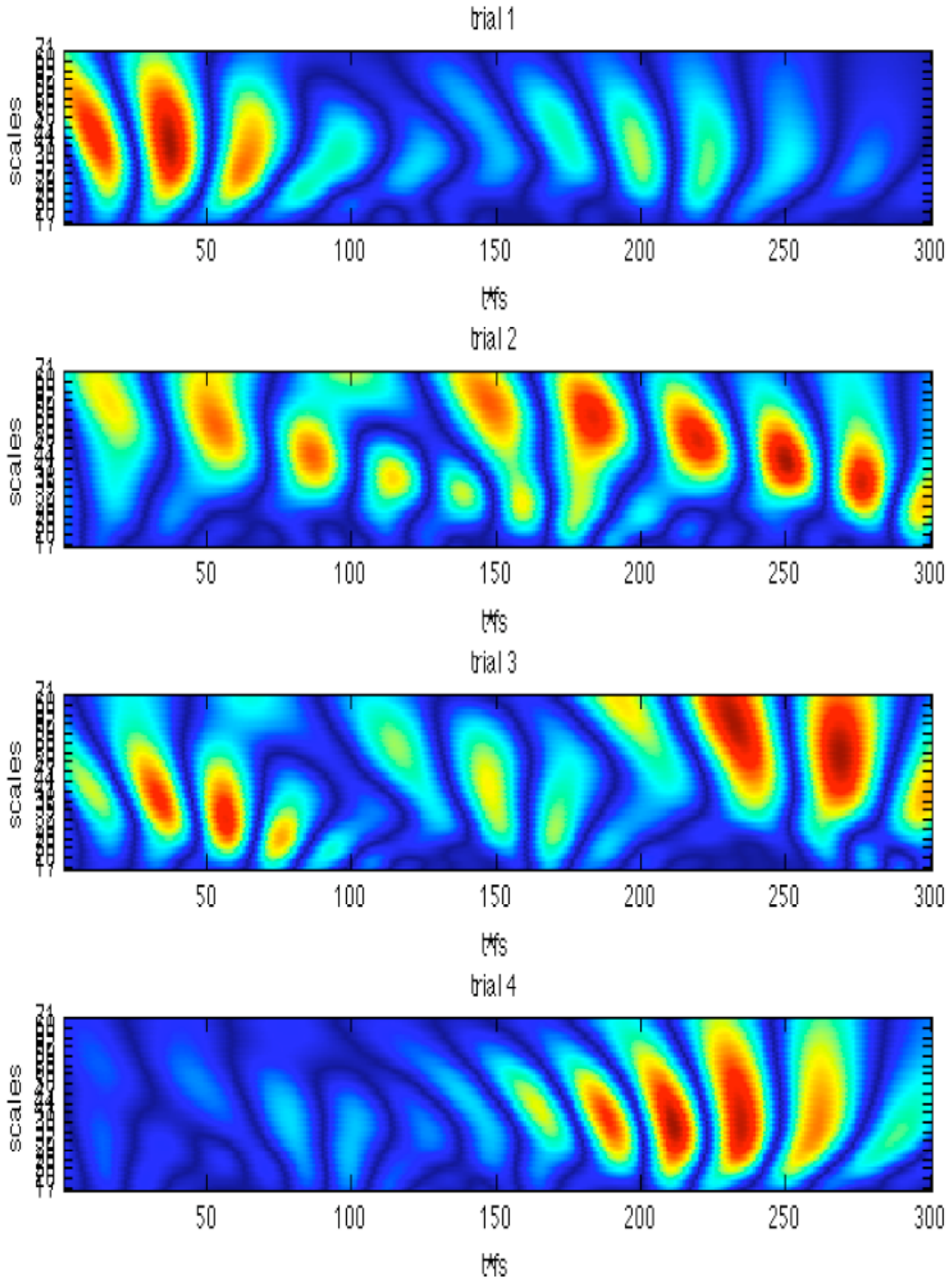

Fig. 32. BAEP CWT plots for data set 3

Shows the CWT applied on averaged responses for data set 3.

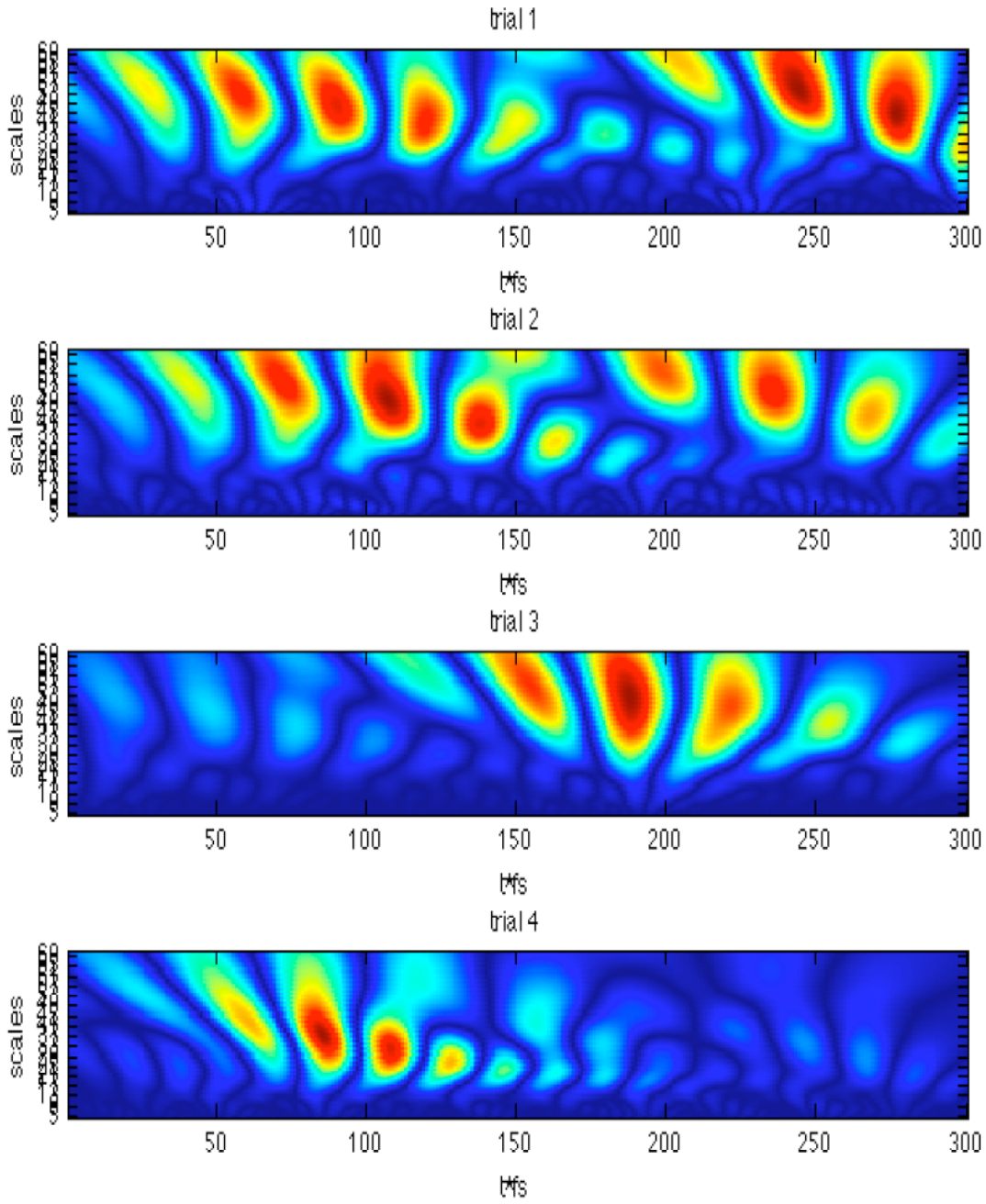

Fig. 33. BAEP CWT plots for data set 4

Shows the CWT applied on averaged responses for data set 4.

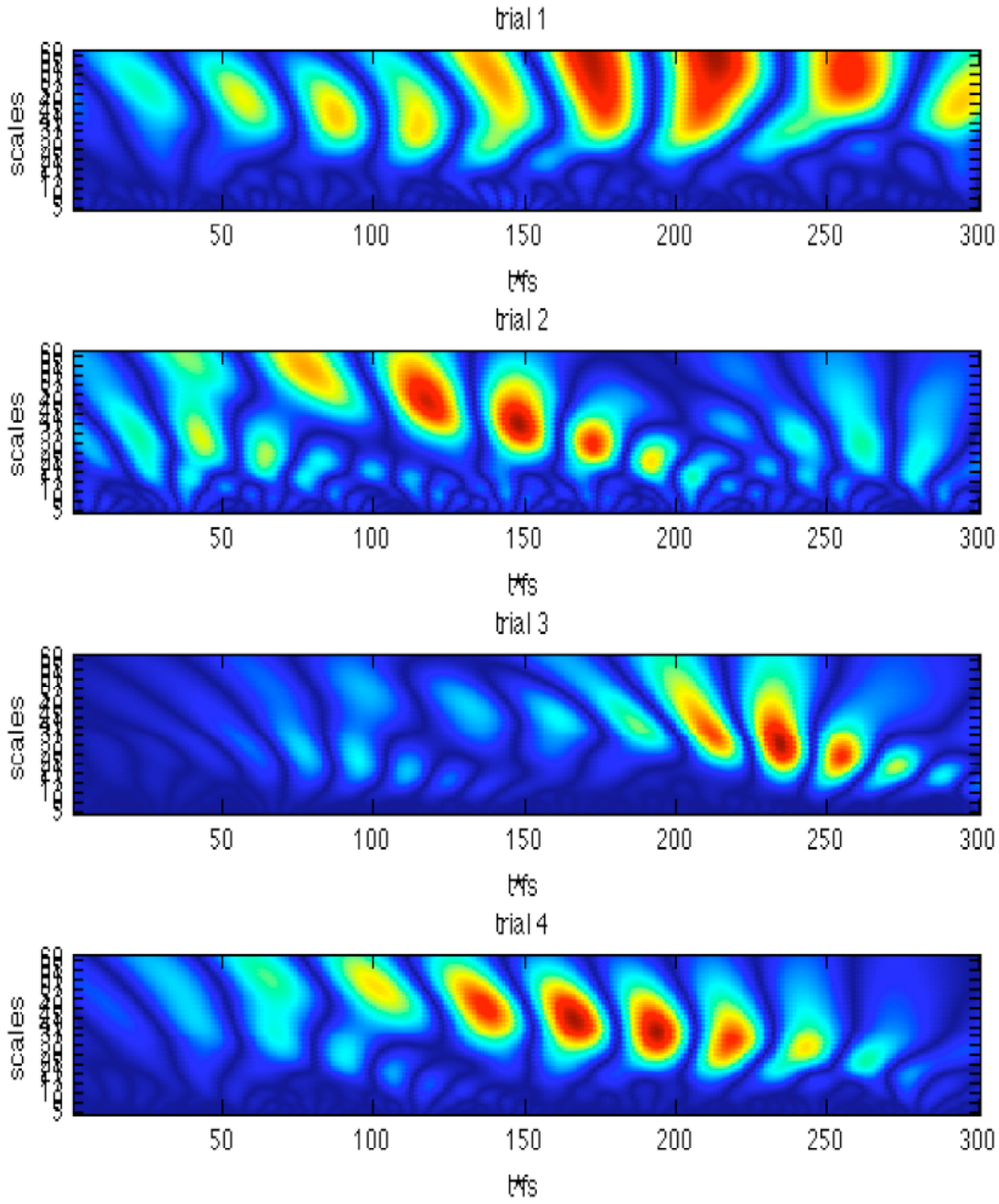

Fig. 34. BAEP CWT plots for data set 5

Shows the CWT applied on averaged responses for data set 5.

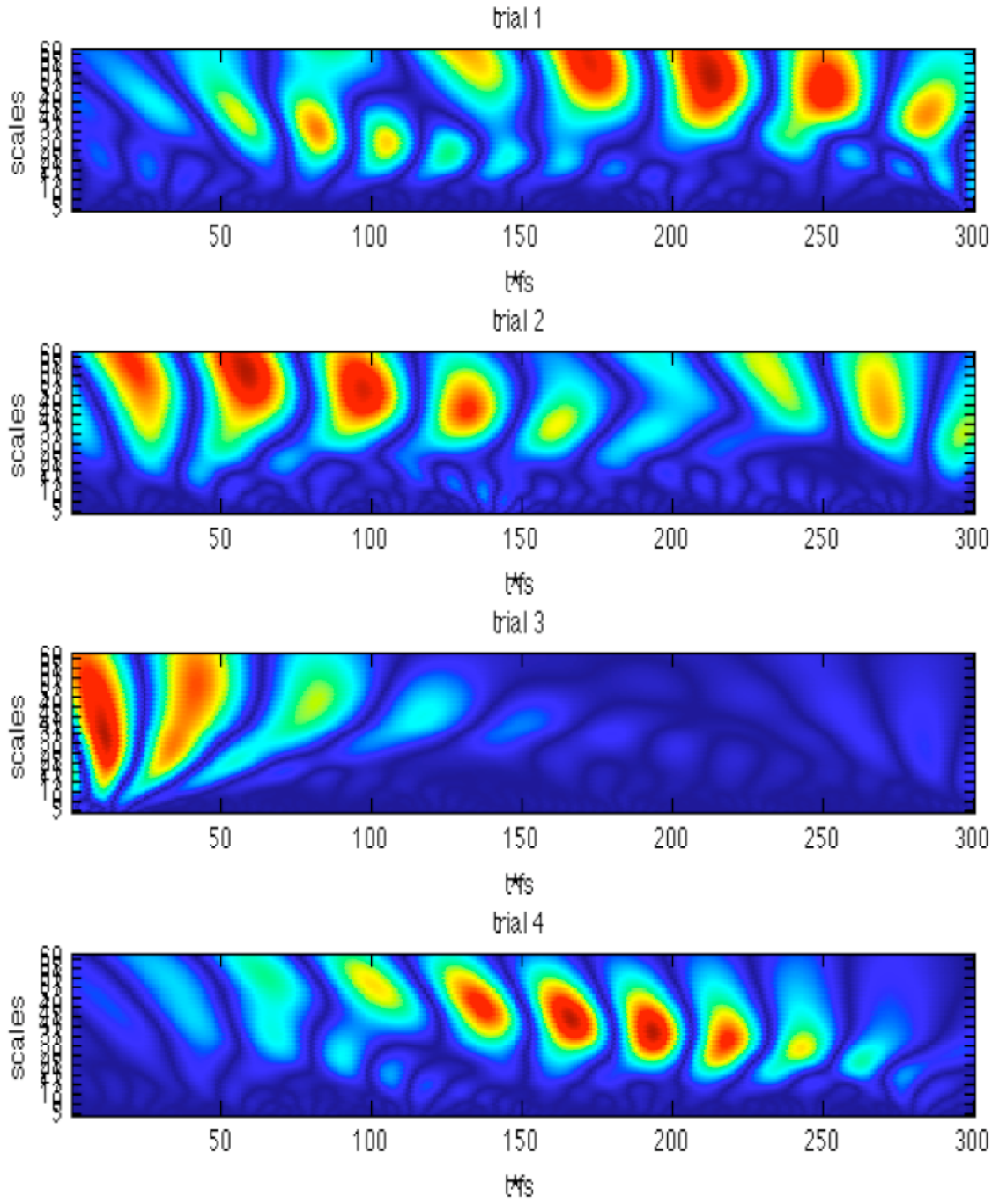

Fig. 35. BAEP CWT plots for data set 6

Shows the CWT applied on averaged responses for data set 6.

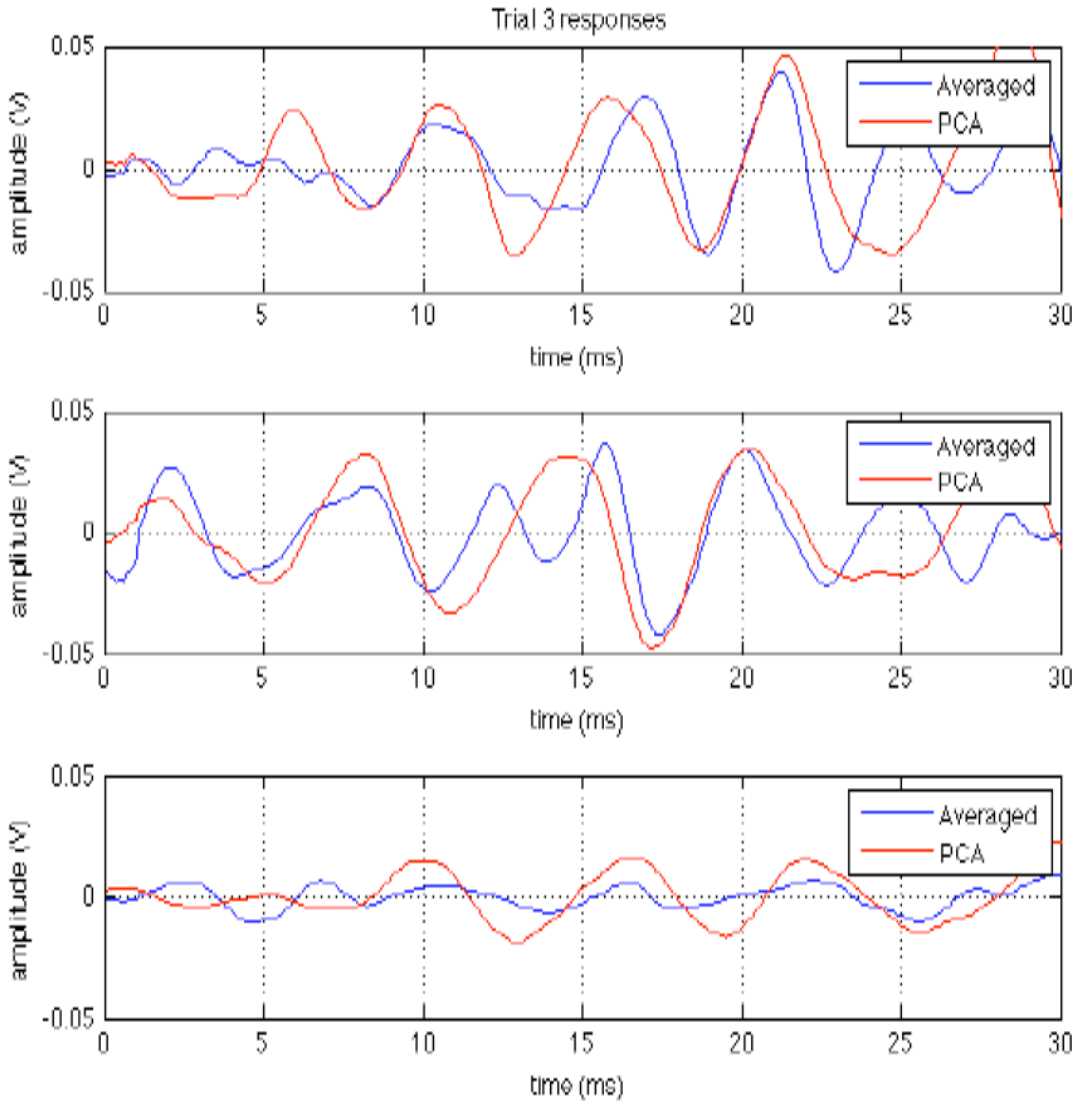

Fig. 36 a. PCA results data sets 1-3

Shows auditory responses in trial 3 from data sets 1-3 obtained using ensemble averaging and PCA methods. AEP extracted using the ensemble averaging method is in blue, and the PCA method in red. PCA method provides a closely correlated response.

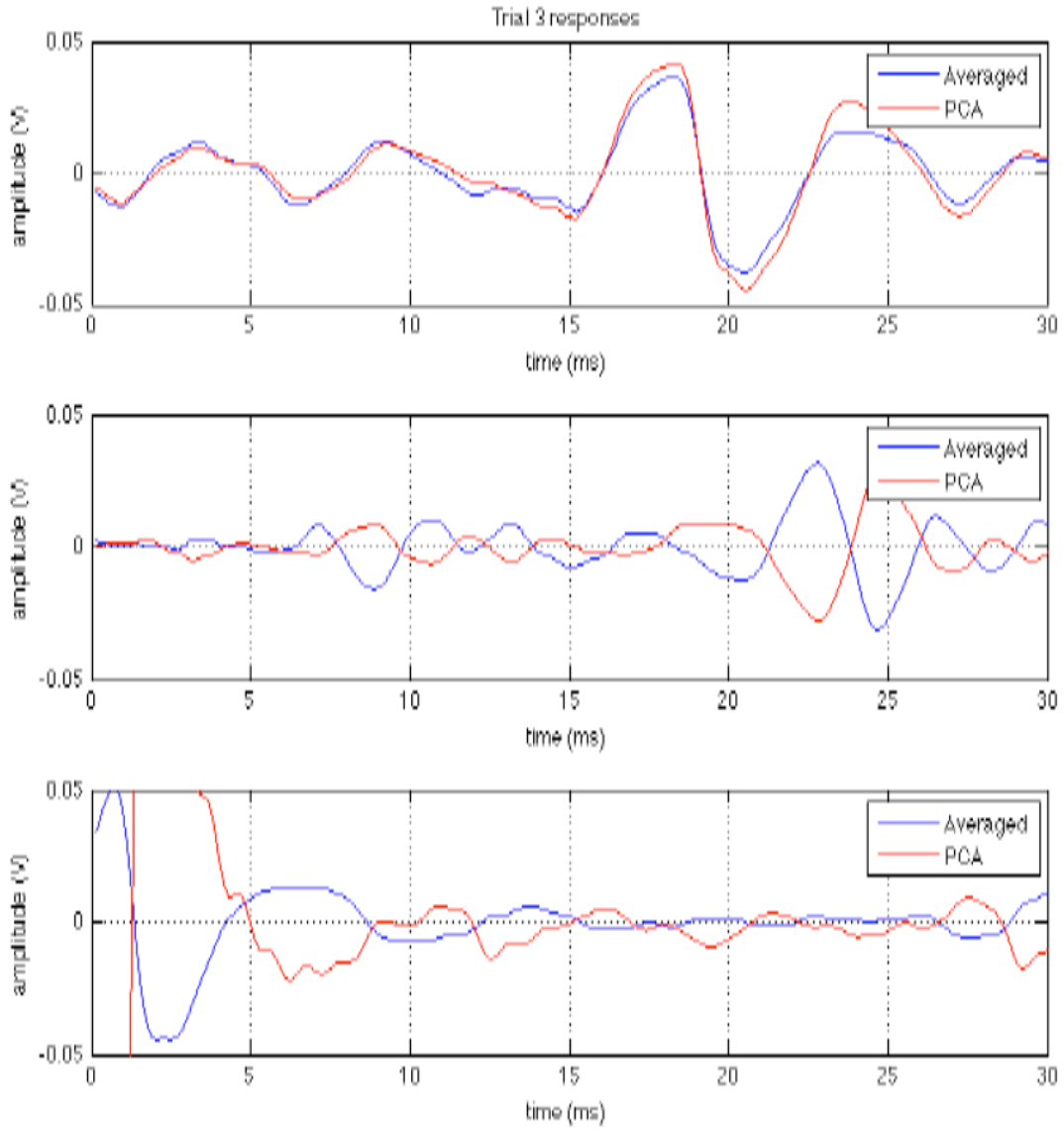

Fig. 36 b. PCA results data sets 4-6

Shows auditory responses in trial 3 from data sets 4-6 obtained using ensemble averaging and PCA methods. Data set 5 and 6 show an anti-correlation.

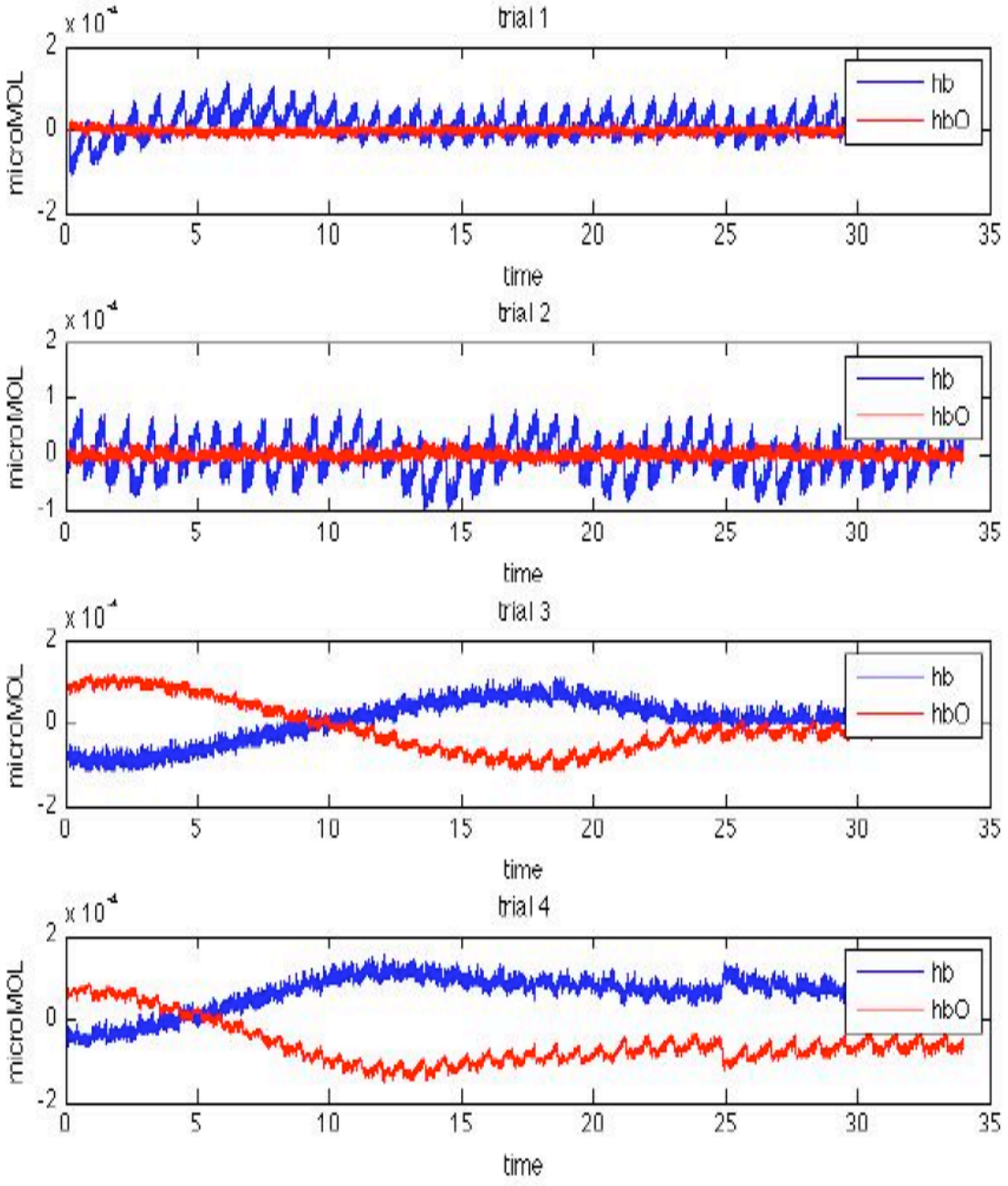

Fig. 37. NIR data

Figure 37 shows brain oxygen concentration as a function of time in seconds. Blue line indicates free hemoglobin (hb), red line indicates O_2 bound hemoglobin (hbO_2).

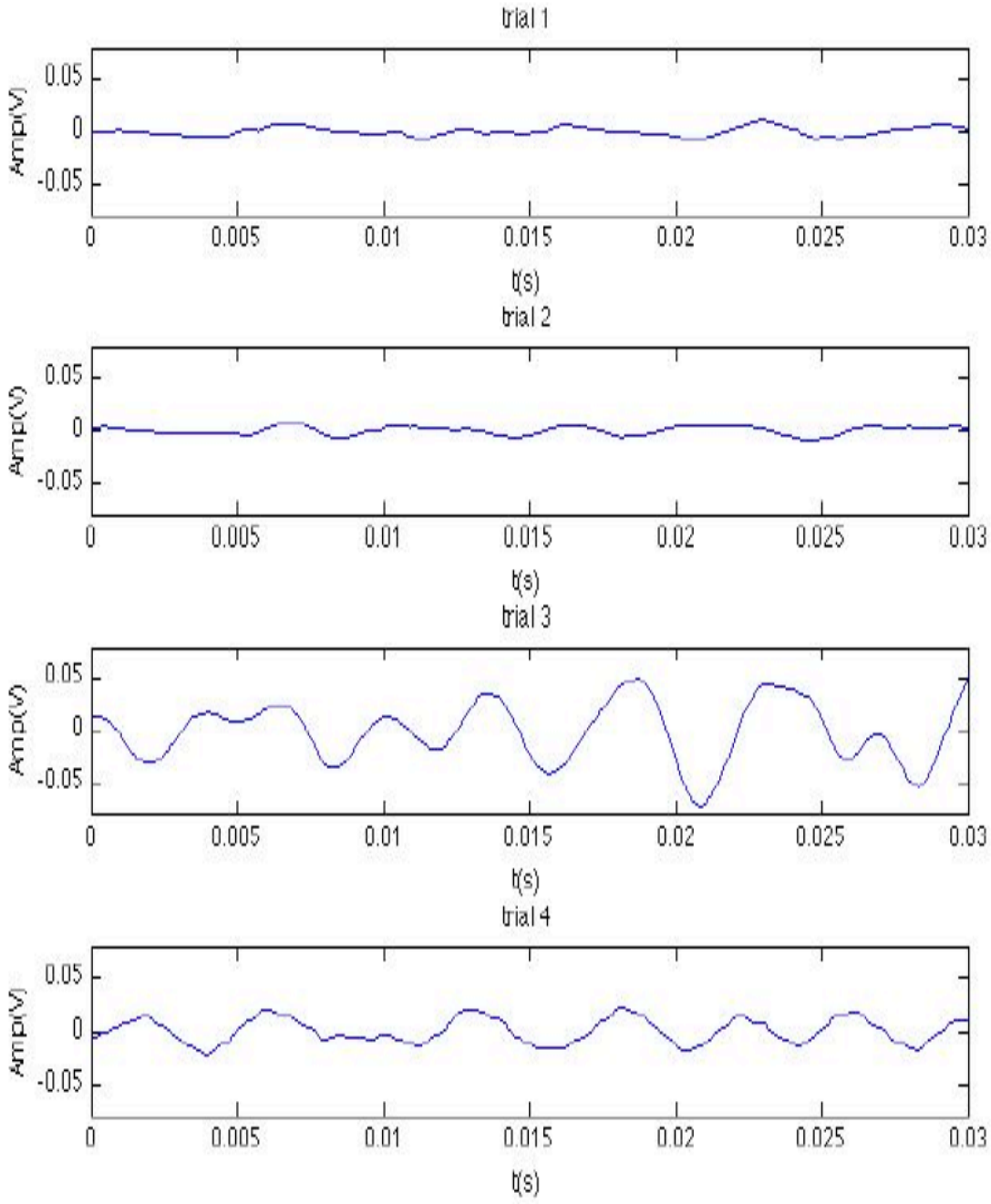

Fig. 38. Corresponding BAEP

BAEP data corresponding to the NIR data in figure 37.

Chapter 5. DISCUSSION AND SUGESTIONS FOR FUTURE RESEARCH

5.1 Discussion

The raw data shows increased fluctuations in trials 3 and 4 where intervention has been applied. This is also seen in the average magnitude of the processed signals. The results in this study suggest that electrical activity in the EEG as well as in the auditory cortex increases under the intervention condition. Studies have shown long periods of HV can cause epileptic activity [11]. This is attributed to the increase in permeability to sodium and potassium ions [11]. Increased permeability can increase the subject's response to the stimulus and make it more prominent in the EEG. Trials 4, in which the auditory stimulus is not applied but the intervention is introduced, show more energy in the signals than in trials 1 and 2, in which intervention is not present. Since the positive electrode is placed near the auditory cortex the increased energy in trials 4 shows that activity increases in the auditory cortex even when no stimulus is present. NIR results in figure 37 show that hypoxia was induced using the intervention conditions. Specifically, hypoxia was induced between 5 – 10 seconds of breath holding after HV. The corresponding BAEPs show a relationship with the NIR data further supporting the findings. The increased electrical activity in the EEG and in the auditory pathway, as seen in the results, is consistent with findings that show that the brain goes through a period of adaptation during sudden decreases in oxygen concentration [17]. Thus, the fluctuating EEG in the intervention trials can be explained by this adaptation. Although the peak amplitudes of the trial 4 signals increased there is significant variation between all data sets. This can be observed in time frequency analysis. In this study CWT is used to further analyze the response. The localization of energy in time varies between all signals

as can be seen from the CWT plots in figures 30-35. Figures 30-35 show the energy variations within 100-1000 Hz over the length of the response. For trial 3, a pattern can be seen in the time frequency characteristics. The energy is low in the first 15 ms of the response and increases significantly between 15 and 25 ms in data sets 1, 2, 4 and 5. This time frame corresponds to the MLR. This is expected since the auditory cortex response is greater in amplitude than the brainstem response due to cortex proximity with electrode [6]. Trial 3 in the 3rd and 6th data sets show a different pattern then trial 3 in remaining data sets. The energy in these trials is greater between 0 and 10 ms, which correspond to ABR. MLR has been shown to reduce under sleep and anesthesia, suggesting that the MLR is governed by the cognitive awareness of the stimulus [7 16]. This is also supported by the fact that the MLR is difficult to record in uncooperative patients such as children, which further demonstrates that the MLR is most prominent when the subject is concentrating on the response [20]. Specifically in trial 3 of data set 6, shown in figure 29a, the subject reported being lightheaded and perceiving the stimulus to be far away. These physiological sensations can be seen in the EEG, BAEP, and CWT plots. The trial 3 EEG in figure 18a shows a rapid fluctuation of high amplitude causing signal saturation. BAEP and CWT plots also show an increase in activity within the time frame of the ABR for this trial. This is because, unlike the auditory cortex response, the brainstem response is not affected by awareness of the stimulus but by the presence of it. The brainstem function is to transmit the auditory signal to the cortex, while it is the cortex function to processes and interpret the signal [20]. Thus, the results in trial 3 of data set 9 can be explained by the subject's physiological state. In trials where intervention is not applied, the energy is relatively constant during the entire response.

The CWT data show random energy distributions between trials and BAEP features cannot be clearly identified.

5.2 Summary

In this study we have developed a device for monitoring BAEP under hypoxic conditions. Our results show that it is possible to extract the BAEP using fewer realizations for averaging under the intervention conditions, suggesting that the BAEP activity increases following sudden unset of hypoxia. We also showed that our methods allow monitoring of oxygen supply to the brain by recording the EEG from the auditory cortex. The technique presented in this study can be used by clinicians to assess hearing and detect abnormal breathing in neonates and adults. In addition, this technique can assist clinicians to assess brain function during surgery since the ABR is not affected by anesthesia and can be used to identify hypoxia.

Recommendations for future study:

In this study our primary focus was to identify changes in the BAEP during sudden onset of hypoxia. However we were not especially concerned with detailed analyses of the BAEP. However, such analysis can provide more incite into how the auditory pathway responds to oxygen concentration changes. Several hardware and experimental protocol adjustments can be made to improve BAEP feature resolution. First, the recordings in this study are taking only from the contralateral side (opposite from the ear where the stimulus is applied). The auditory nerve and cochlear nuclei are on the ipsilateral side (same side as the ear where the stimulus is applied). Therefore Wave I and II of the ABR cannot be detected. Applying the stimulus to both ears can potentially solve this problem by stimulating the ipsilateral side. Adjustments to the

circuit can also be made to improve the SNR of the BAEP. Even though machine noise is reduced by the application of a digital comb filter, some amount of noise is still detected as can be seen in figures 24-29b. An addition of an analog notch filter as well as adjustment of the sampling frequency can further reduce this noise. Finally, additional subjects could be included to substantiate present findings in future studies and future clinical applications.

REFERENCES

1) Acir, N. "The Effects of Reference Inputs in the BAEP signal acquisition using adaptive filter." *IEEE EMBS Conference on Neural Engineering,* 685-688, 2009.
2) Antonio, J. Gnecchi, G. Rogelio, L. Lara, S. Cesar, J. Garcia, H. "Design and Construction of an EEG Data Acquisition System for Measurement of Auditory Evoked Potentials." *Electronics, Robotics and Automotive Mechanics Conference,* 547-552, 2008.
3) Baas, J. M.P. Milstein, J. Donlevy, M. Grillon, C. "Brainstem Correlates of Defensive States in Humans." *Biol Psychiatry,* 59:588–593, 2006.
4) Changzhi, L.V. Di, F. Min, W. Guangheng, G. "A Wireless Collector for EEG Signal of Freely Behaving White Mice." *2nd International Congress on Image and Signal Processing*, 1-4, 2009.
5) Cherrid, N. Naıt-Ali, A. Siarry, P. "Optimized Brainstem Auditory Evoked Potentials Estimation Using Simulated Annealing." *Journal of Clinical Monitoring and Computing,* 19: 231–238, 2005.
6) Gazzaniga, M. S. Ivry, R. B. Mangun, G. R. "Cognitive Neuroscience The biology of the Mind." *W.W. Norton & Company, Inc.,* second edition, 2002.
7) Huang, J. W. Lu, Y. Nayak, A. Roy, R. J. "Depth of Anesthesia Estimation and Control." *IEEE Transactions On Biomedical Engineering*, 46:1, 1999.
8) Kandel, E. R. Schwartz, J. H. Jessell, T. M. "Principles of Neural Science." *McGraw-Hill Companies,* fourth edition, 2000.
9) Lakany, H. Conway, B. A. "Classification of Wrist Movements using EEG-based

Wavelets Features." *Engineering in Medicine and Biology 27th Annual Conference,* 5404-5407, 2005.

10) Lehninger, A. L. Nelson, D. L., Cox, M. M. "Lehninger Principles of Biochemistry", *W.H. Freeman and Company*, Fifth Edition, 450-451, 2008.

11) Leonhardt, G. Greiff, A. Marks, S. Ludwig, T. Doerfler, A. Forsting, M. Konermann, S. Hufnagel, A. "Brain diffusion during hyperventilation: Diffusion-weighted MR-monitoring in patients with temporal lobe epilepsy and in healthy volunteers." *Epilepsy Research,* 51:269-278, 2002.

12) Li, J. K-J. Wang, T. Zhang, H. "Rapid Noninvasive Continuous Monitoring of Oxygenation in Cerebral Ischemia and Hypoxia", Cardiovascular Engineering, 10:213-217, 2010.

13) Lijaun, D. Zhiyu, Q. Huinan, W. Min, P. "Noninvasive monitoring adult hemodynamic and oxygenation variables' changes in response to sensory stimulation by near-infrared spectrodcopy." *International Symposium on Biophotonics, Nanophotonics and Metamaterials,* 159-162, 2006.

14) Misulis, K. E. Head, T. C. "Essentials of Clinical Neurophysiology." *Elsevier Science (USA)*, Third Edition, 211-220, 2003.

15) Naït-Ali, A. Siarry, P. "Optimal Estimation of Temporal Non-stationary Signals Using Simulated Annealing: Application to Brainstem Auditory Evoked Potentials." *Biomedical Engineering*, 37:175-180, 2003.

16) Nayak, A. Roy, R. J. "Anesthesia Control Using Midlatency Auditory Evoked Potentials." *IEEE Transactions On Biomedical Engineering,* 45:409-421, 1998.

17) Ortiz-Prado, E. Natah, S. Srinivasan, S. Dunn, J. F. "A method for measuring

brain partial pressure of oxygen in unanesthetized unrestrained subjects: The effect of acute and chronic hypoxia on brain tissue PO_2." *Journal of Neuroscience Methods* 193:217-225, 2010.

18) Ozaki, H. Watanabe, S. Suzuki, H. "Topographic EEG changes due to hypobaric hypoxia at simulated high altitude." *Electroencephalography and Clinical Neurophysiology,* 94:349-356, 1995.

19) Semmlow, J. L. "Biosignal and Medical Image Processing." *Taylor & Francis, New York,* 2009

20) Stach, B. A. "Clinical Audiology." *Thomson Delmar Learning*, 1998.

21) Zhu, X. Chen, W. "In vivo oxygen-17 NMR for imaging brian oxygen metabolism at high field." *Progress in Nuclear Magnetic Resonance Spectroscopy,* 59:319-335, 2011.

APPENDIX

Appendix I: Matlab programs for BAEP extraction and processing.

```
function [B, M, BAEP]=dataLCAve(fs,data) %input is 2D dataDsplit dfr B pad M
dfr=abs(diff(data(:,2)));
i=1;
j=1;
 time=1050;
 t=(1:time)/fs;
 for n=1:length(dfr);

    if abs(dfr(n))>1
        Dsplit{j}=data(i:n+1,1);
        pad=time-length(Dsplit{j});
        B{j} = padarray(Dsplit{j}, [pad,0], 'post');
          j=j+1;
          i=n+1;
    else
          j=j;
          i=i;
    end
 end

 C=B';
 M=[C{:}];
 M=M';
 M=M(2:end,1:900);

 M=center(M);
 M=LC(M);

 BAEP=mean(M)

%does latency correction
%uses xcorr
function[Mb]=LC(M)
[m n]=size(M)
for i=1:m
[c,lags] = xcorr(M(1,:),M(i,:),10);
LT=find(c==max(c));
   if lags(LT)>=0
         Mbar{i} = padarray(M(i,:), [0 lags(LT) ],'pre');
         Mbar{i}=Mbar{i}(1:500);
```

```
    else if lags(LT)<0
            Mbar{i}=M(i,abs(lags(LT)):end);
            Mbar{i}=Mbar{i}(1:500);
        end
    end
end

Mbar=Mbar';
Mb(1,:)=M(1,1:500);
clear i
for i=1:length(Mbar)
    Mb(i+1,:)=Mbar{i};
end

%FIR bandpass filter
%fs is the sampling frequency
%w are cutoff frequency in Hz
%data is input data
function [y]=filtEEG(fs,w, data)

N=length(data(:,1));
wn=w./(fs/2);
b = fir1(200,wn);
y=filter(b,1,data(:,1));
y=[y, data(:,2)];

function[combed]=combsig(fs,fo,q,data)
%fs = 10000; fo = 180;  q = 70;
bw = (fo/(fs/2))/q;
[b,a] = iircomb(500,bw,'notch'); % Note type flag 'notch'
combed=filter(b,a,data(:,1));
combed=[combed, data(:,2)];

%implements Singular value decompostion to perform principal component
%analyses
function[tp fp eigen PC]=PcAEP(M)
%input a matrix M of latency corrected responces
%principal components
fs=10000;
[n m]=size(M);
[U,S,PC]=svd(M);
N=500;
eigen=diag(S).^2;
eigen=eigen/N;
PC=PC(:,1:n);
```

```
tp=(1:N)/fs;
fp=(1:N)*(fs/N);
for i=1:n;
   PC(:,i)=PC(:,i)*sqrt(eigen(i));
end


clear all
close all

fs=10000;
data{1}=load('jeffclk1218.txt');
data{2}=load('jeffnclk1218.txt');
data{3}=load('jeffhclk1218.txt');
data{4}=load('jeffhnclk1218.txt');

f1=figure(1);
set(f1, 'color', 'white');
for i=1:4
   y=filtEEG(fs,[100 1000], data{i});
   y=combsig(fs,180,70,y);
   fs=10000;
   [B, M, BAEP(i,:)]=dataLCAve(fs,y);
   LCM{i}=M;
   [tp fp PC{i}]=PcAEP(M);

   N=length(BAEP);
   t=(1:N)/fs;
   f=(1:N)*(fs/N);
   subplot(4,1,i); plot(t*1000,BAEP(i,:)); xlim([0 30]); ylim([-.07 .07]); title(['trial
',num2str(i)]); xlabel('t(ms)'); ylabel('Amp(V)')
   tmax(i)=find(BAEP(i,1:300)==max(BAEP(i,1:300)));
   tmax(i)=tmax(i)/10
end

f2=figure(2);
set(f2, 'color', 'white');
for i=1:4
   FBAEP(i,:)=abs(fft(BAEP(i,:)));
   subplot(4,1,i); plot(f,FBAEP(i,:)); xlim([0 1500]); ylim([0 5]); title(['trial
',num2str(i)]); xlabel('f(Hz)'); ylabel('Mag');
   Ave(i)=mean(FBAEP(i,:))
end
f3=figure(3)
set(f3, 'color', 'white');
for i=1:4
```

```
   subplot(4,1,i);  C{i}=cwt(BAEP(i,1:300),17:71,'db6','plot');    title(['trial  ',num2str(i)]);
xlabel('t*fs'); ylabel('scales');colormap(jet);
end


%find peaks
%clear all; close all;
%load BAEP12183

function [time]=findmax(fs, Data)
Data=Data(1:300);
N=length(Data);
D=diff(Data);
t=((1:N)/fs)*1000;
j=1;
for i=1:length(D)-1

   if (sign(D(i)) ~= sign(D(i+1))) && (D(i)>D(i+1))
      index(j)=i;
   j=j+1;
   else end
end
k=1;
 plot(t,Data);
for i=1:length(index);

   if (Data(index(i))>0) && (index(i)/fs*1000 >=1.8)
      hold on
      time(k)=(index(i)/fs) *1000;
      k=k+1;
      plot((index(i)/fs)*1000, Data(index(i)), 'r*'); ylim([-.05 .05]); grid on
   else end
end
```